Final Performance Report

March 1, 2022 – February 28, 2026

As Required By

Matagorda Bay Mitigation Trust
Contract No. 022

Trophic Linkages and Habitat Connectivity of Popular Sportfish in the Matagorda Bay System

Prepared by:
Kesley Gibson-Banks, Ph.D. (PI)
Matthew Streich, Ph.D. (Co-PI)
Jessica Dutton, Ph.D. (Co-PI)

Trophic linkages and habitat connectivity of popular sportfish in the Matagorda Bay system

Personnel:

Principal Investigator(s):
PI: Kesley G. Banks, Ph.D., kesley.banks@tamucc.edu
Co-PI: Matthew Streich, Ph.D., matthew.streich@tamucc.edu
Co-PI: Jessica Dutton, Ph.D., jdutton@txstate.edu
[1]Harte Research Institute, Texas A&M University-Corpus Christi, 6300 Ocean Drive, Corpus Christi, TX 78412
[2]Texas State University, 601 University Drive, San Marcos, TX 78666

Significant Deviation:

A year no-cost extension (NCE) was granted due to additional time needed to analyze the contaminate and stable isotope datasets, which were much larger than anticipated. The NCE allowed for the acoustic array to remain in place for several additional months, completing the project with approximately 1.5 years of movement data for tagged fish in the system.

Objectives:

The overall **goal** of this study was to evaluate the movement patterns, trace element concentrations (i.e., potential contaminants), and trophic linkages between three recreationally exploited sportfish species (black drum, red drum, and spotted seatrout) and their prey items in Matagorda Bay to determine whether movements throughout the bay system identified via acoustic tracking expose these sportfish to varying concentrations of trace elements. The **specific objectives** of the study were to:

1) Characterize the movement patterns of spotted seatrout, red drum, and black drum in the Matagorda Bay system using acoustic telemetry.
2) Measure and compare the concentration of essential and nonessential trace elements in red drum, black drum, and spotted seatrout and their prey at each location to determine whether individual elements are biomagnifying, biodiluting, or do not significantly change in concentration at this trophic step.
3) Determine the stable isotope ratios (δ13C, δ34S, and δ15N) in sportfish muscle tissue and representative prey to elucidate the diet, foraging habitat, and trophic position, respectively, of each sportfish species and determine which prey poses the greatest risk of exposure to each trace element for each sportfish species within different areas of the bay system.

Introduction:

Recreational fishing represents a multibillion-dollar industry with over one million saltwater anglers in Texas. Spotted seatrout (*Cynoscion nebulosus*), red drum (*Sciaenops ocellatus*), frequently referred to as redfish, and black drum (*Pogonias cromis*) are the most commonly caught and consumed estuarine sportfish. Because of the large numbers of fish consumed by the local population, concerns about contaminant levels found in these fish naturally arise (Islam and

Tanaka 2004, Stunz and Robillard 2011, Hernout et al. 2020). Fish are primarily exposed to contaminants through their diet (Dutton and Fisher 2010, 2014).

The Alcoa Point Comfort Operations (PCO) Plant opened as an aluminum smelter in 1948 and began refining bauxite in 1958. Between 1966 and 1979, a chlor-alkali production plant was operational on the site. Mercury (Hg) wastewater from the chlor-alkali production plant contaminated the water, sediment, and biota in the bay next to the facility. This area of Lavaca Bay has been closed to the retention of finfishes and blue crab since 1988. In 1994, the area was added to the National Priorities List as a Superfund Site and long-term environmental monitoring is ongoing. As part of the biomonitoring effort, the concentration of Hg in red drum and juvenile blue crab is measured on an annual basis. While Hg concentrations in juvenile blue crab in the Superfund site are now comparable to other areas of Lavaca Bay, Hg concentrations in red drum are still elevated (U.S. EPA 2021). For fishes, biomonitoring only focuses on red drum, and other commercially and/or recreationally important fishes (e.g., black drum and spotted seatrout) which have different life spans and diets have been overlooked. Since Hg bioaccumulates in fishes and biomagnifies in estuarine food webs, it is critical to investigate Hg concentration in a variety of species.

Elevated Hg concentrations in red drum indicate that environmental Hg concentrations (i.e., sediment) are still high in some areas of the Superfund site and Hg is trophically transferred up the food web to top predators. It is therefore important to investigate the Hg concentrations in red drum, black drum, and spotted seatrout and their commonly consumed prey items to elucidate how Hg is transferred to these three focal species. To do this, stable isotopes [carbon (C), nitrogen (N), sulfur (S)] can be used to understand feeding ecology. Specifically, $\delta^{13}C$ reflects whether the investigated species feeds in the water column (pelagic) or bay floor (benthic) environment, $\delta^{15}N$ provides insights into the investigated species trophic position, and $\delta^{34}S$ can reflect foraging habitat in relation to salinity gradients (Fry and Chumchal 2011, Marley et al. 2019, Millie et al. 2021). Combined, stable isotope analysis helps elucidate potential sources of variation in Hg accumulation among species.

To date, toxicology research in the Alcoa Superfund site has focused on Hg, due to Hg discharges into the bay next to the facility in the 1960s and 70s that contaminated the sediment and food web. However, bauxite was refined at the facility between 1958 and 2016, and bauxite residue entered the bay, either through wind-blown dust or runoff from land. Bauxite is a naturally occurring, reddish-brown heterogeneous sedimentary rock that is primarily composed of one or more aluminum (Al) hydroxide minerals including gibbsite [$Al(OH)_3$], boehmite [γ-AIO(OH)], and diaspore [α-AIO(OH)], and the Al clay mineral kaolinite [$Al_2Si_2O_5(OH)_4$] (USGS, 2024). Globally, it is the predominant source of Al which is used in building and construction, transportation, packaging, and other applications. In addition to Al, bauxite also contains many other elements that are toxic to wildlife and humans at elevated concentrations including arsenic (As), beryllium (Be), cadmium (Cd), cesium (Cs), chromium (Cr), gallium (Ga), iron (Fe), lead (Pb), lithium (Li), manganese (Mn), Hg, molybdenum (Mo), nickel (Ni), Se, silver (Ag), thorium (Th), tin (Sn), uranium (U), vanadium (V), and zinc (Zn) (Ismail et al. 2018, Staun et al. 2018, Van Gosen and Choate 2021). Nonessential trace elements (i.e., have no biological function; e.g., As, Cd, Hg, Pb) are toxic at low concentration, whereas essential trace elements (i.e., have a biological function; e.g., Cu, Cr, Mn, Se, Zn) can be toxic at greater concentrations. Depending on the trace element, adverse biological effects in biota can include, but are not limited to, damage to the central nervous system, cardiovascular system, liver, kidney, gills, and olfactory system, altered DNA, reduced reproductive success, and maternal transfer to offspring resulting in delayed growth, development, and physical deformities such as spinal curvature and craniofacial defects (Wood et al. 2012a,b). It is therefore important to measure the concentration of trace elements found in elevated levels in bauxite in fishes and their respective prey in the Superfund and compare those concentrations to conspecifics in other areas of the Matagorda Bay system.

The type of prey sportfish consume (e.g., polychaete worms, crabs, oysters, and forage fishes) can have varying concentrations of contaminants and trace elements due to their habitat (i.e., whether benthic or pelagic) and trophic position. In addition, there can be spatial distribution in contaminant and trace element concentrations in the sediment and water throughout the Matagorda Bay system, resulting in spatial variation in the concentration of these individual pollutants in prey items. These fish are highly mobile; thus, they can be exposed to significantly different concentrations across their range, which can impact tissue-specific trace element concentrations and the risk of developing deleterious health effects. By comparing the concentration of each trace element in sportfish and their prey, we can determine whether each trace element biomagnifies (sportfish have a higher tissue concentration than prey), biodilutes (sportfish have a lower tissue concentration than prey) or does not significantly change in concentration at that trophic step. Furthermore, stable isotopes can be incorporated to help explain that relationship.

Stable isotope ratios (e.g., δ13C, δ15N, and δ34S) provide and integrate information on diet and habitat, acting as biotracers (Layman et al. 2012); thus, stable isotope values of sportfish and their prey provide critical information on how each investigated trace element enter food webs and which prey pose the greatest exposure risk to each trace element, particularly non-essential trace elements, to sportfish. Stable isotopes are frequently used in ecotoxicology to identify contaminated food sources and estimate consumer trophic position. Stable isotope values of a consumer and their potential prey items can be used in dietary mixing models, which provide estimates of the proportional contribution of different food items to an organism's diet (Parnell et al. 2012); therefore, stable isotopes are a wide-spread and reliable method to estimate the contribution of different food items to each sportfish species or which food chain each species may be foraging from. Dietary proportions can then be explicitly related to food item and sportfish trace element concentrations to elucidate each investigated trace element exposure risk to sportfish.

Differences in fish ecology can exasperate or mediate their contaminant exposure. For example, fish that are more migratory may leave the contaminated area reducing their exposure compared to more resident species. However, the bioaccumulation in those mobile species may also increase the risk to human health in areas away from the contamination source (do Amaral Kehrig and Maim 1999). Red drum and spotted seatrout have been reported to demonstrate high residency to small regions within bays (Moulton et al. 2017), which would allow for increased exposure to contaminants. However, seasonally directed movements have been documented for these species occurring primarily in the winter and spring following the passages of cold fronts (Callihan et al. 2014, Dance and Rooker 2015, Moulton et al. 2017). These movements may allow for retention of contaminated fish in areas away from the contamination site or give time for increased levels of contaminates to decrease. Historically, animal movement has rarely been quantitatively incorporated in ecotoxicological studies (Taylor et al. 2017), but the use of acoustic telemetry to monitor the movement of red drum, black drum, and spotted seatrout throughout the Matagorda Bay system provided a unique opportunity to investigate the spatial variation in contaminant and trace element concentrations in prey items and determine which area(s) of the bay expose sportfish to the greatest concentration of non-essential trace elements.

Methods:

Acoustic telemetry was used to characterize movement patterns and habitat connectivity of sportfish in the Matagorda Bay system. Combining movement patterns and habitat connectivity with trace elements and stable isotope sampling provided a method to evaluate the connectivity and spatial variation of trace elements across the entire Matagorda Bay system. To assess the biomagnification of total Hg (THg) within the Superfund site, this study measured the Hg concentration and $\delta^{15}N$ value in 27 species ranging from lower trophic levels to apex predators to calculate the trophic magnification slope (TMS). To elucidate potential differences in THg accumulation among red drum, black drum, and spotted seatrout, this study measured isotopic ratios ($\delta^{13}C$, $\delta^{15}N$, and $\delta^{34}S$) to estimate the isotopic niche and trophic position of each species. Finally, for red drum, black drum, and spotted seatrout, the estimated dietary source contributions were estimated using dietary mixing models using stable isotope signatures in each species and their putative prey items. This study investigated the concentration of essential (Co, Cu, Fe, Mn, Ni, Se, Zn) and nonessential (Ag, Al, As, Cd, Cs, Hg, Pb, Sn, Th, U) trace elements in red drum, black drum, and spotted seatrout and their commonly consumed prey (striped mullet, Atlantic

Figure 1. Map of the acoustic receiver (pink triangles) array in Matagorda Bay system.

croaker, blue crab, white shrimp, eastern oyster) in the Alcoa Superfund site and compared the concentrations to the same species caught in western Lavaca Bay (Port Lavaca), Tres Palacios Bay, and northeastern and southwestern Matagorda Bay.

Movement Patterns

Thirty-five acoustic receivers ("listening stations"; VEMCO/Innovasea, Nova Scotia) were deployed around Matagorda Bay using PCV poles or on structures already present in the area (e.g., pilings). The array was composed of 21 VR2W and 14 VRTX receivers). All receivers were deployed prior to the start of the project (March 2022) or August 2022 (after project start; **Figure 1**).

Sampling was conducted under Texas Parks and Wildlife Department Scientific Permit #SPR-0303-279 and IACUC protocols #2020-04-001, #2021-06-016, #2021-06-017, and #2023-007. Sportfish (red drum, black drum and spotted seatrout) were tagged from four regions within the bay system, including the Superfund site near the Alcoa/Formosa plants. Three regions away from the Superfund site acted as control tagging locations. These included areas near Port O'Connor (POC), Palacios/Lavaca Bay, and the Colorado River Delta (CRD). Fish were implanted with VEMCO/Innovasea acoustic transmitters ("pingers") following Robillard et al. (2015). Briefly, the fish were placed dorsoventrally in a surgical cradle allowing for the head and gills to be submerged in seawater during the surgery. Transmitters were inserted into the peritoneal cavity through a small incision made down the midline posterior to the pelvic fins (**Figure 2**). The incision was then closed with a single suture secured with a surgeon's knot. A uniquely numbered dart tag with PI contact information was externally inserted into the dorsal tissue of the fish in case of recapture by anglers. Individual fish movement tracks were calculated using the tagging date and last day of detection (Appendix I). Days a liberty were calculated as last day of detection minus tagging date. Distance traveled was calculated as largest straight distance between receivers that individual fish was detected on. Residency was determined using the R package "igraph".

Figure 2. Acoustic transmitter being implanted into the peritoneal cavity of a red drum.

Mercury analysis

Specimens (**Table 1**) were collected from the Alcoa Superfund site (**Figure 3**) between Dredge Island and the Alcoa facility and entrance to Calhoun Port Authority using gillnets, rod-and-reel, gigging, trawl nets, hand nets/dip nets, epibenthic sled, and hand collection. All species were collected between August 2022 and July 2023. Specimens were stored on ice and transported to Texas State University and stored at -20°C until processing.

After thawing, the body length of each specimen was recorded, and a tissue sample placed into a 50 ml trace metal clean tube, freeze dried (FreeZone$^{2.5}$; Labconco, Kansas City, MO), and homogenized into a powder or cut into 5 mm pieces (marsh grass only). Depending on the species, the shell length (hooked mussel), shell height (eastern oyster), total length (teleost and elasmobranch fishes, shrimp), carapace width (crabs), or wingspan (cownose ray) was recorded. For teleost and elasmobranch fishes, a muscle axial sample was dissected, claw and leg tissue was dissected for blue crab, all soft tissue was processed for white shrimp and mollusks, whereas grass shrimp, fiddler crabs, and mud crabs were processed whole, and marsh grass was separated into stem and blade.

Table 1. Species investigated in this study and their sample size (n). [a] n = 3 for blade and 4 for stem.

	Species	Scientific name	n
Marsh grass	Smooth cordgrass	*Spartina alterniflora*	3/4[a]
Mollusks	Eastern oyster	*Crassostrea virginica*	10
	Hooked mussel	*Ischadium recurvum*	9
Crustaceans	Grass shrimp	*Palaemonetes pugio*	6
	White shrimp	*Litopenaeus setiferus*	10
	Fiddler crab	*Uca longisignalis*	8
	Mud crab	*Panopeus obesus*	4
	Blue crab	*Callinectes sapidus*	10
Teleost fishes	Atlantic croaker	*Micropogonias undulatus*	10
	Spot	*Leiostomus xanthurus*	3
	Sand seatrout	*Cynoscion arenarius*	10
	Gizzard shad	*Dorosoma cepedianum*	5
	Gulf menhaden	*Brevoortia patronus*	10
	Pinfish	*Lagodon rhomboides*	4
	Ladyfish	*Elops saurus*	3
	Striped mullet	*Mugil cephalus*	10
	Hardhead catfish	*Ariopsis felis*	10
	Gafftopsail catfish	*Bagre marinus*	6
	Sheepshead	*Archosargus probatocephalus*	8
	Southern flounder	*Paralichthys lethostigma*	10
	Spotted seatrout	*Cynoscion nebulosus*	27
	Black drum	*Pogonias cromis*	30
	Red drum	*Sciaenops ocellatus*	30
Elasmobranch fishes	Cownose ray	*Rhinoptera bonasus*	5
	Bonnethead shark	*Sphyrna tiburo*	3
	Scalloped hammerhead shark	*Sphyrna lewini*	9
	Bull shark	*Carcharhinus leucas*	9

Depending on the species, the concentration of Hg was determined in 15 to 35 mg of dried sample using a Direct Mercury Analyzer (DMA-80; Milestone Inc., Shelton, CT). Quality control included blanks, certified reference materials (DORM-4 and DORM-5 fish protein; National Research Council Canada), and duplicate samples. Following lipid and urea extraction, samples were packaged and sent to the Stable Isotope Ratio Facility for Environmental Research (SIRFER) at the University of Utah (Salt Lake City, UT) for C, N, and S stable isotope analysis. Quality control included reference materials (bovine muscle, UU-CN-1, UU-CN-2) and duplicate samples.

The R package "nicheROVER" was to determine the niche region and niche overlap among red drum, black drum, and spotted seatrout, whereas the R package "trps" was used to estimate their trophic position, and the R package "MixSIAR" was used to estimate the dietary contributions of each species.

Figure 3. Map of the Alcoa (Point Comfort) Superfund site in Lavaca Bay. The red line shows the boundary of the Superfund site in Lavaca Bay. The light blue area shows the region of the Alcoa Superfund site where species were collected. DI = Dredge Island.

Trace element analysis

All fishes and shellfishes were collected from the Alcoa Superfund site using the methods described under "*Mercury analysis*". Red drum, black drum, and spotted seatrout were caught using rod-and-reel in Port Lavaca and at cleaning stations or fishing tournaments in Palacios, Port O'Connor, and Matagorda. It was confirmed that fish sampled in Palacios were caught in Tres Palacios Bay, fish sampled in Matagorda were caught in the northeastern region of Matagorda Bay, and fish sampled in Port O'Connor were caught in the southwestern region of Matagorda Bay. Hardhead catfish were caught using rod-and-reel in all locations. Atlantic croaker, striped mullet, white shrimp, blue crab, and eastern oyster were purchased from bait shops or seafood stores in the respective towns. At time of purchase, it was confirmed the species was caught or collected nearby. Concentration of the other trace elements were determined in each sample was determined by digesting ~0.25 g of dried sample in 5 ml of nitric acid (HNO_3) in a high temperature, high pressure microwave (Ethos-UP; Milestone, Shelton, CT) and diluting with 25 ml of Milli-Q water (MilliporeSigma, Burlington, MA) for a final volume of ~30 ml. The samples were then shipped to the Trace Element Analysis Core Lab at Dartmouth College (Hanover, NH) for ICP-MS analysis (Agilent 8900; Agilent Technologies, Santa Clara, CA). Quality control included blanks, certified reference materials (DORM-4, DORM-5), spiked samples, and duplicate samples. One set of quality control was included with every 20 samples analyzed. At each location, the maximum sample size was 30 for red drum, black drum, and spotted seatrout, and 10 for Atlantic croaker, striped mullet, white shrimp, blue crab, and eastern oyster.

Note: A sister study was conducted in conjunction with this project and measured the Hg and Se concentrations and calculated the Se:Hg molar ratios in 27 species (marsh grass, two mollusk species, five crustacean species, 15 teleost species, and four elasmobranch species) collected from the Alcoa Superfund site. The relationship between mean Se:Hg molar ratio and mean Hg concentration for each species was examined and for each species, the percentage of individuals that had a Se:Hg molar ratio < 1:1, between 1:1 and 5:1, and > 5:1 was calculated. Results can be found in Appendix II.

The chosen trace elements were investigated because they are readily added to the environment through urban and agricultural runoff, industrial activities, coal-fired power plants, atmospheric deposition, and boating activities/marinas. The concentration of trace elements (excluding Hg) in all biota and sediment samples were measured using microwave assisted acid digestion and Inductively Coupled Mass Spectrometry (ICP-MS) analysis. In summary, 0.25 g of sample were digested in 5 ml of nitric acid in a microwave digestion system (Ethos-UP; Milestone Inc., Shelton, CT) in Co-PI Dutton's lab, diluted with 20 ml of Milli-Q water and sent to the Trace Element Analysis Core Lab at Dartmouth College (Hanover, NH) for ICP-MS analysis (Agilent 8900; Agilent Technologies, Santa Clara, CA) following EPA Method 6020A (U.S. EPA, 1998). Quality assurance/quality control (QA/QC) included blanks, digested and analytical duplicate samples, spiked samples, and certified reference materials [DORM-4 (fish protein), DOLT-5 (dogfish liver), and TORT-3; from the National Research Council Canada (NRCC); ERM-CE464 (tuna) from European Reference Materials; and NIST 1566b (oyster tissue) from the National Institute of Standards and Technology]. One set of QA/QC was included with every 20 samples analyzed. All sediment samples were digested and analyzed at Dartmouth College.

Table 2. Species investigated in this study with the corresponding sample size (n) and body length (mean ± standard deviation; minimum – maximum in parentheses). [a] n = 5 for stem and 6 for blade. * shell height; ** shell length, *** total length; **** carapace width; ***** wingspan. ND = not determined.

	Species	Scientific name	n	Body length (cm)
Marsh grass	Smooth cordgrass	*Spartina alterniflora*	5/6[a]	ND
Mollusks	Eastern oyster	*Crassostrea virginica*	12	7.6 ± 1.5 (5.5 - 10.2) *
	Hooked mussel	*Ischadium recurvum*	9	3.5 ± 0.4 (2.9 - 4.0) **
Crustaceans	Grass shrimp	*Palaemonetes pugio*	6	3.0 ± ND (2.5 - 3.5) ***
	White shrimp	*Litopenaeus setiferus*	10	12.8 ± 1.3 (11.2 - 15.0) ***
	Fiddler crab	*Uca longisignalis*	8	1.4 ± 0.2 (1.2 - 1.8) ****
	Mud crab	*Panopeus obesus*	5	1.3 ± 0.4 (0.8 - 1.7) ****
	Blue crab	*Callinectes sapidus*	10	12.5 ± 2.7 (7.5 - 15.6) ****
Teleost fishes	Atlantic croaker	*Micropogonias undulatus*	10	16.0 ± 5.9 (9.5 - 24.2) ***
	Spot	*Leiostomus xanthurus*	3	17.0 ± 2.0 (15.7 - 19.3) ***
	Sand seatrout	*Cynoscion arenarius*	10	15.5 ± 3.5 (12.0 - 23.0) ***
	Gizzard shad	*Dorosoma cepedianum*	5	26.0 ± 1.3 (24.8 - 27.5) ***
	Gulf menhaden	*Brevoortia patronus*	10	15.7 ± 1.1 (14.0 - 17.2) ***
	Pinfish	*Lagodon rhomboides*	5	15.8 ± 2.4 (12.2 - 18.1) ***
	Ladyfish	*Elops saurus*	3	35.9 ± 13.7 (24.4 - 51.0) ***
	Striped mullet	*Mugil cephalus*	10	15.5 ± 6.5 (9.2 - 24.0) ***
	Hardhead catfish	*Ariopsis felis*	10	26.1 ± 4.9 (19.8 - 35.5) ***
	Gafftopsail catfish	*Bagre marinus*	7	33.4 ± 11.3 (19.5 - 50.0) ***
	Sheepshead	*Archosargus probatocephalus*	8	33.3 ± 4.0 (29.0 - 40.3) ***
	Southern flounder	*Paralichthys lethostigma*	10	39.9 ± 4.0 (35.5 - 47.3) ***
	Spotted seatrout	*Cynoscion nebulosus*	27	40.9 ± 9.2 (26.7 - 57.5) ***
	Black drum	*Pogonias cromis*	30	52.1 ± 28.9 (21.1 - 108.4) ***
	Red drum	*Sciaenops ocellatus*	30	45.6 ± 14.2 (27.6 - 103.0) ***
Elasmobranch	Cownose ray	*Rhinoptera bonasus*	5	52.7 ± 8.7 (46.0 - 63.4) *****
	Bonnethead shark	*Sphyrna tiburo*	3	60.6 ± 7.2 (52.4 - 65.7) ***
	Scalloped hammerhead shark	*Sphyrna lewini*	9	64.9 ± 8.4 (50.5 - 80.5) ***
	Bull shark	*Carcharhinus leucas*	9	110.1 ± 12.5 (88.9 - 123.9) ***

Results and Discussion:

Fish movement

A total of 89 sportfish were tagged in the Matagorda Bay system, comprising of 26 black drum, 30 red drum, and 33 spotted seatrout (**Table 3**). Tagged red drum ranged from 361 – 1,118 mm TL (mean ± SD = 543 ± 176 mm TL) while black drum ranged from 285 – 810 mm TL (363 ± 107 mm). Spotted seatrout ranged from 305 – 451 mm TL (370 ± 32.7 mm). Most of the tagging effort was concentrated in the Superfund site, resulting in 48 fish being tagged (53.9%). Five of each species were tagged in each of the other three regions (n = 15 fish/region), except for POC where only one black drum was tagged (n = 11 fish).

Of the 89 tagged fish, 33 fish were never detected on receivers (37.1%). From the 56 fish (63.9%) that were detected, 30,653 detections were recorded. Of those, 16,023 detections were from red drum (52.3%), 12,868 detections were from black drum (42.0%), and 1,762 detections were from spotted seatrout (5.7%). Red drum and black drum were detected longer in the array than spotted seatrout. Red drum were detected from 3 – 690 days at liberty (DAL; 163 ± 230 DAL), with 7 fish detected over a year while black drum were detected from 4 – 746 DAL (170 ± 244 DAL), with 6 fish detected over a year within the array. Spotted seatrout were tracked from 2 -309 DAL (34 ± 71 DAL) with no fish detected over a year. Detections within each tagging region differed. The Superfund site had the highest reported detections with 23,180 detections, with Palacios having 6,147 detections, the CRD having 1,108 detections and POC having 218 detections. The increased detections in the Superfund site may be an artifact of the increased tagging effort in the this region compared to other regions.

Movement patterns generally varied by species with some individuals making large movements across the bay system (**Appendix 1**). Black drum showed high residency to tagging locations with 65% (n = 13 fish) classified as resident and 35% (n = 7 fish) classified as transient. Overall, black drum had a mean displacement distance of 11.2 km. However, BD3 was tagged and tracked in the Superfund site but it was detected on receivers in the jetties before ceasing reporting, suggesting a potential offshore migration. Conversely, red drum were more transient with 70.6% (n = 12 fish) classified as transient and 29.4% (n = 5 fish) classified as resident. Mean displacement distance was 31.6 km. Most red drum tagged in the Superfund site were detected within the site or on receivers within Lavaca Bay, suggesting minimal movement of these fish across the bay. For example, RD6 left the Superfund site but remained more resident in Lavaca Bay. However, RD11 had the largest movement from the Superfund site, transiting east to the CRD. RD14 moved from the Superfund site to the jetties with the last detection at the receiver there, suggesting a potential offshore migration. For red drum tagged outside the Superfund site, fish remained relatively resident to their tagging bays, except for two. RD17 made large movements between the CRD and the jetties while RD27 made a directed movement to the jetties before ceasing reporting suggesting a potential offshore migration. Spotted seatrout showed a mix of resident and transient behaviors with 47.4% (n = 9 fish) were classified as resident and 52.6% (n = 10 fish) were classified as transient. Mean displacement distance for spotted seatrout was 9.11 km. Spotted seatrout largely remained in their tagging areas for the duration of the study and demonstrated no cross-bay system movements. Overall, relatively few fish from closed area moved to other areas of the bay and Hg concentrations (see results below) declined as distance from closed area increased. This means there are lower health/consumption risks for fish further from closed area.

Only two fish were recaptured during the study. Both were spotted seatrout and released after recapture. SS28 was recaptured near its tagging location in the CRD 11 days after tagging. However, this fish was never detected on any receivers. The second spotted seatrout recapture was recaptured near an RV park by the bride up the Colorado River. The angler failed to record the tag number so no additional information can be determined (e.g., DAL, distance traveled, etc.).

Table 3. Fish tagged as part of the movement student. Grayed out lines indicated fish that did not report after release.

Date	Species	Fish	Site Location	Lat	Long	TL (mm)	Days At Liberty	Number of Detections
10/6/22	Black Drum	BD1	Impact	28.6567	-96.57172	405	416	38
7/12/23	Black Drum	BD10	Impact	28.6602	-96.5689	515	155	541
7/12/23	Black Drum	BD11	Impact	28.6602	-96.5689	320	746	1303
7/12/23	Black Drum	BD12	Impact	28.6602	-96.5689	345	308	625
7/12/23	Black Drum	BD13	Impact	28.6602	-96.5689	372	39	31
7/12/23	Black Drum	BD14	Impact	28.6516	-96.5668	368	0	1
7/12/23	Black Drum	BD15	Impact	28.6516	-96.5668	315	642	8661
8/10/23	Black Drum	BD16	POC	28.434	-96.337	810	0	1
11/9/23	Black Drum	BD17	Palacios	28.6098	-96.2492	326	0	1
11/9/23	Black Drum	BD18	Palacios	28.611	-96.168	345	0	0
11/9/23	Black Drum	BD19	Palacios	28.6112	-96.1696	348	0	0
7/12/23	Black Drum	BD2	Impact	28.6579	-96.5684	307	5	137
11/9/23	Black Drum	BD20	Palacios	28.6112	-96.1696	405	0	0
11/9/23	Black Drum	BD21	Palacios	28.6112	-96.1696	330	4	70
12/5/23	Black Drum	BD22	Delta	28.63145	-96.00315	440	595	148
12/5/23	Black Drum	BD23	Delta	28.631867	-95.99515	330	0	3
12/5/23	Black Drum	BD24	Delta	28.631867	-95.99515	295	62	30
12/5/23	Black Drum	BD25	Delta	28.63035	-95.994483	320	0	0
12/5/23	Black Drum	BD26	Delta	28.623667	-95.99485	435	572	510
7/12/23	Black Drum	BD3	Impact	28.6579	-96.5684	285	454	189
7/12/23	Black Drum	BD4	Impact	28.6579	-96.5684	308	111	122
7/12/23	Black Drum	BD5	Impact	28.6579	-96.5684	290	20	24
7/12/23	Black Drum	BD6	Impact	28.6579	-96.5684	295	31	245
7/12/23	Black Drum	BD7	Impact	28.6579	-96.5684	300	0	0
7/12/23	Black Drum	BD8	Impact	28.6579	-96.5684	294	262	188

7/12/23	Black Drum	BD9	Impact	28.6579	-96.5684	345	0	0
10/6/22	Red Drum	RD1	Impact	28.6567	-96.57172	500	208	20
8/5/22	Red Drum	RD10	Impact	28.65353	-96.56792	458	125	6
8/5/22	Red Drum	RD11	Impact	28.6534	-96.5676	432	14	72
8/4/22	Red Drum	RD12	Impact	28.6538	-96.56796	560	0	0
8/4/22	Red Drum	RD13	Impact	28.65347	-96.56796	453	0	0
8/4/22	Red Drum	RD14	Impact	28.65339	-96.5679	437	449	500
8/4/22	Red Drum	RD15	Impact	28.65416	-96.56787	540	0	0
8/10/23	Red Drum	RD16	POC	28.434	-96.337	1016	422	1707
8/10/23	Red Drum	RD17	POC	28.434	-96.337	1118	625	752
8/10/23	Red Drum	RD18	POC	28.434	-96.337	890	421	3687
8/10/23	Red Drum	RD19	POC	28.434	-96.337	690	0	0
10/6/22	Red Drum	RD2	Impact	28.6567	-96.57172	540	0	0
8/10/23	Red Drum	RD20	POC	28.42509	-96.40919	470	0	0
11/9/23	Red Drum	RD21	Palacios	28.6075	-96.1769	380	0	0
11/9/23	Red Drum	RD22	Palacios	28.61125	-96.2087	494	0	0
11/9/23	Red Drum	RD23	Palacios	28.61125	-96.2087	361	0	0
11/9/23	Red Drum	RD24	Palacios	28.614	-96.168	555	0	0
11/9/23	Red Drum	RD25	Palacios	28.614	-96.168	456	0	0
12/5/23	Red Drum	RD26	Delta	28.636467	-95.9996	560	0	0
12/5/23	Red Drum	RD27	Delta	28.636467	-95.9996	555	496	85
12/5/23	Red Drum	RD28	Delta	28.631867	-95.99515	430	614	33
12/5/23	Red Drum	RD29	Delta	28.631867	-95.99515	395	0	0
10/6/22	Red Drum	RD3	Impact	28.6567	-96.57172	541	690	166
12/5/23	Red Drum	RD30	Delta	28.631867	-95.99515	389	3	23
10/6/22	Red Drum	RD4	Impact	28.6563	-96.57135	505	317	39
10/6/22	Red Drum	RD5	Impact	28.6563	-96.57135	560	32	265
8/5/22	Red Drum	RD6	Impact	28.6317	-96.563024	445	76	250
8/5/22	Red Drum	RD7	Impact	28.63621	-96.56306	462	33	291

8/5/22	Red Drum	RD8	Impact	28.63669	-96.56287	620	349	8072
8/5/22	Red Drum	RD9	Impact	28.65353	-96.56792	464	16	55
10/7/22	Spotted Seatrout	SS1	Impact	28.65421	-96.56823	390	0	0
8/10/23	Spotted Seatrout	SS10	POC	28.420317	-96.399517	370	0	0
8/10/23	Spotted Seatrout	SS11	POC	28.420317	-96.399517	355	0	0
8/10/23	Spotted Seatrout	SS12	POC	28.410467	-96.3988	340	0	0
8/10/23	Spotted Seatrout	SS13	POC	28.410467	-96.3988	386	0	0
8/10/23	Spotted Seatrout	SS14	POC	28.42509	-96.40919	405	0	0
8/18/23	Spotted Seatrout	SS15	Impact	28.659	-96.5707	375	34	24
8/18/23	Spotted Seatrout	SS16	Impact	28.659	-96.5707	373	229	150
8/18/23	Spotted Seatrout	SS17	Impact	28.659	-96.5707	339	2	6
8/18/23	Spotted Seatrout	SS18	Impact	28.659	-96.5707	340	0	0
8/18/23	Spotted Seatrout	SS19	Impact	28.659	-96.5707	351	0	0
10/7/22	Spotted Seatrout	SS2	Impact	28.66141	-96.57108	391	0	4
8/18/23	Spotted Seatrout	SS20	Impact	28.659	-96.5707	357	2	2
8/18/23	Spotted Seatrout	SS21	Impact	28.659	-96.5707	390	187	105
8/18/23	Spotted Seatrout	SS22	Impact	28.659	-96.5707	425	0	0
11/9/23	Spotted Seatrout	SS23	Palacios	28.6098	-96.2492	391	309	43
11/9/23	Spotted Seatrout	SS24	Palacios	28.589	-96.189	370	5	23
11/9/23	Spotted Seatrout	SS25	Palacios	28.589	-96.189	390	31	6
11/9/23	Spotted Seatrout	SS26	Palacios	28.589	-96.189	366	34	56
11/9/23	Spotted Seatrout	SS27	Palacios	28.589	-96.189	410	46	19
12/5/23	Spotted Seatrout	SS28	Delta	28.6404	-95.9952	425	0	0
12/5/23	Spotted Seatrout	SS29	Delta	28.6404	-95.9952	344	13	36
10/7/22	Spotted Seatrout	SS3	Impact	28.6365	-96.57171	388	0	0
12/5/23	Spotted Seatrout	SS30	Delta	28.6404	-95.9952	350	12	163
12/5/23	Spotted Seatrout	SS31	Delta	28.6404	-95.9952	360	18	68
12/5/23	Spotted Seatrout	SS32	Delta	28.6404	-95.9952	378	65	9
10/7/22	Spotted Seatrout	SS33	Impact	28.65421	-96.56823	376	0	5

8/5/22	Spotted Seatrout	SS4	Impact	28.65431	-96.51339	309	0	0
10/7/22	Spotted Seatrout	SS5	Impact	28.6543	-96.56803	353	0	0
7/12/23	Spotted Seatrout	SS6	Impact	28.6579	-96.5684	324	49	42
7/12/23	Spotted Seatrout	SS7	Impact	28.6602	-96.5689	451	0	0
7/12/23	Spotted Seatrout	SS8	Impact	28.6602	-96.5689	305	61	374
7/12/23	Spotted Seatrout	SS9	Impact	28.6602	-96.5689	338	11	627

Mercury

A significant positive relationship was found between Log_{10} THg concentration and $\delta^{15}N$ indicating that Hg is biomagnifying within the food web in the Superfund site (**Figure 4**). The calculated TMS of 0.0968 falls within a global meta-analysis range of −0.19 and 0.48 for aquatic food webs (mean ± standard deviation: 0.16 ± 0.11) (Lavoie et al., 2013).

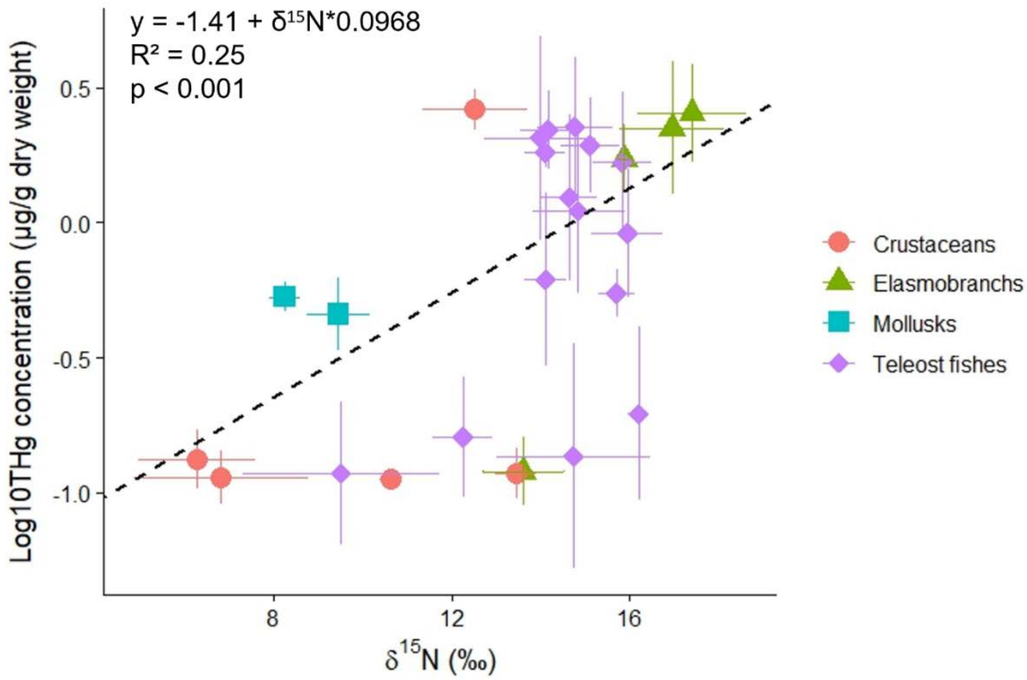

Figure 4. Relationship between Log10 THg concentration (µg/g dry weight) and δ^{15} N. Data is presented as mean ± standard deviation for each species. The linear regression (dashed line) is for all data points. The slope of the line represents the TMS.

Mercury concentrations were greatest in red drum, followed by black drum, and spotted seatrout (**Figure 5**). This difference among species is most likely due to differences in habitat/movement patterns, diet, and age. There was a positive relationship between Hg concentration and total length for each species (**Figure 5**), indicating that Hg is bioaccumulating in each species. Despite higher $\delta^{15}N$, which can indicate higher trophic position, spotted seatrout had lower Hg concentrations compared to red drum and black drum (**Figure 5**). This may indicate that spotted seatrout are incorporating N from a different baseline source and/or spending more time outside of the Superfund site.

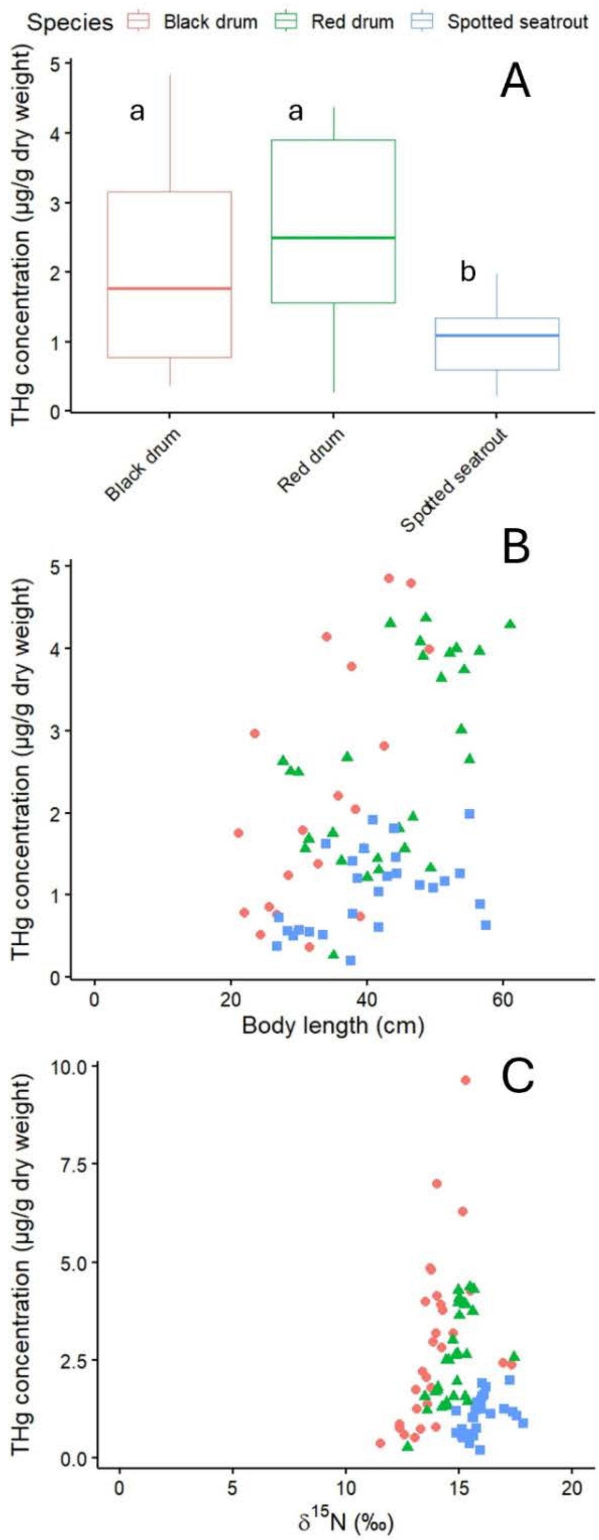

Figure 5. Panel A shows the THg concentrations in red drum, black drum, and spotted seatrout of comparable body lengths. Black drum and red drum > 75 cm were excluded. Panel B shows the relationship between THg concentration and body length, and Panel C shows the relationship between THg concentration and $\delta^{15}N$.

Estimated trophic position was highest for spotted seatrout (median 3.91, credible interval 3.65 – 4.26) followed by red drum (median 3.54, credible interval 3.33 – 3.83), and black drum <50 cm (median 3.14, credible interval 2.97 – 3.36) (**Figure 6**). The trophic positions calculated for the focal species are similar to those previously reported for black drum, red drum, and spotted seatrout in Lavaca Bay (Simons et al., 2015) and Galveston Bay (Livernois et al., 2024).

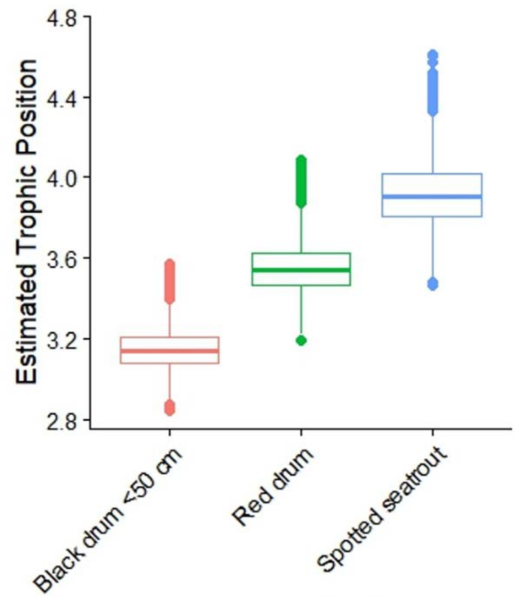

Figure 6. Estimated trophic position of black drum, red drum, and spotted seatrout in the Alcoa Superfund site.

MixSIAR estimated that black drum had the greatest estimated proportion of the diet attributed to mollusks, whereas the greatest estimated dietary contributions for red drum were striped mullet, grass shrimp, and mollusks. The estimated proportions of dietary contributions for spotted seatrout were highly variable (**Figure 7**).

Trace element

All data has been collected and data analysis and interpretation are ongoing. This study resulted in a much larger dataset than expected and as a result, has taken longer to analyze. The resulting manuscript will be provided to the Matagorda Bay Mitigation Trust once published. The results of the data should help determine whether species in the Alcoa Superfund site are accumulating greater concentrations of trace elements found at elevated concentrations in bauxite, and combined with the fish telemetry data, determine how far these fish are moving.

Dissemination of all findings to the public (fieldwork/lab work/publications/conference presentation)

- Social media (Instagram and Facebook) @matbaytoxstudy; @hgtxseafood
- Summary of studies will be made available on a website that is being constructed under MBMT contract #065.

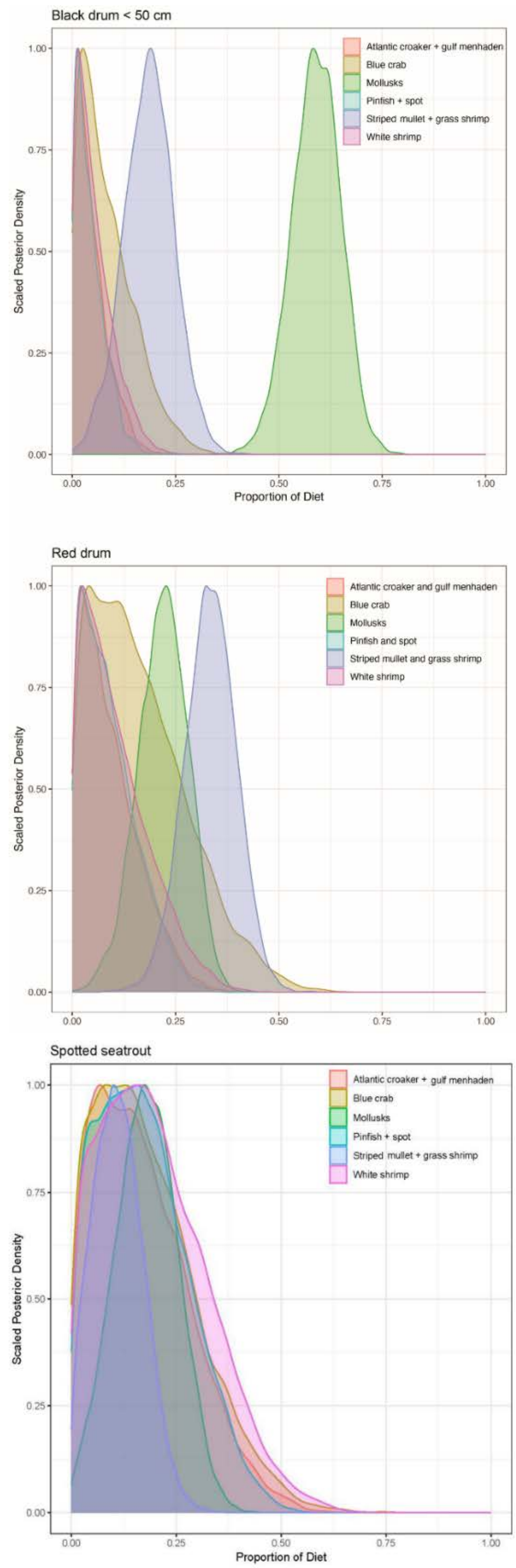

Figure 7. MixSIAR estimated dietary contributions for black drum, red drum, and spotted seatrout.

References

Burger, J., M. Gochfeld, C. Jeitner, M. Donio, and T. Pittfield .2012. Interspecific and intraspecific variation in selenium:mercury molar ratios in saltwater fish from the Aleutians: potential protection on mercury toxicity by selenium. Science of the Total Environment 431:46-56.

Callihan, J.L., Cowan Jr., J.H., and Harbison, M.D. 2014. Sex-specific movement response of an estuarine sciaenid (*Cynoscion nebulosus*) to freshets. Estuaries and Coasts. 38(5):1-13.

Dance, M.A., and Rooker, J.R. 2015. Habitat- and bay-scale connectivity of sympatric fishes in an estuarine nursery. Estuarine, Coastal and Shelf Science. 167: 447-457.

do Amaral Kehrig, H., and Maim, O., 1999. Methylmercury in fish as a tool for understanding the Amazon mercury contamination. Applied Organometallic Chemistry. 13:689-696.

Dutton, J., and Fisher, N.S. 2010. Intraspecific comparisons of metal bioaccumulation in the juvenile Atlantic silverside (*Menidia menidia*). Aquatic Biology. 10:211-226.

Dutton, J., and Fisher, N.S. 2014. Modeling metal bioaccumulation and tissue distribution in killifish (*Fundulus heteroclitus*) in three contaminated estuaries. Environmental Toxicology and Chemistry. 33(1):89-101.

Fry, B., and M.M. Chumchal. 2011. Sulfur stable isotope indicators of residency in estuarine fish. Limnology and Oceanography 56(5):1563-1576.

Hernout, B., Leleux, J., Lynch, J., Ramaswamy, K., Faulkner, P., Matich, P., and Hala, D. 2020. The integration of fatty acid biomarkers of trophic ecology with pollutant body-burdens of PAHs and PCBs in four species of fish from Sabine Lake, Texas. Environmental Advances. 1: https://doi.org/10.1016/j.envadv.2020.100001.

Islam, M.S., and Tanaka, M. 2004. Impacts of pollution on coastal and marine ecosystems including coastal and marine fisheries and approach for management: a review and synthesis. Marine Pollution Bulletin 48:624-649.

Ismail, S.N.S., E.Z. Abidin, and S.M. Praveena. 2018. Heavy metals in soil of a tropical climate bauxite mining area in Malaysia. Journal of Physical Science 29:7-14.

Kaneko, J.J., and N.V.C. Ralston. 2007. Selenium and mercury in pelagic fish in the central north Pacific near Hawaii. Biological Trace Element Research 119:242-254.

Lavoie, R.A., T.D. Jardine, M.M. Chumchal, K.A. Kidd, and L.M. Campbell. 2013. Biomagnification of mercury in aquatic food webs: a worldwide meta-analysis. Environmental Science & Technology, 47(23), 13385-13394.

Layman, C.A., Araujo, MS., Boucek, R., Hammerschlag-Peyer, C.M. Harrison, E. Jud, Z.R., Matich, P., Rosenblatt, A.E., Vaudo, J.J., Yeager, L.A., Post, D.M., and Bearhop, S. 2012. Applying stable isotopes to examine food-web structure: an overview of analytical tools. Biological Reviews. 87:545-562.

Livernois, M.C., R.J. Rezek, and R.D. Wells. 2024. Spatial and ontogenetic trophic dynamics of co-occurring predatory fishes in a Northern Gulf of Mexico Estuary. Estuaries and Coasts 47(4):1119-1138.

Marley, G., A.J. Lawrence, D.A. Phillip, and B. Hayden. 2019. Mangrove and mudflat food webs are segregated across four trophic levels, yet connected by highly mobile top predators. Marine Ecology Progress Series 632:13-25.

Mille, T., A. Bisch, N. Caill-Milly, P. Cresson, J. Deborde, A. Gueux, G. Morandeau, and M. Monperrus. 2021. Distribution of mercury species in different tissues and trophic levels of commonly consumed fish species from the south Bay of Biscay (France). Marine Pollution Bulletin 166:112172.

Moulton, D.L., Dance, M.A., Williams, J.A., Sluis, M.Z., Stunz, G.W., and Rooker, J.R. 2017. Habitat partitioning and seasonal movement of red drum and spotted seatrout. Estuaries and Coasts. 40:905-916.

Parnell, A.C., Phillips, D.L., Bearhop, S., Semmens, B.X., Ward, E.J., Moore, J.W., Jackson, A.L., Grey, J., Kelly, D.J., and Inger, R. 2012. Bayesian stable isotope mixing models. Environmetrics. 24:387-399.

Robillard, M.M.R., Payne, L.M., Vega, R.R., and Stunz, G.W. 2015. Best practices for surgically implanting acoustic transmitters in spotted seatrout. Transactions of the American Fisheries Society. 144:81-88.

Simons, J. D., K. Withers, T. Weatherall, C.C. Council, and M. Porter. 2015. Assessment of mercury in selected game fish food webs in the Texas coastal zone. Texas A&M University – Corpus Christi. TAMU-CC-1501-CCS. 102 p.

Staun, C., J. Vaughan, M.A. Lopez-Anton, M. Rumayor, and M.R. Martínez-Tarazona. 2018. Geochemical speciation of mercury in bauxite. Applied Geochemistry 93:30-35.

Stunz, G.W., and Robillard, M. 2011. Contaminant level of fishes in several coastal bend estuaries: screening investigation. Final Report to Coastal Bend Bays & Estuaries Program. Texas A&M University, Corpus Christi, TX.

Taylor, M.D., Babcock, R.C., Simpfendorfer, C.A., and Crook, D.A. 2017. Where technology meets ecology: acoustic telemetry in contemporary Australian aquatic research and management. Marine and Freshwater Research. 68:1397-1402.

U.S. EPA. 2021. Third five-year review report for Alcoa (Point Comfort)/Lavaca Bay Superfund Site, Calhoun County, Texas. U.S. Environmental Protection Agency – Region 6, Dallas, Texas.

U.S. EPA, 1998. Method 6020A: Inductively Coupled Plasma-Mass Spectrometry. US Environmental Protection Agency, Washington, DC.

USGS. 2024. Bauxite and alumina statistics and information. https://www.usgs.gov/centers/national-minerals-information-center/bauxite-and-alumina-statistics-and-information.

Van Gosen, B.S., and L.M. Choate. 2021. Reconnaissance study of the major and trace element content of bauxite deposits in the Arkansas bauxite region, Saline and Pulaski Counties, Central Arkansas. U.S. Geological Survey Open-File Report 2021-1073. 18 p.

Wood, C.M., Farrell, A.P., and Brauner, C.J. 2012a. Homeostatis and toxicology of non-essential metals. Fish physiology: vol 31B. Academic Press, New York

Wood, C.M., Farrell, A.P., and Brauner, C.J. 2012b. Homeostatis and toxicology of essential metals. Fish physiology: vol 31A. Academic Press, New York

Appendix I: Maps of movement patterns for individual fish

Black Drum

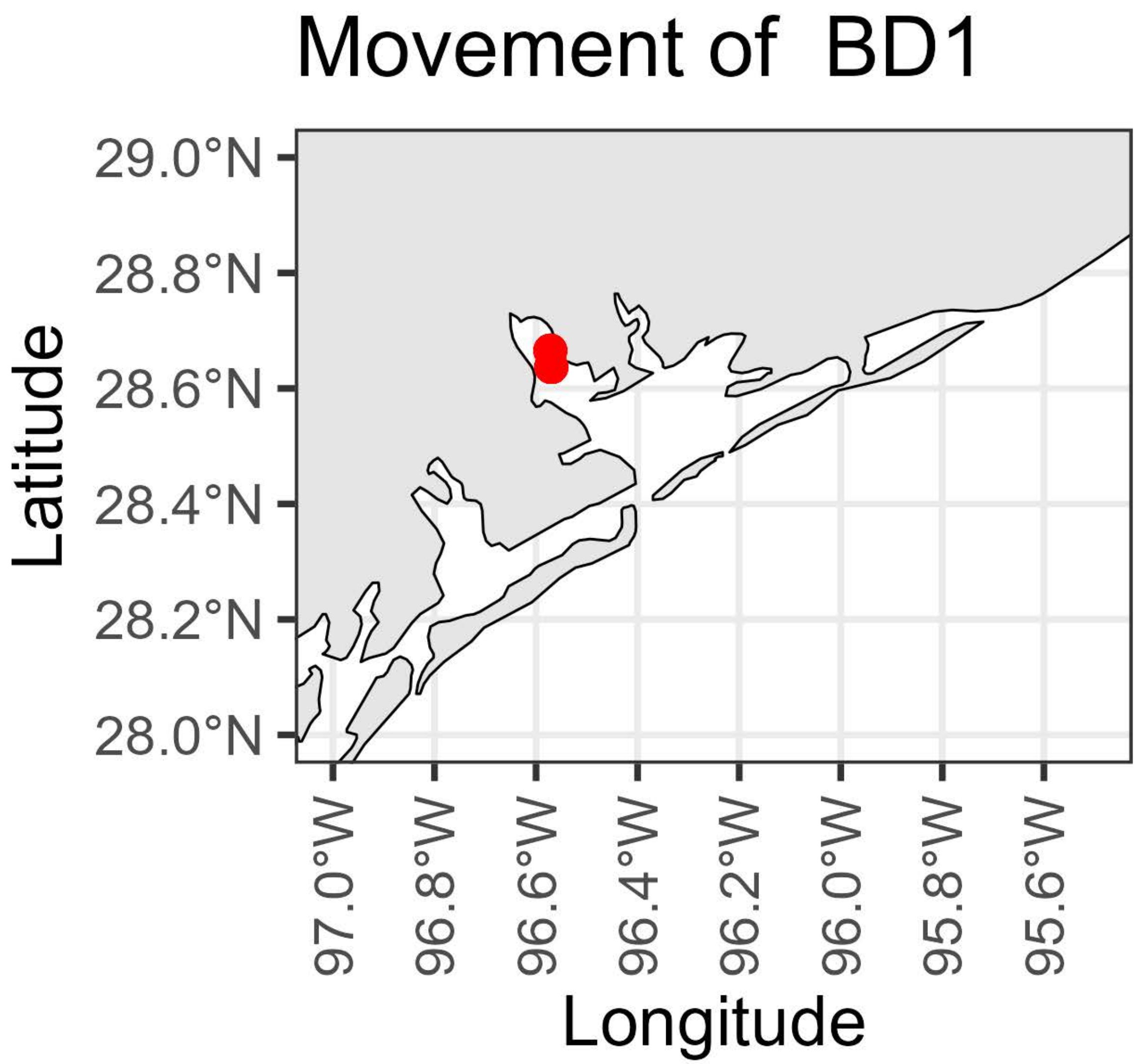

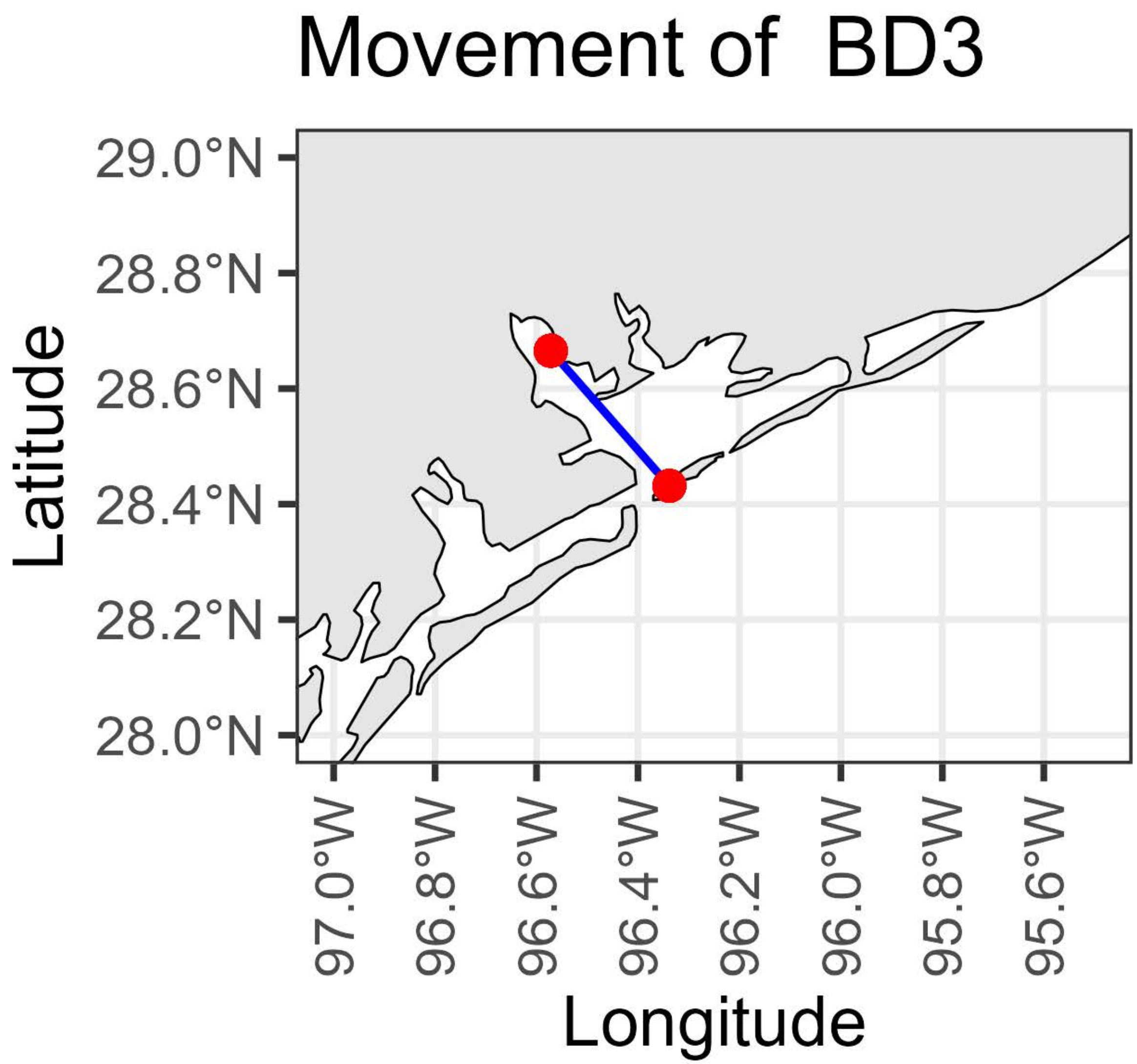
Movement of BD3
29.0°N
28.8°N
28.6°N
28.4°N
28.2°N
28.0°N
Latitude
97.0°W
96.8°W
96.6°W
96.4°W
96.2°W
96.0°W
95.8°W
95.6°W
Longitude

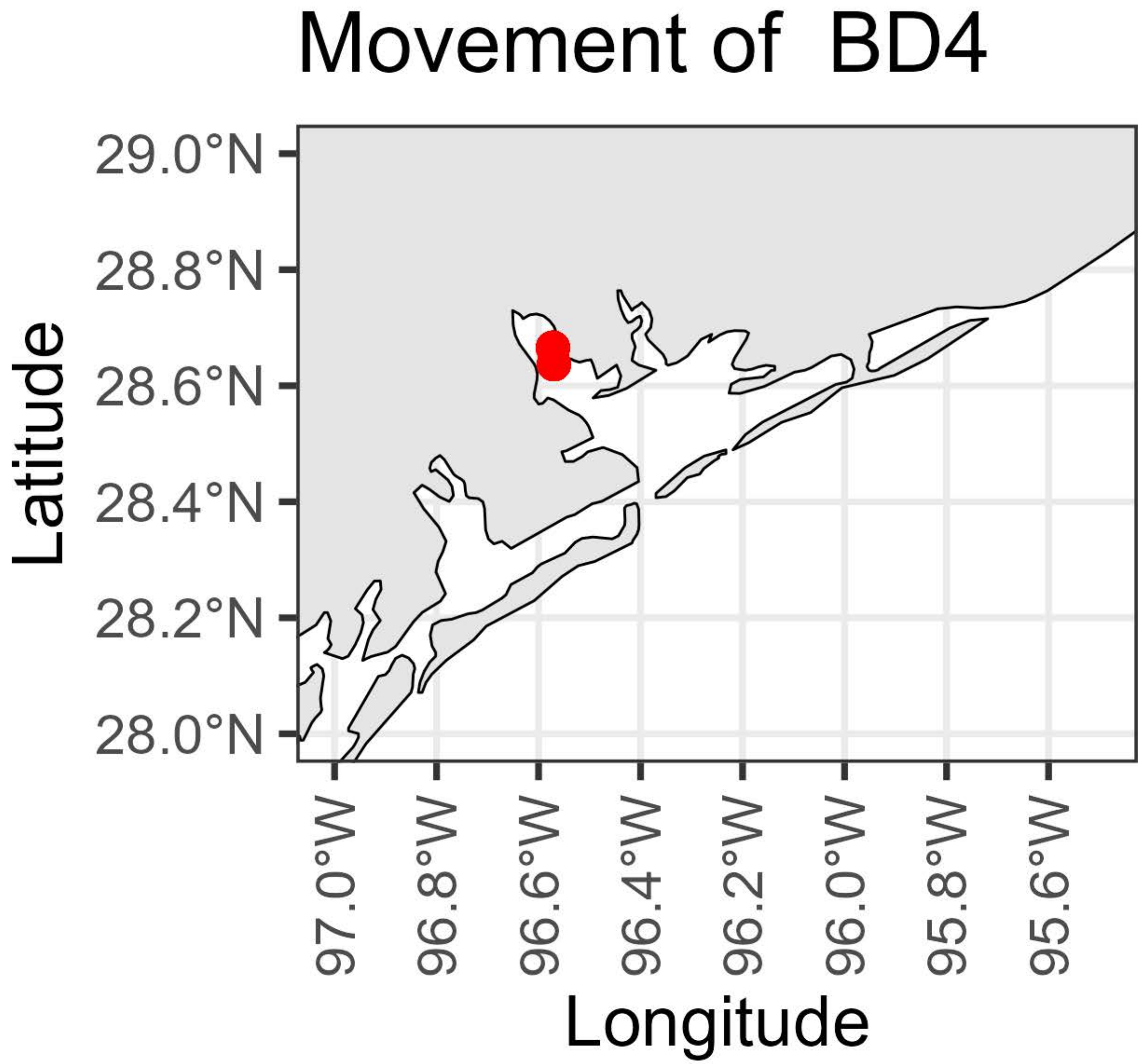
Movement of BD4
29.0°N
28.8°N
28.6°N
28.4°N
28.2°N
28.0°N
Latitude
97.0°W
96.8°W
96.6°W
96.4°W
96.2°W
96.0°W
95.8°W
95.6°W
Longitude

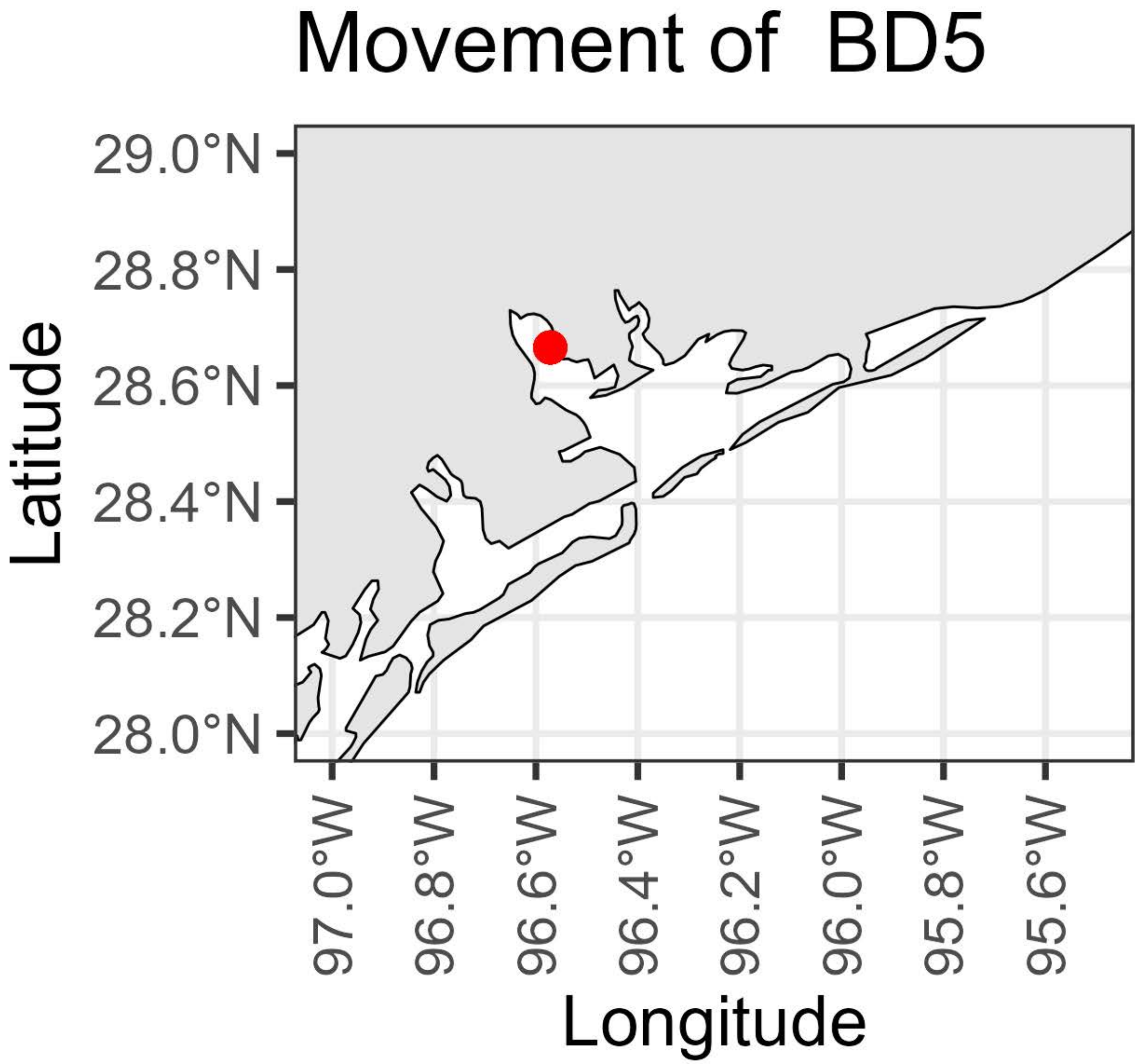
Movement of BD5
29.0°N
28.8°N
28.6°N
28.4°N
28.2°N
28.0°N
Latitude
97.0°W
96.8°W
96.6°W
96.4°W
96.2°W
96.0°W
95.8°W
95.6°W
Longitude

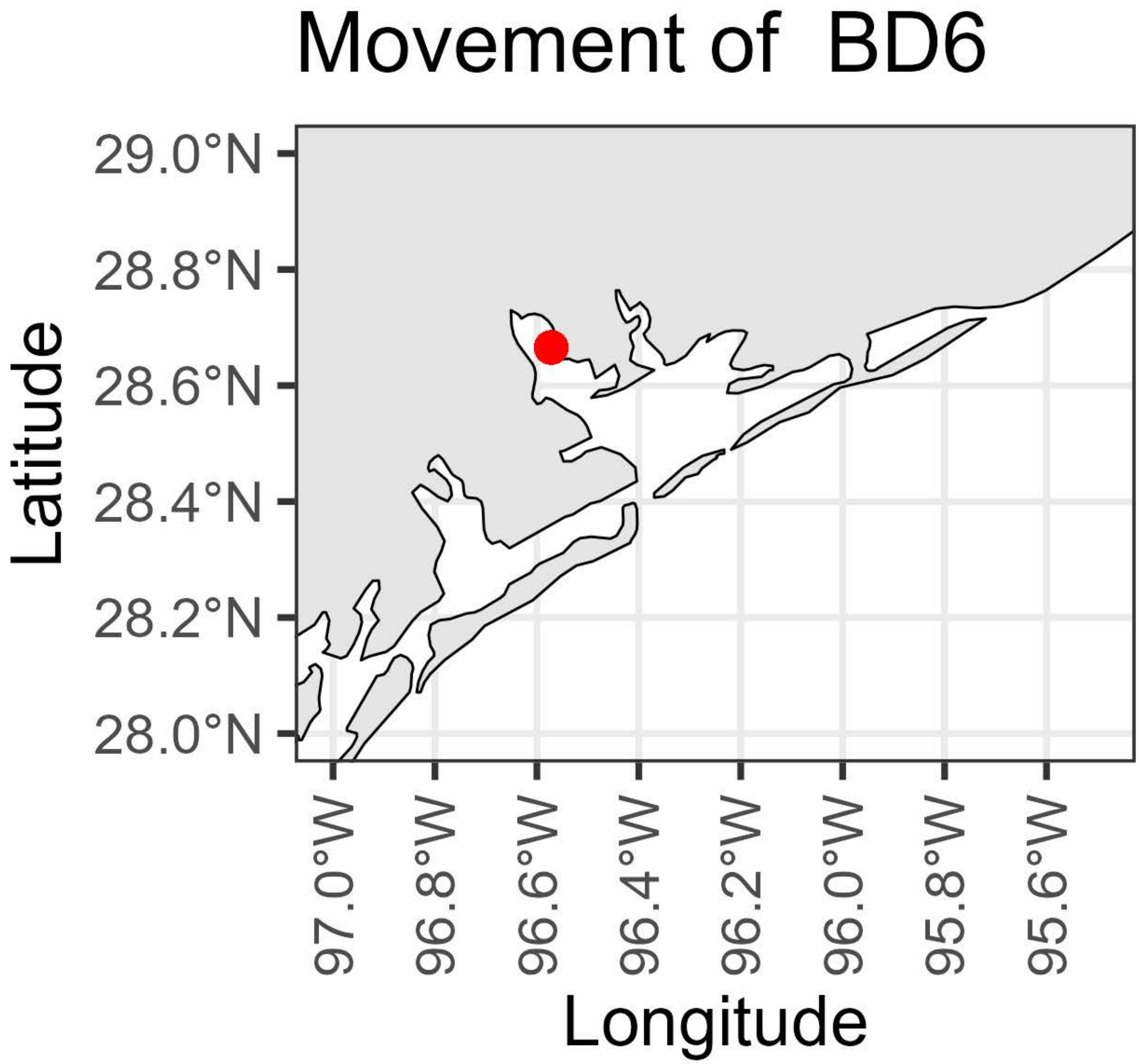
Movement of BD6
Latitude
29.0°N
28.8°N
28.6°N
28.4°N
28.2°N
28.0°N
97.0°W
96.8°W
96.6°W
96.4°W
96.2°W
96.0°W
95.8°W
95.6°W
Longitude

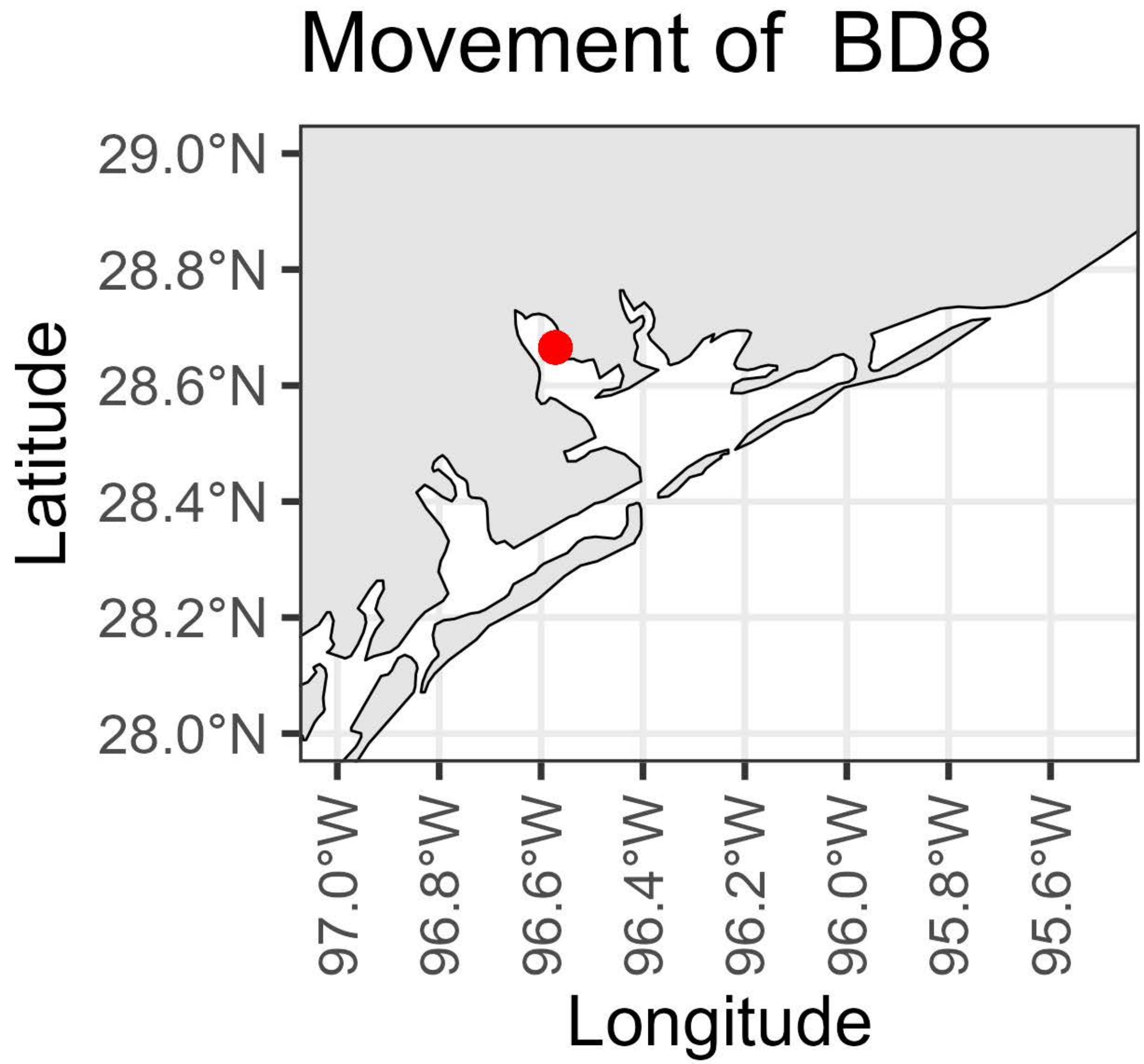
Movement of BD8
29.0°N
28.8°N
28.6°N
28.4°N
28.2°N
28.0°N
Latitude
97.0°W
96.8°W
96.6°W
96.4°W
96.2°W
96.0°W
95.8°W
95.6°W
Longitude

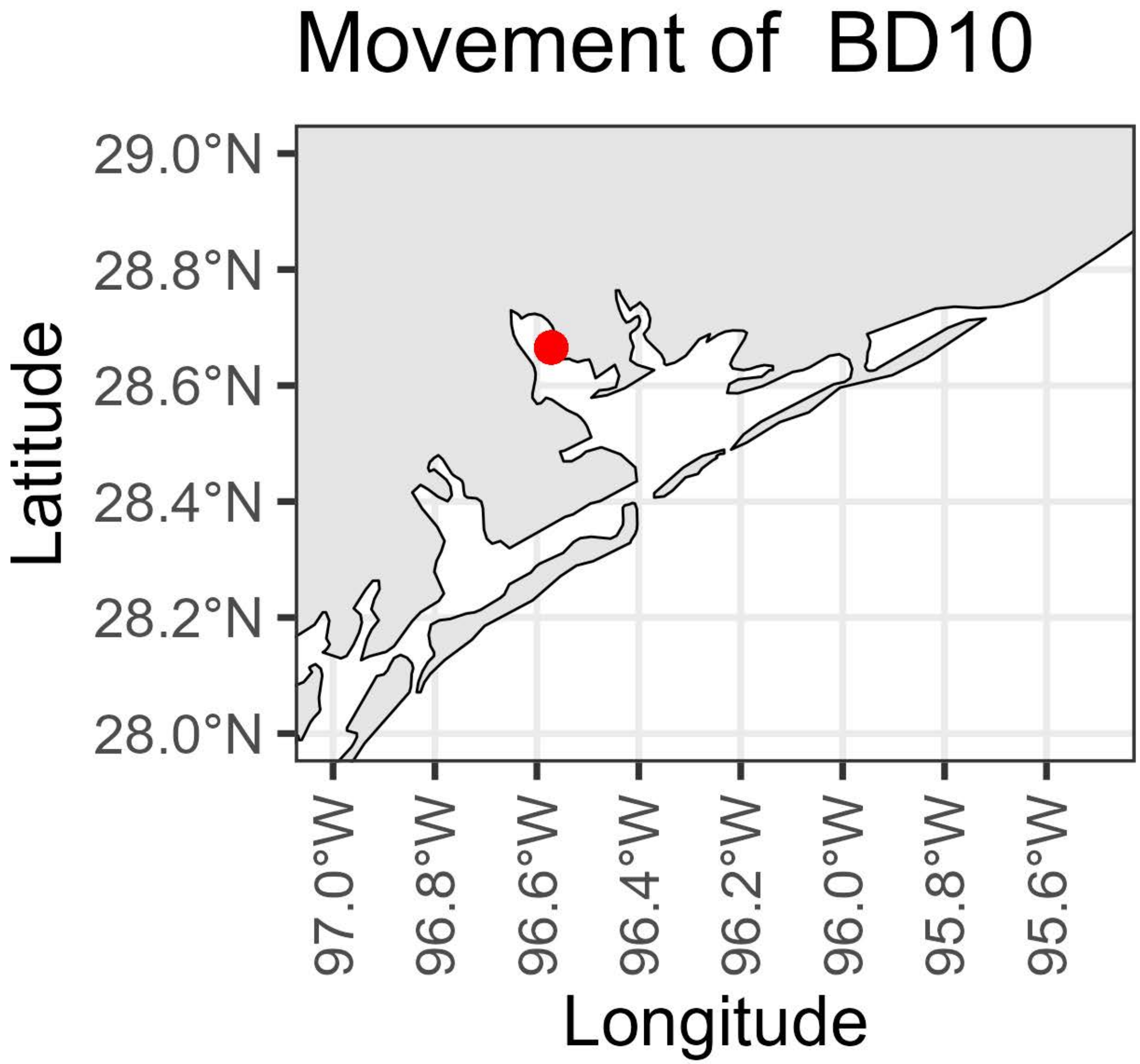
Movement of BD10
29.0°N
28.8°N
28.6°N
28.4°N
28.2°N
28.0°N
Latitude
97.0°W
96.8°W
96.6°W
96.4°W
96.2°W
96.0°W
95.8°W
95.6°W
Longitude

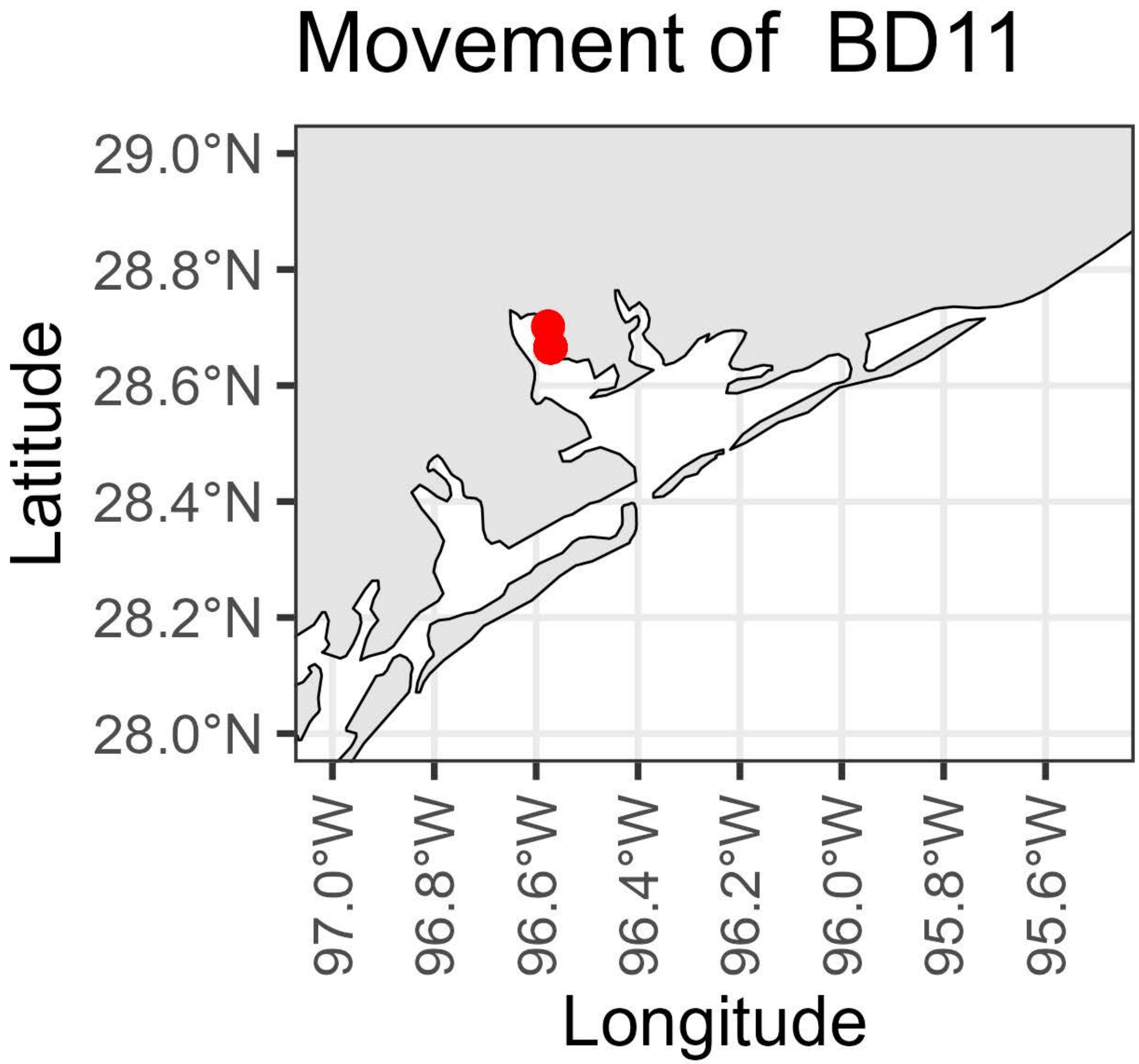
Movement of BD11
29.0°N
28.8°N
28.6°N
28.4°N
28.2°N
28.0°N
Latitude
97.0°W
96.8°W
96.6°W
96.4°W
96.2°W
96.0°W
95.8°W
95.6°W
Longitude

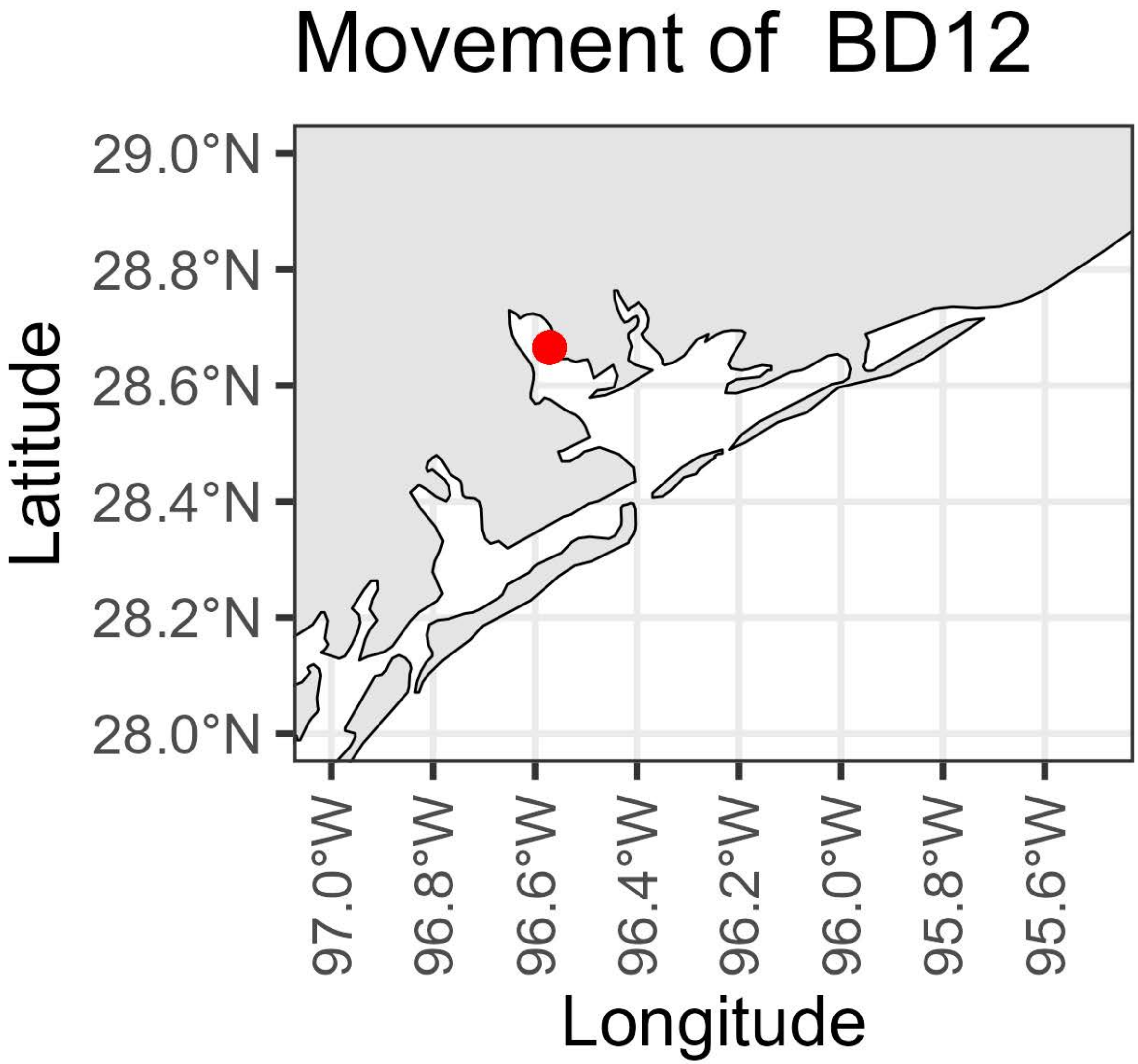
Movement of BD12
29.0°N
28.8°N
28.6°N
28.4°N
28.2°N
28.0°N
Latitude
97.0°W
96.8°W
96.6°W
96.4°W
96.2°W
96.0°W
95.8°W
95.6°W
Longitude

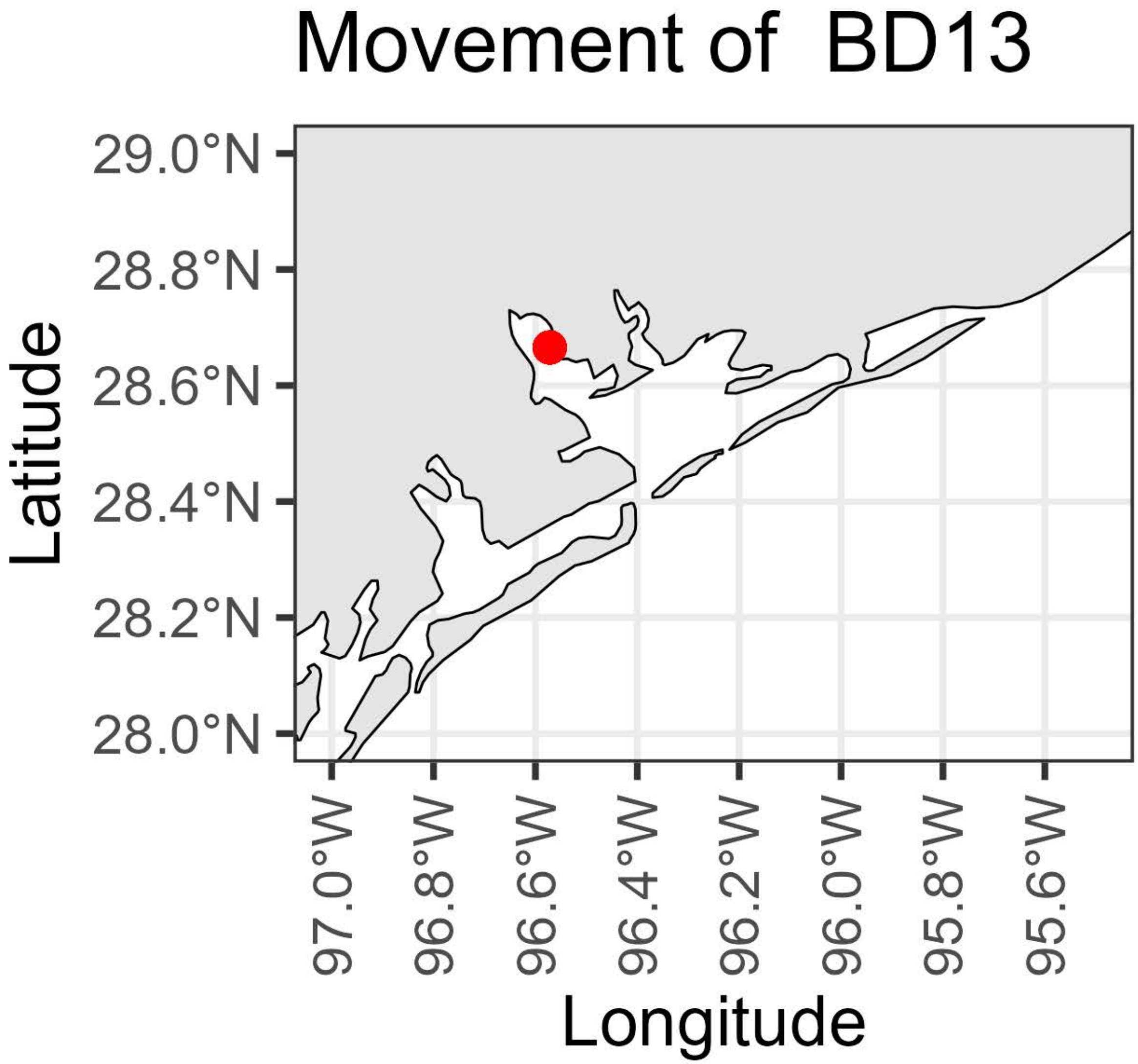
Movement of BD13
Latitude
29.0°N
28.8°N
28.6°N
28.4°N
28.2°N
28.0°N
97.0°W
96.8°W
96.6°W
96.4°W
96.2°W
96.0°W
95.8°W
95.6°W
Longitude

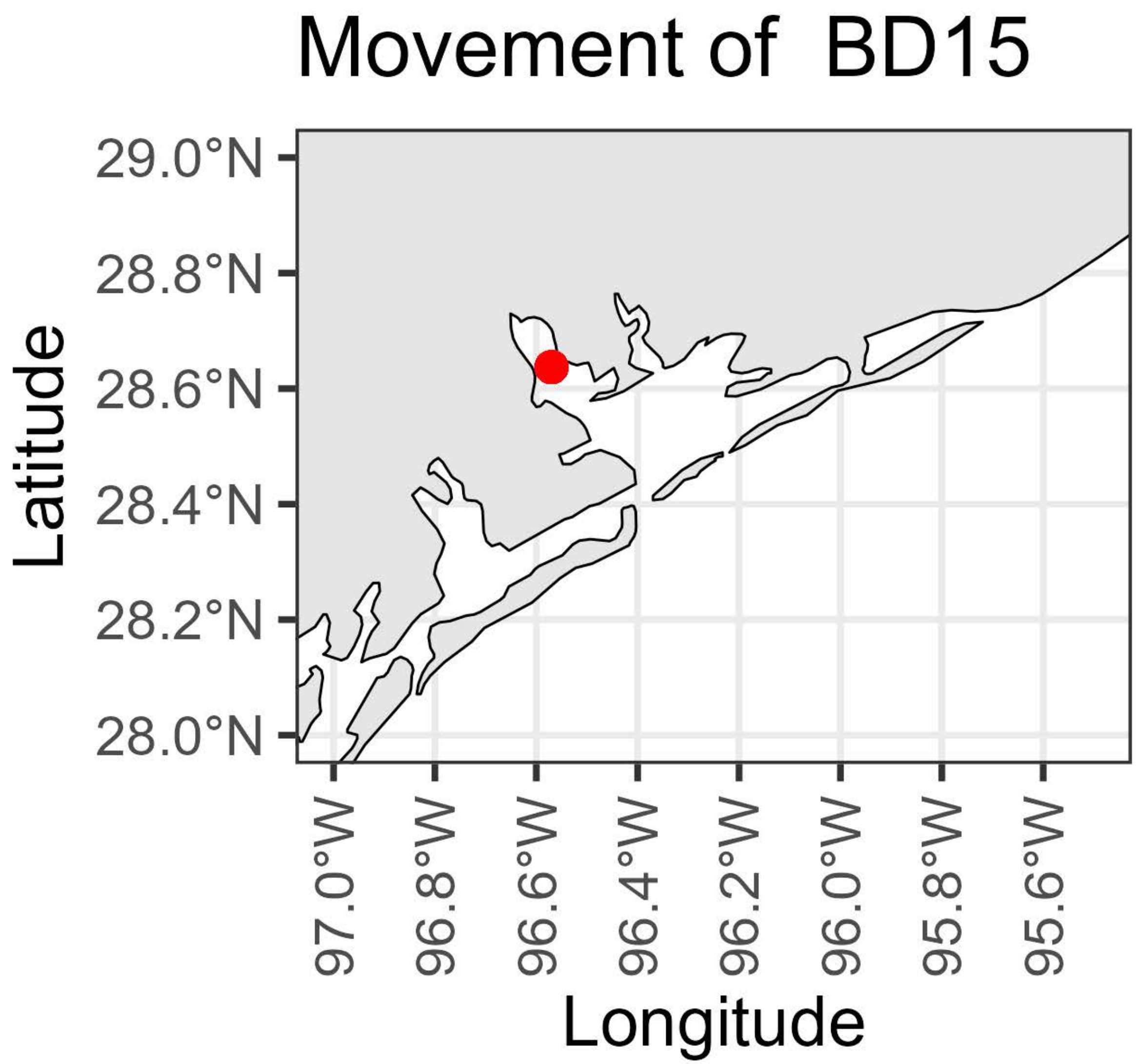
Movement of BD15
Latitude
29.0°N
28.8°N
28.6°N
28.4°N
28.2°N
28.0°N
97.0°W
96.8°W
96.6°W
96.4°W
96.2°W
96.0°W
95.8°W
95.6°W
Longitude

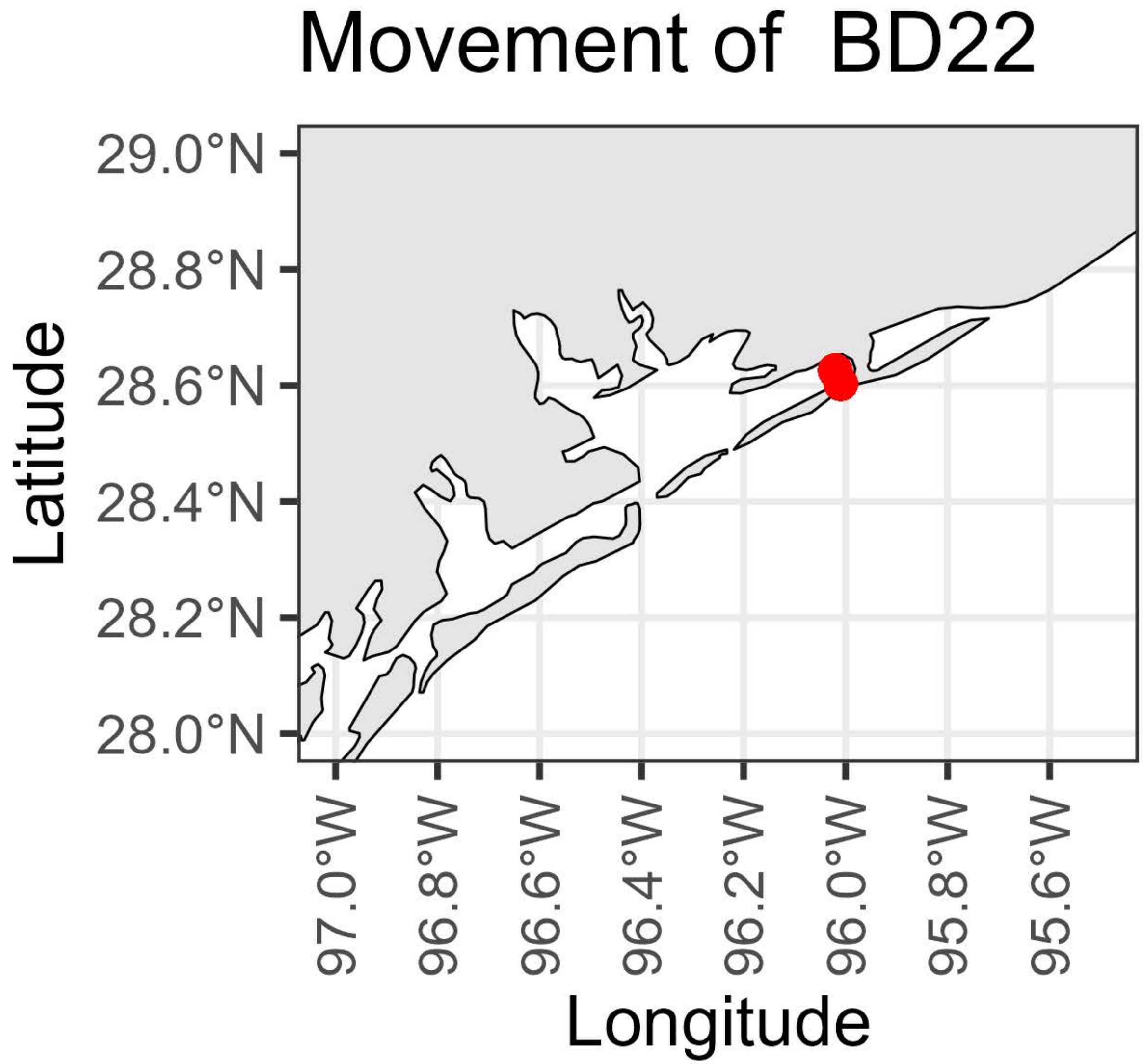
Movement of BD22
Latitude
29.0°N
28.8°N
28.6°N
28.4°N
28.2°N
28.0°N
Longitude
97.0°W
96.8°W
96.6°W
96.4°W
96.2°W
96.0°W
95.8°W
95.6°W

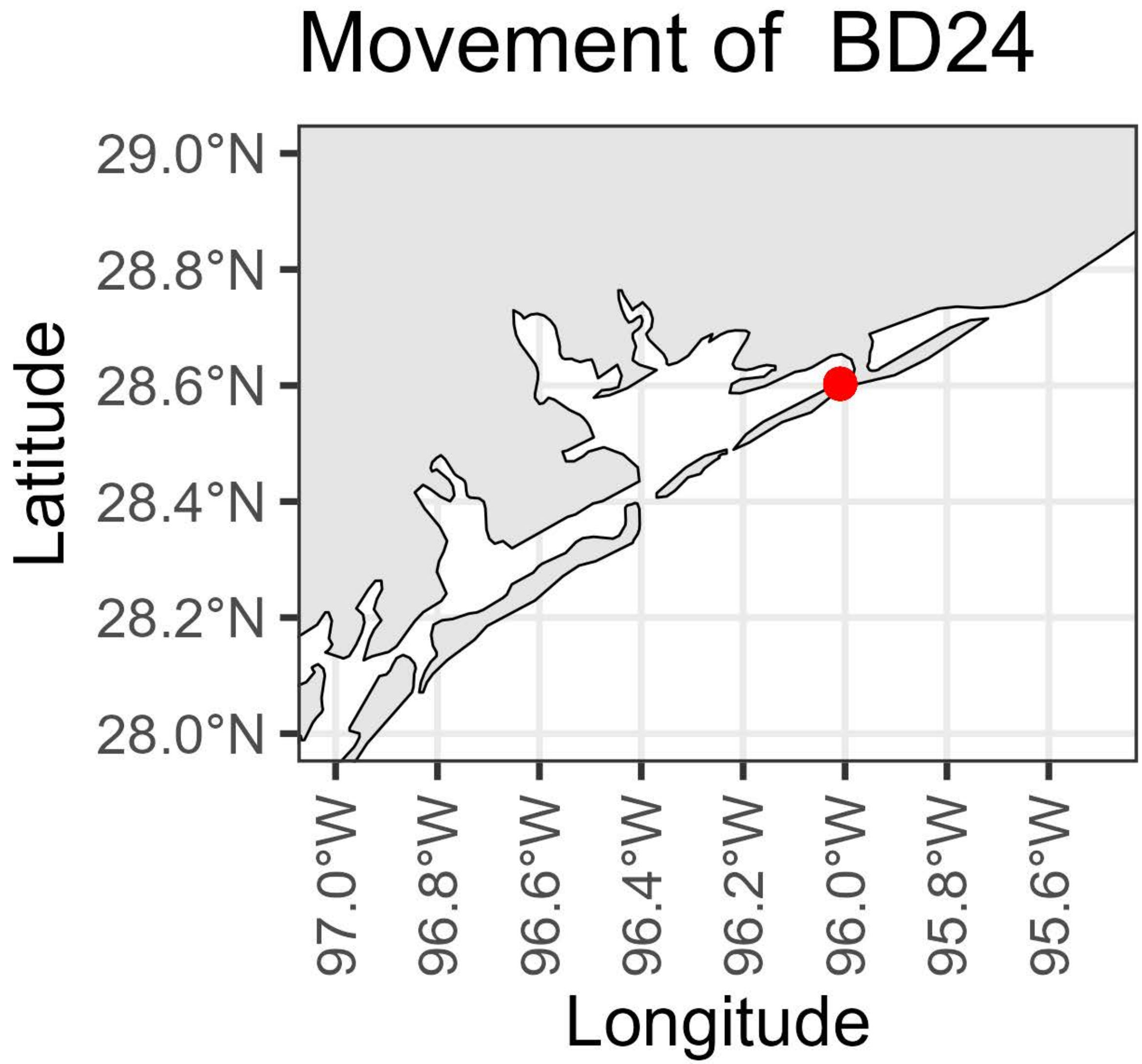
Movement of BD24
29.0°N
28.8°N
28.6°N
28.4°N
28.2°N
28.0°N
Latitude
97.0°W
96.8°W
96.6°W
96.4°W
96.2°W
96.0°W
95.8°W
95.6°W
Longitude

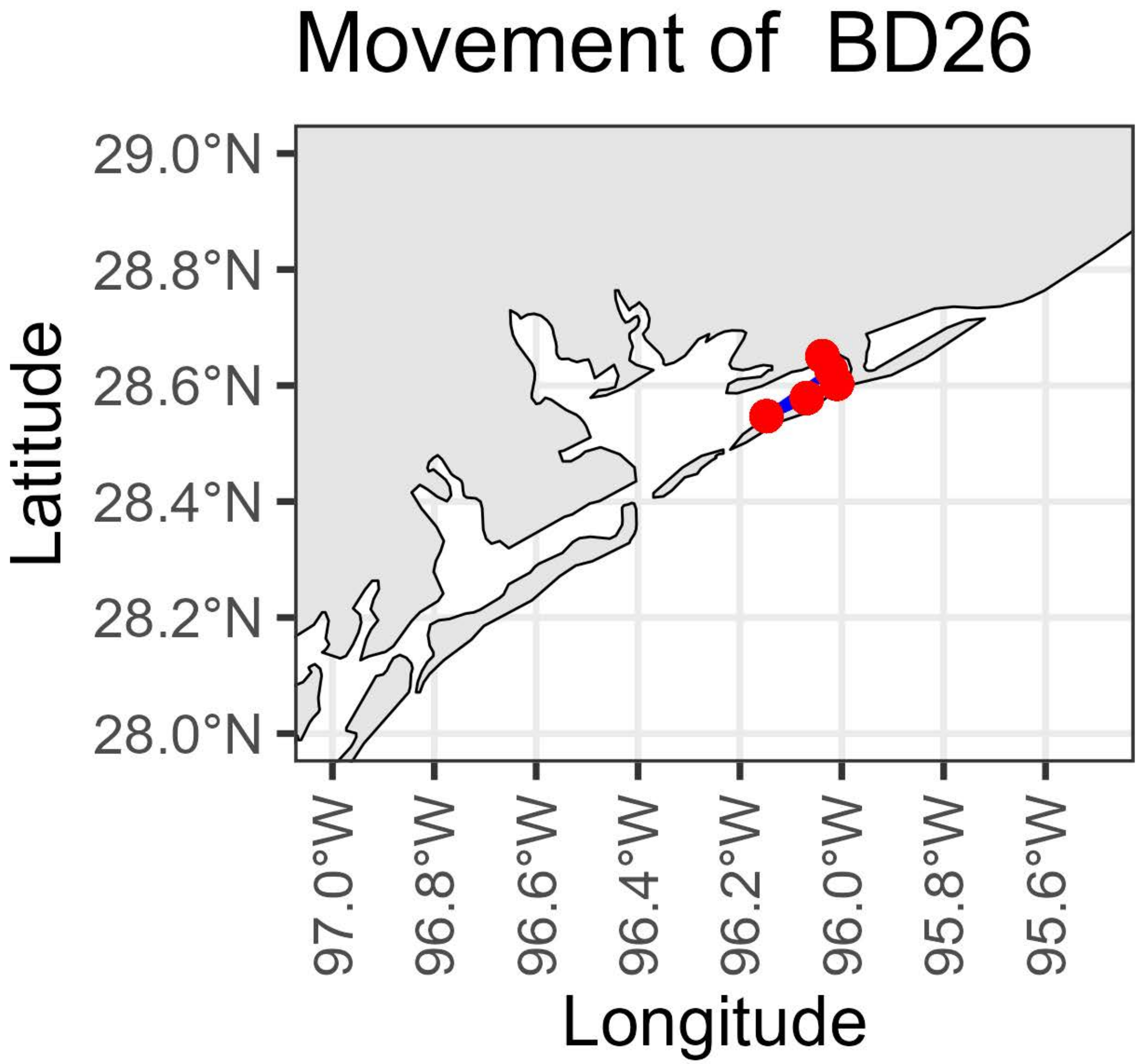
Movement of BD26
29.0°N
28.8°N
28.6°N
28.4°N
28.2°N
28.0°N
Latitude
97.0°W
96.8°W
96.6°W
96.4°W
96.2°W
96.0°W
95.8°W
95.6°W
Longitude

Red Drum

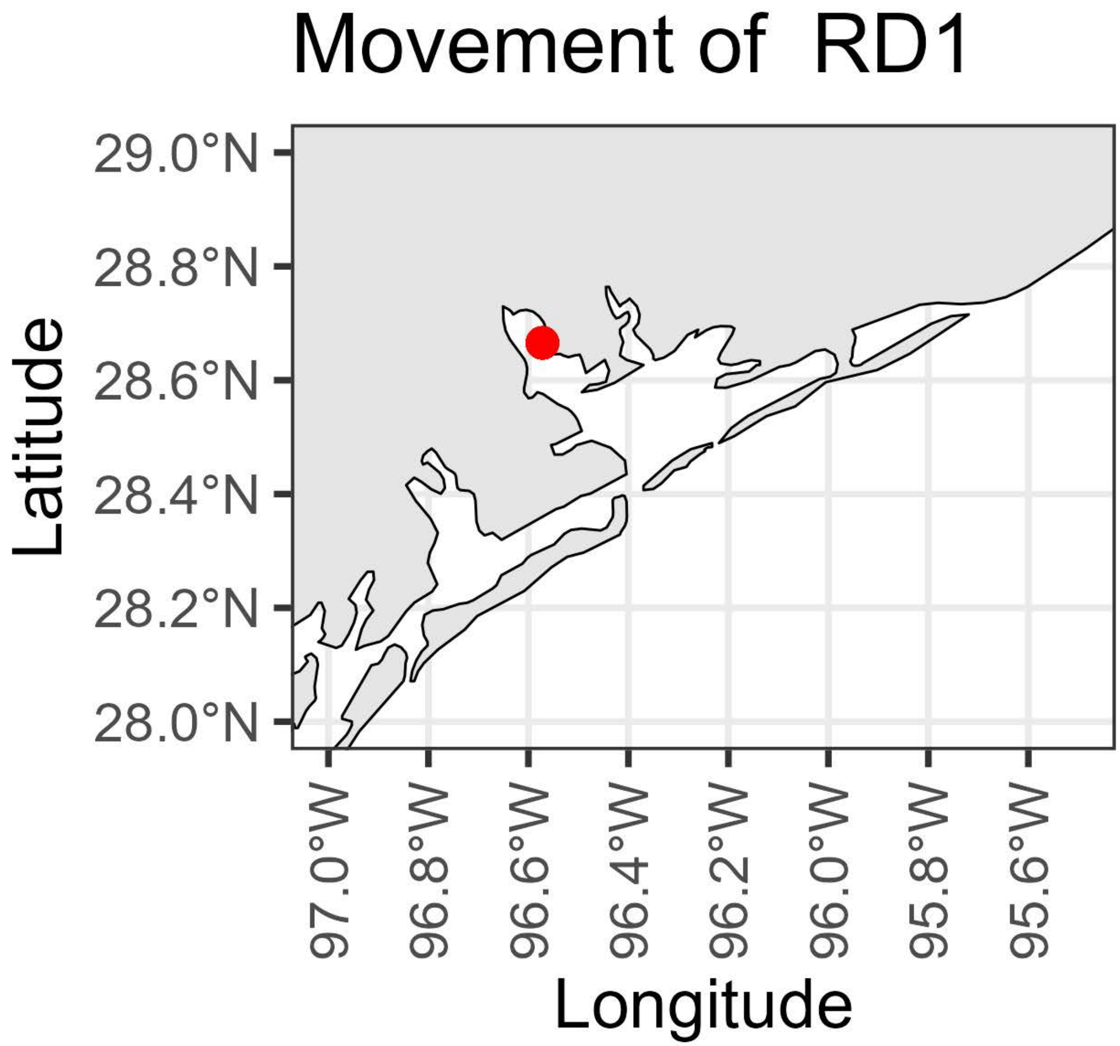
Movement of RD1
Latitude
29.0°N
28.8°N
28.6°N
28.4°N
28.2°N
28.0°N
97.0°W
96.8°W
96.6°W
96.4°W
96.2°W
96.0°W
95.8°W
95.6°W
Longitude

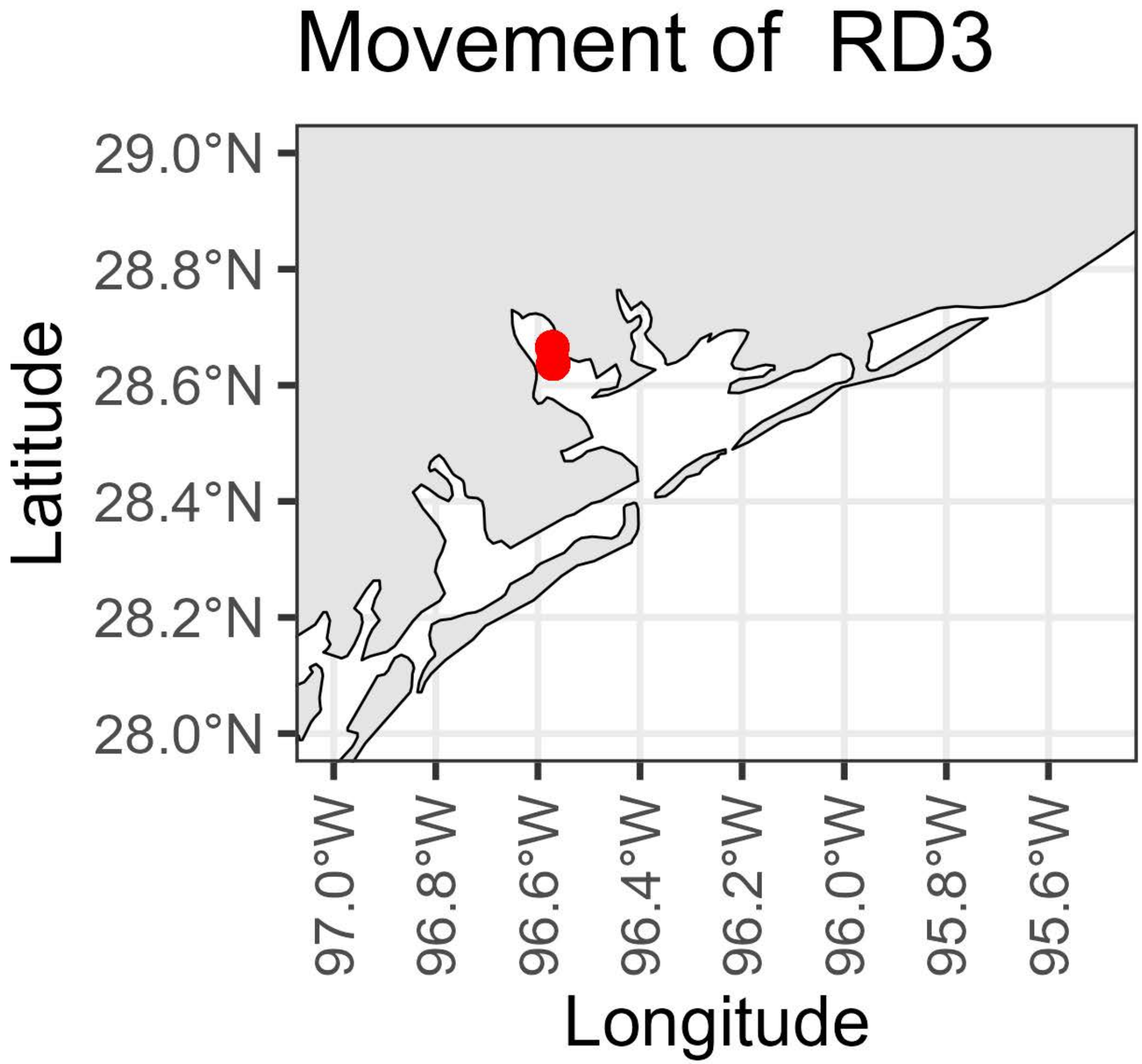
Movement of RD3
29.0°N
28.8°N
28.6°N
28.4°N
28.2°N
28.0°N
Latitude
97.0°W
96.8°W
96.6°W
96.4°W
96.2°W
96.0°W
95.8°W
95.6°W
Longitude

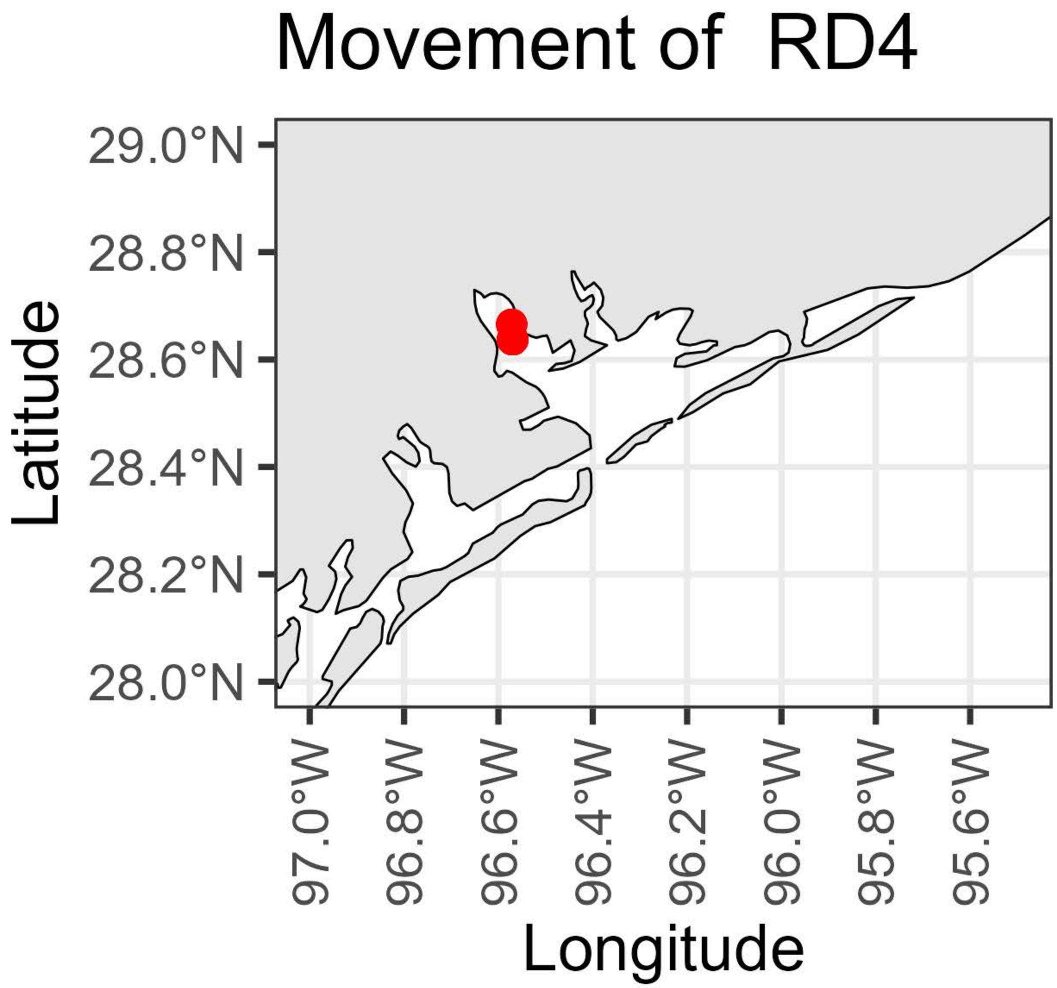
Movement of RD4
29.0°N
28.8°N
28.6°N
28.4°N
28.2°N
28.0°N
Latitude
97.0°W
96.8°W
96.6°W
96.4°W
96.2°W
96.0°W
95.8°W
95.6°W
Longitude

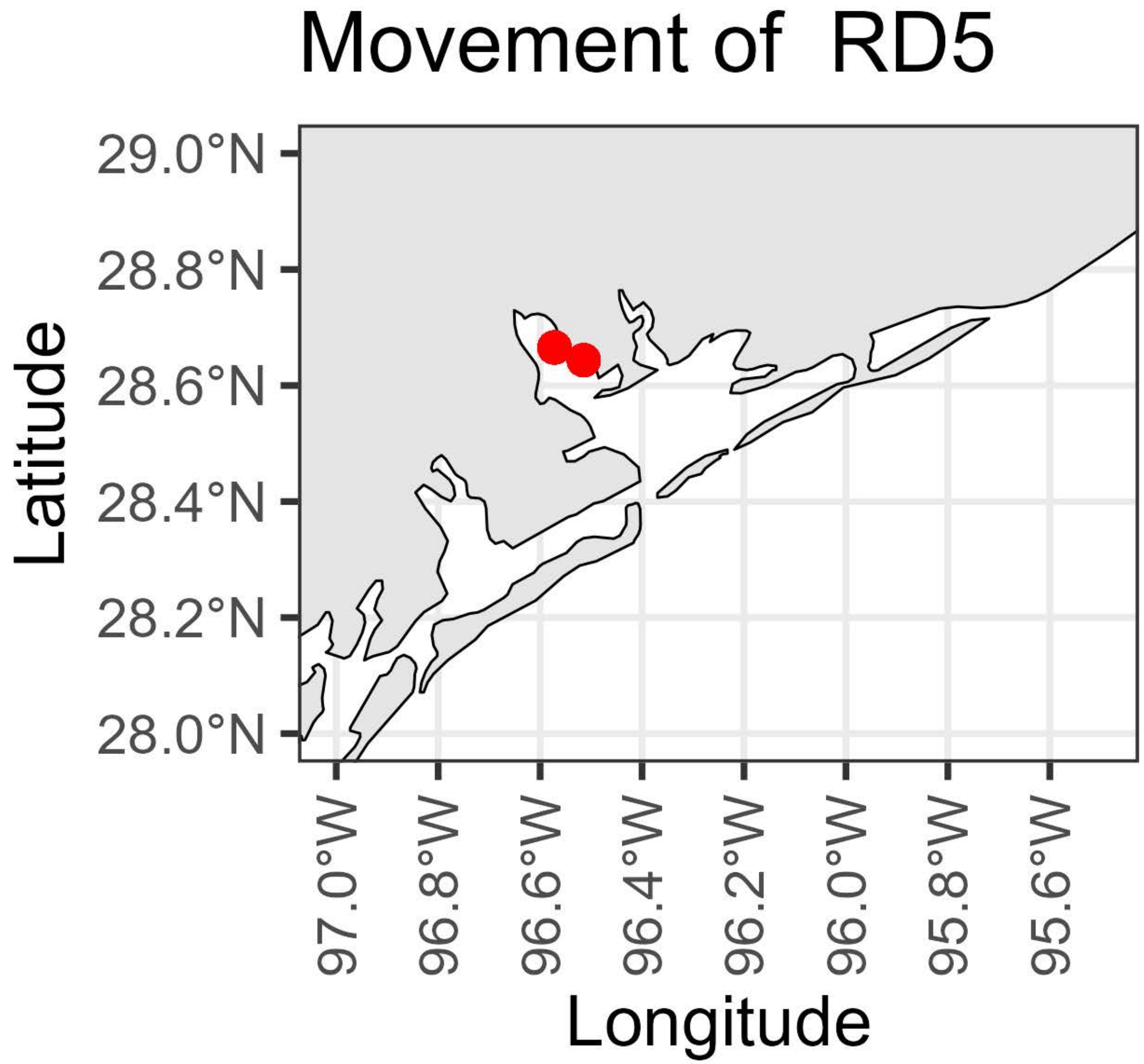
Movement of RD5
29.0°N
28.8°N
28.6°N
28.4°N
28.2°N
28.0°N
Latitude
97.0°W
96.8°W
96.6°W
96.4°W
96.2°W
96.0°W
95.8°W
95.6°W
Longitude

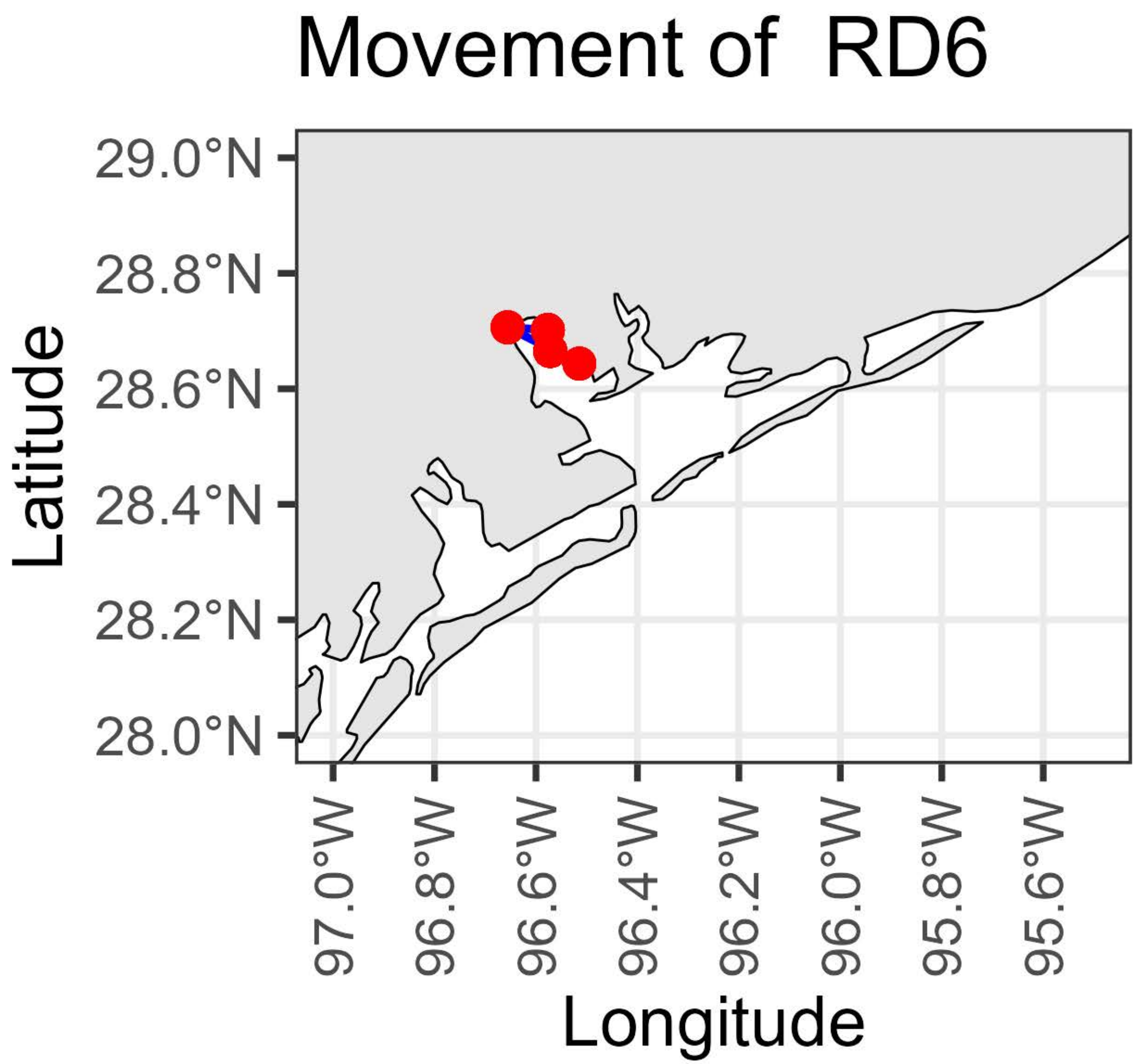
Movement of RD6
Latitude
29.0°N
28.8°N
28.6°N
28.4°N
28.2°N
28.0°N
Longitude
97.0°W
96.8°W
96.6°W
96.4°W
96.2°W
96.0°W
95.8°W
95.6°W

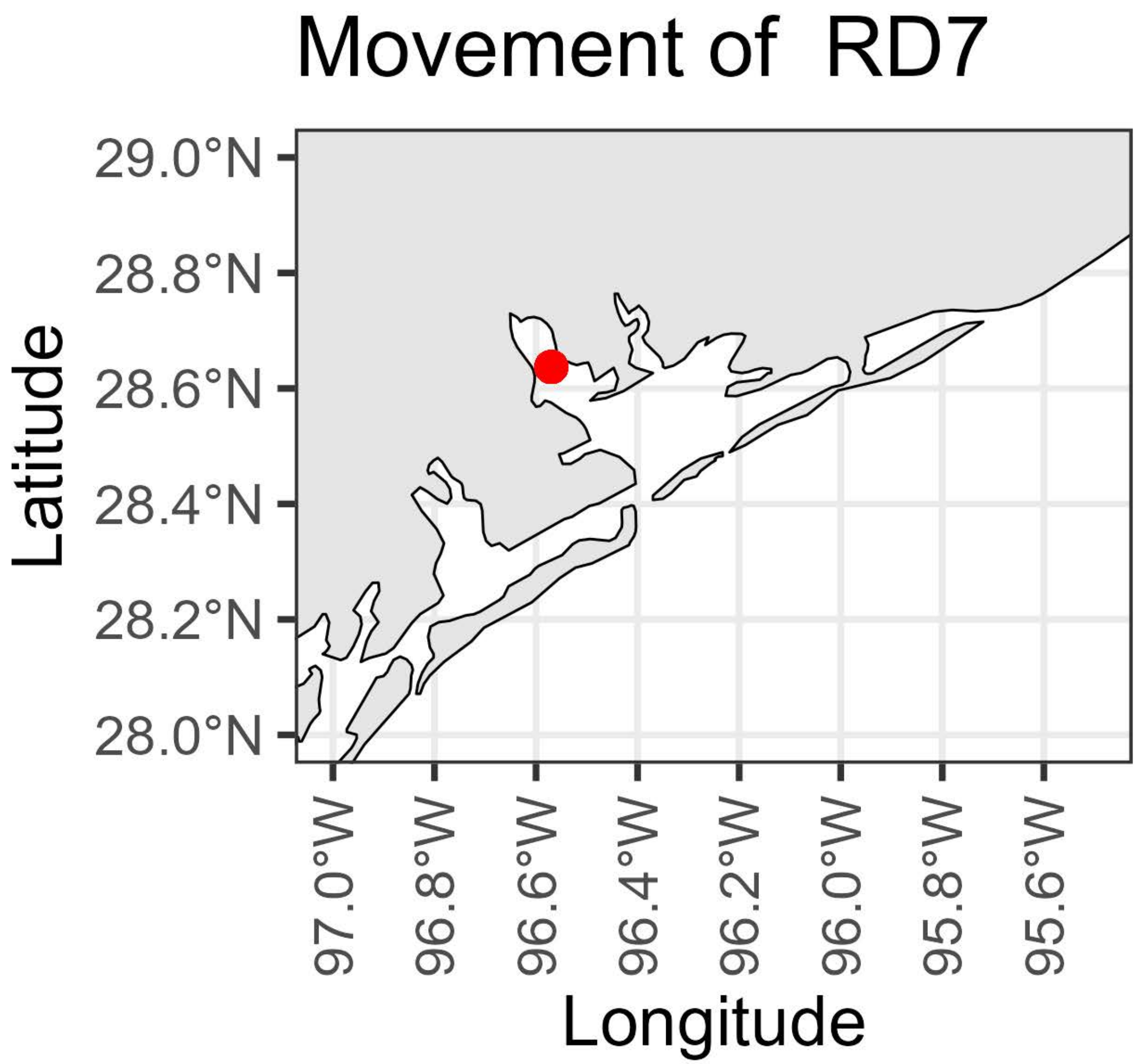
Movement of RD7
29.0°N
28.8°N
28.6°N
28.4°N
28.2°N
28.0°N
Latitude
97.0°W
96.8°W
96.6°W
96.4°W
96.2°W
96.0°W
95.8°W
95.6°W
Longitude

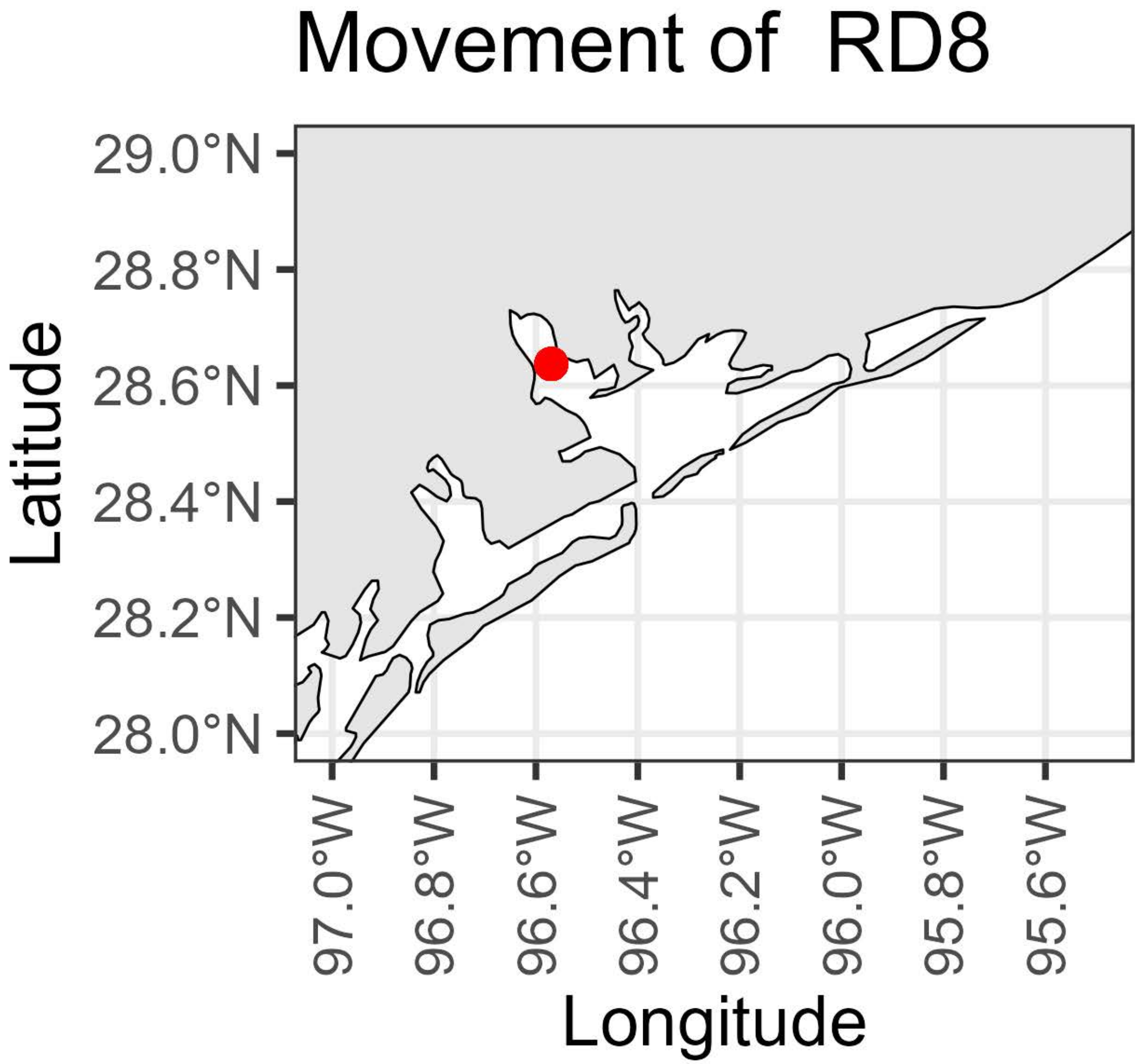
Movement of RD8
29.0°N
28.8°N
28.6°N
28.4°N
28.2°N
28.0°N
Latitude
97.0°W
96.8°W
96.6°W
96.4°W
96.2°W
96.0°W
95.8°W
95.6°W
Longitude

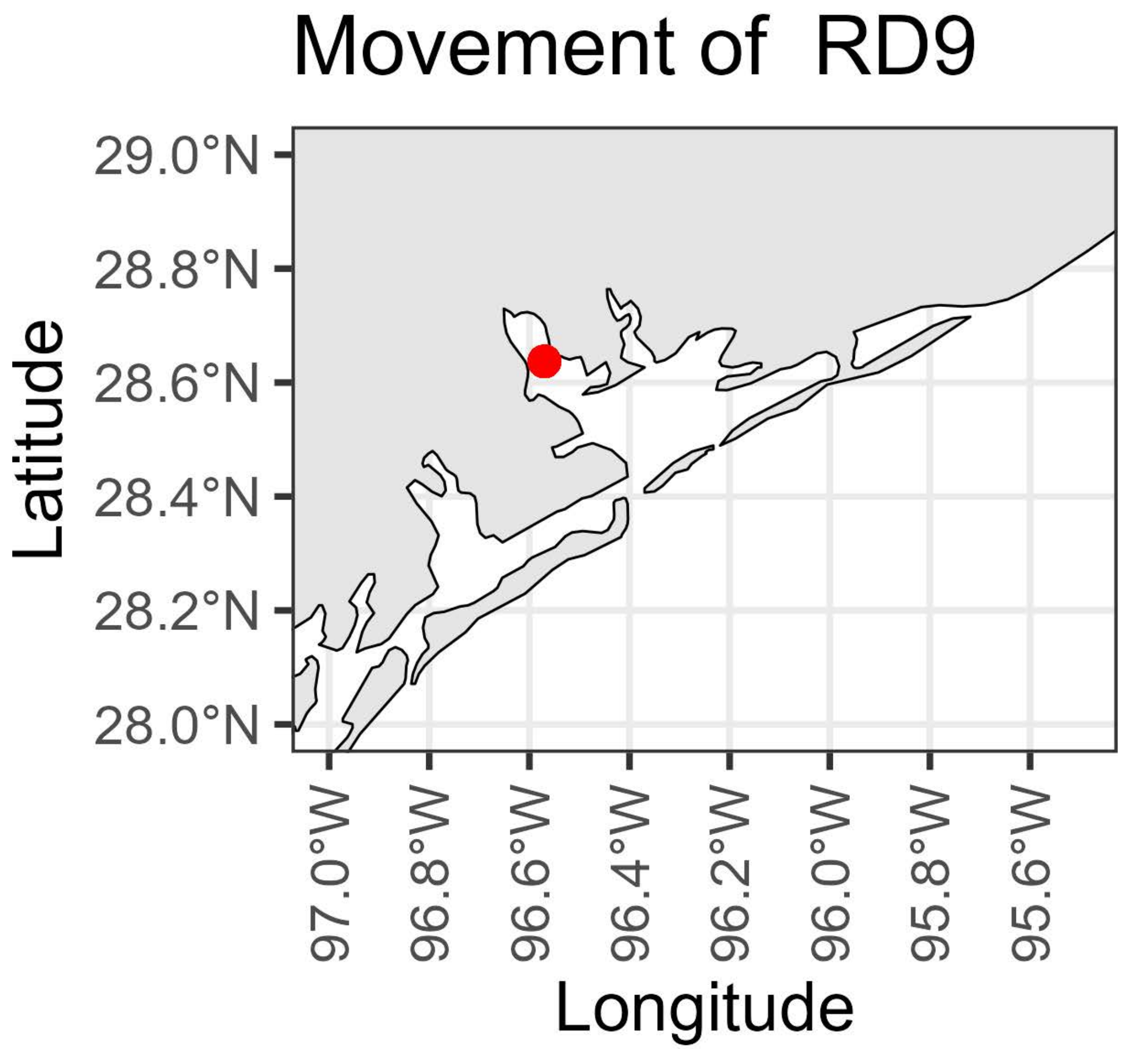
Movement of RD9
Latitude
29.0°N
28.8°N
28.6°N
28.4°N
28.2°N
28.0°N
97.0°W
96.8°W
96.6°W
96.4°W
96.2°W
96.0°W
95.8°W
95.6°W
Longitude

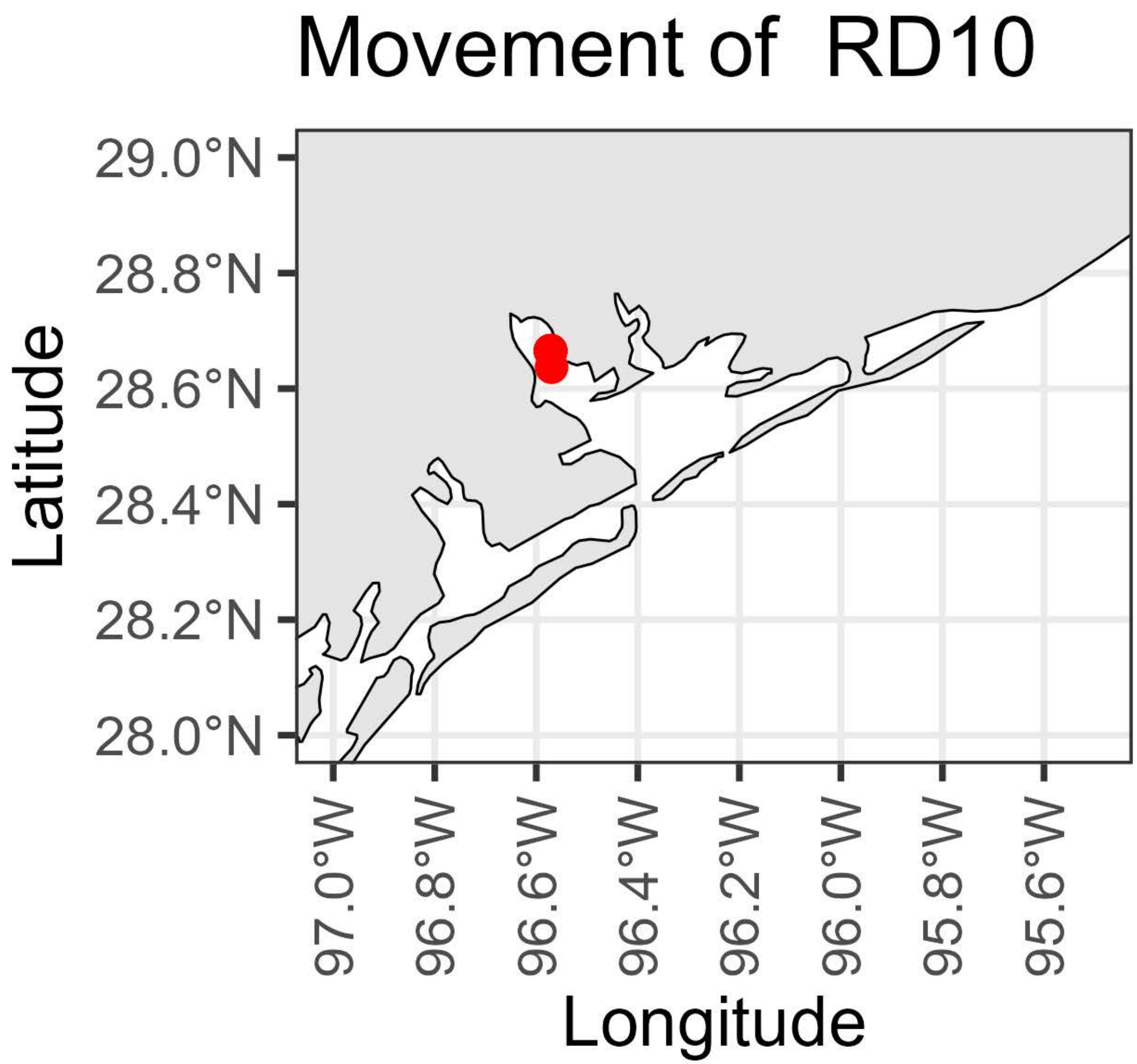
Movement of RD10
Latitude
29.0°N
28.8°N
28.6°N
28.4°N
28.2°N
28.0°N
97.0°W
96.8°W
96.6°W
96.4°W
96.2°W
96.0°W
95.8°W
95.6°W
Longitude

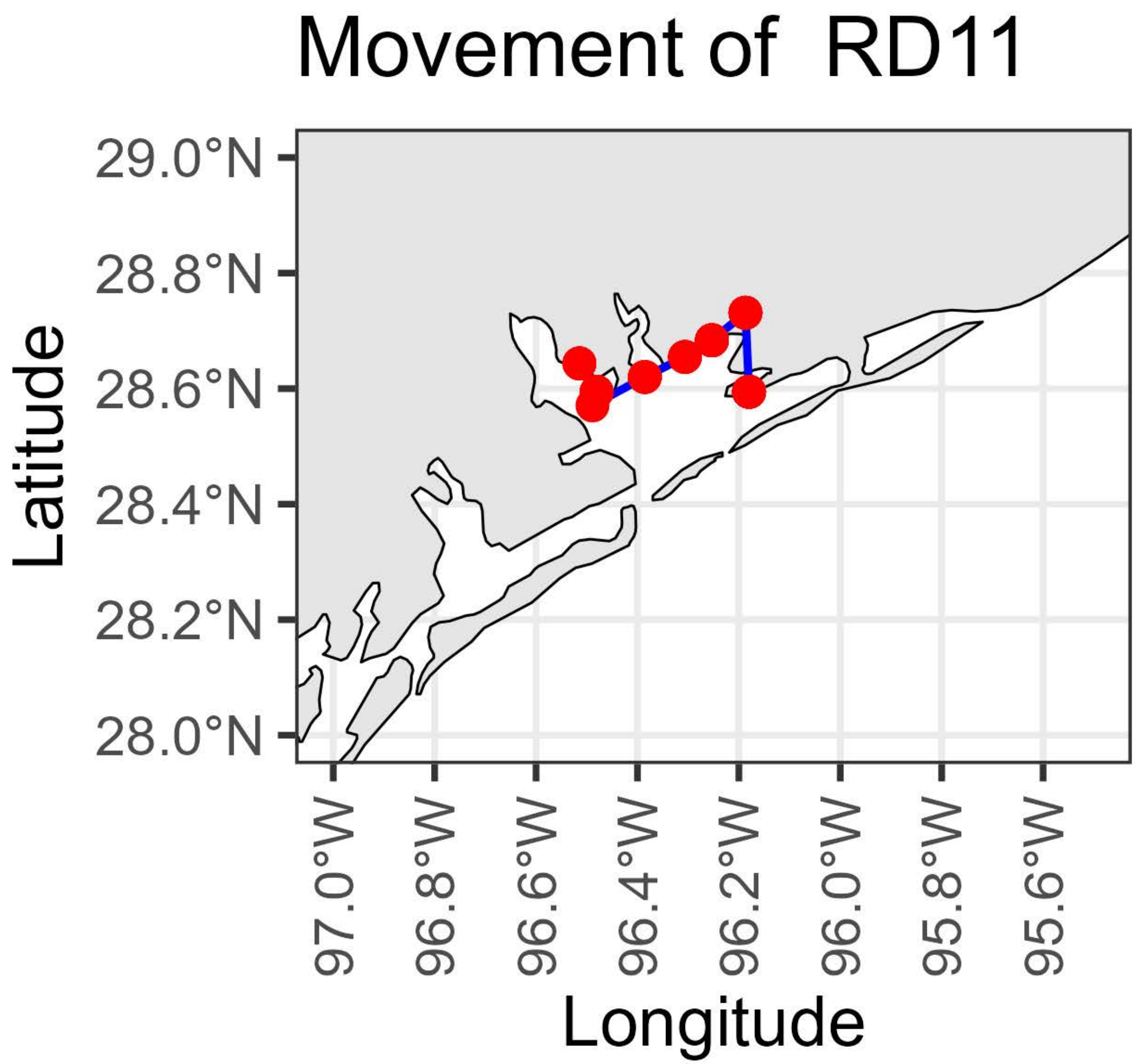
Movement of RD11
29.0°N
28.8°N
28.6°N
28.4°N
28.2°N
28.0°N
Latitude
97.0°W
96.8°W
96.6°W
96.4°W
96.2°W
96.0°W
95.8°W
95.6°W
Longitude

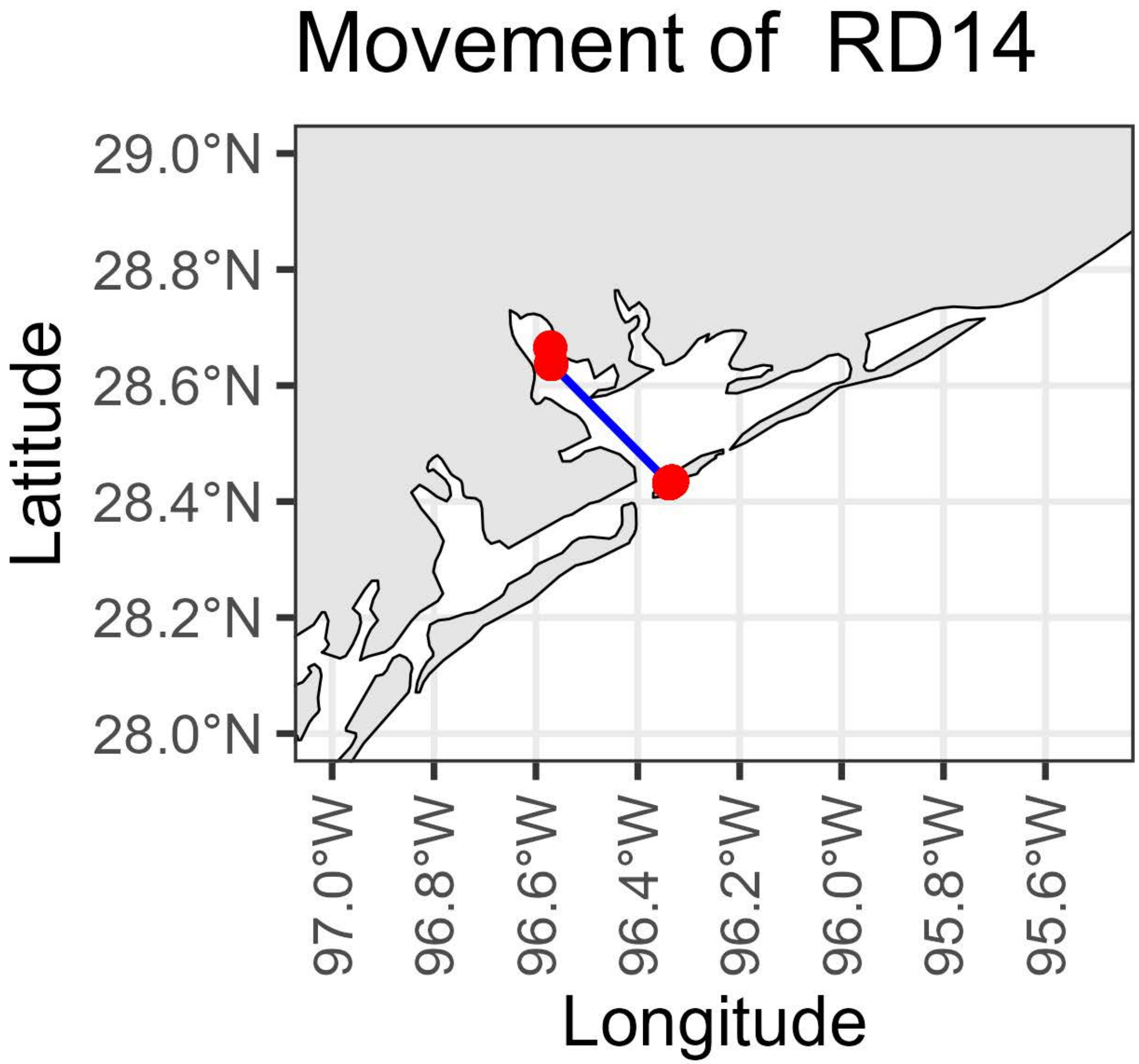
Movement of RD14
29.0°N
28.8°N
28.6°N
28.4°N
28.2°N
28.0°N
Latitude
97.0°W
96.8°W
96.6°W
96.4°W
96.2°W
96.0°W
95.8°W
95.6°W
Longitude

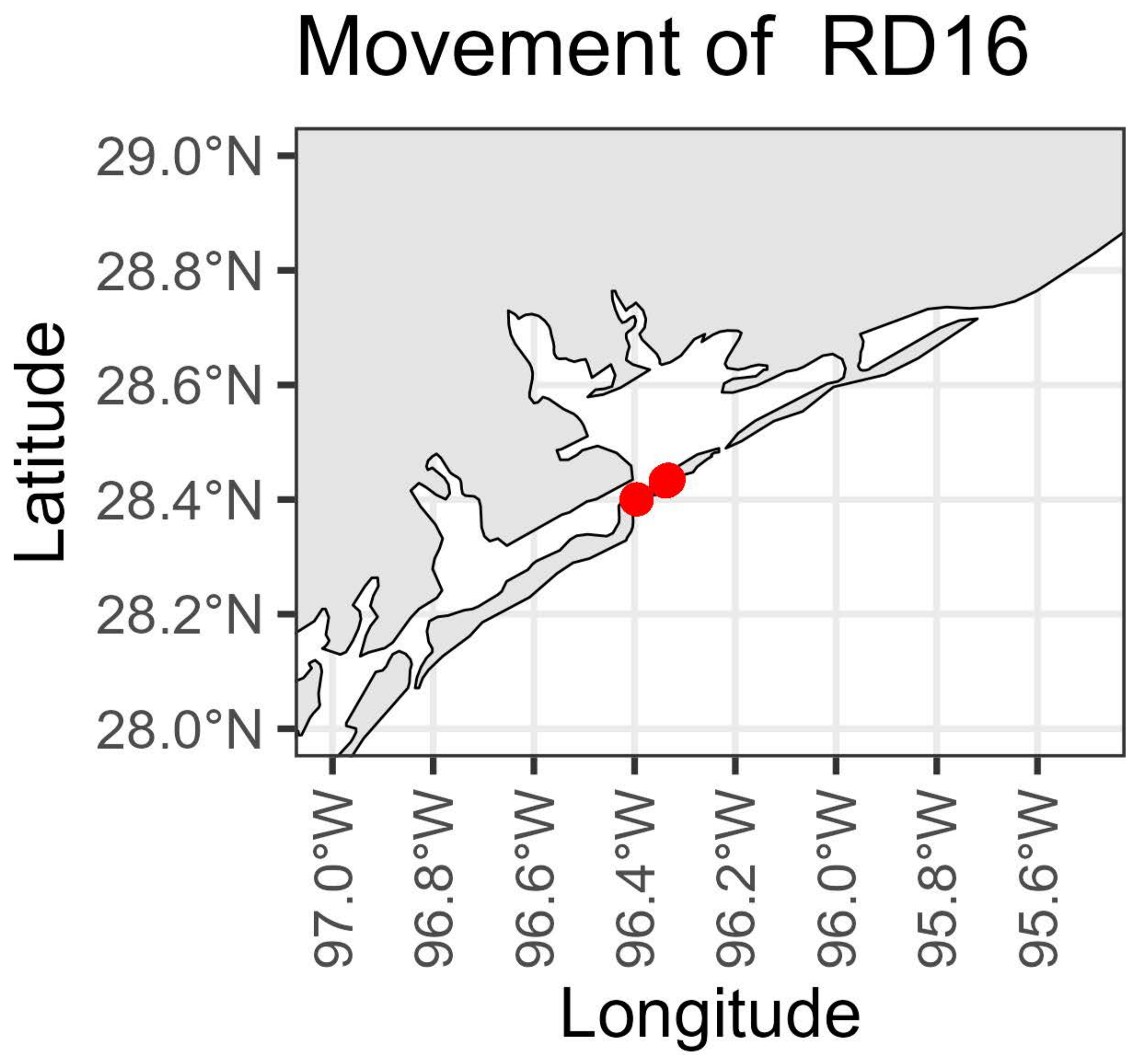
Movement of RD16
Latitude
29.0°N
28.8°N
28.6°N
28.4°N
28.2°N
28.0°N
97.0°W
96.8°W
96.6°W
96.4°W
96.2°W
96.0°W
95.8°W
95.6°W
Longitude

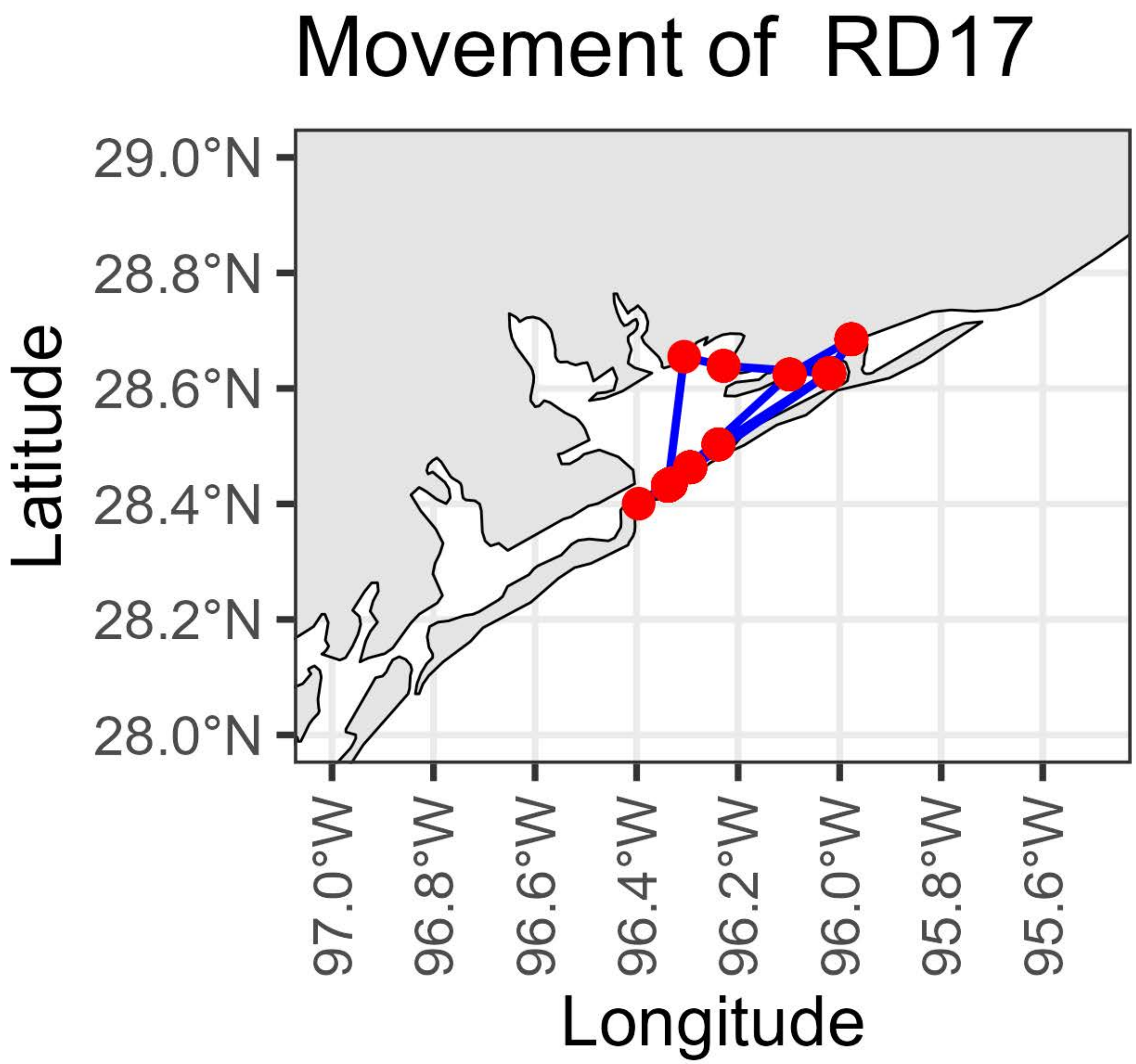
Movement of RD17
29.0°N
28.8°N
28.6°N
28.4°N
28.2°N
28.0°N
Latitude
97.0°W
96.8°W
96.6°W
96.4°W
96.2°W
96.0°W
95.8°W
95.6°W
Longitude

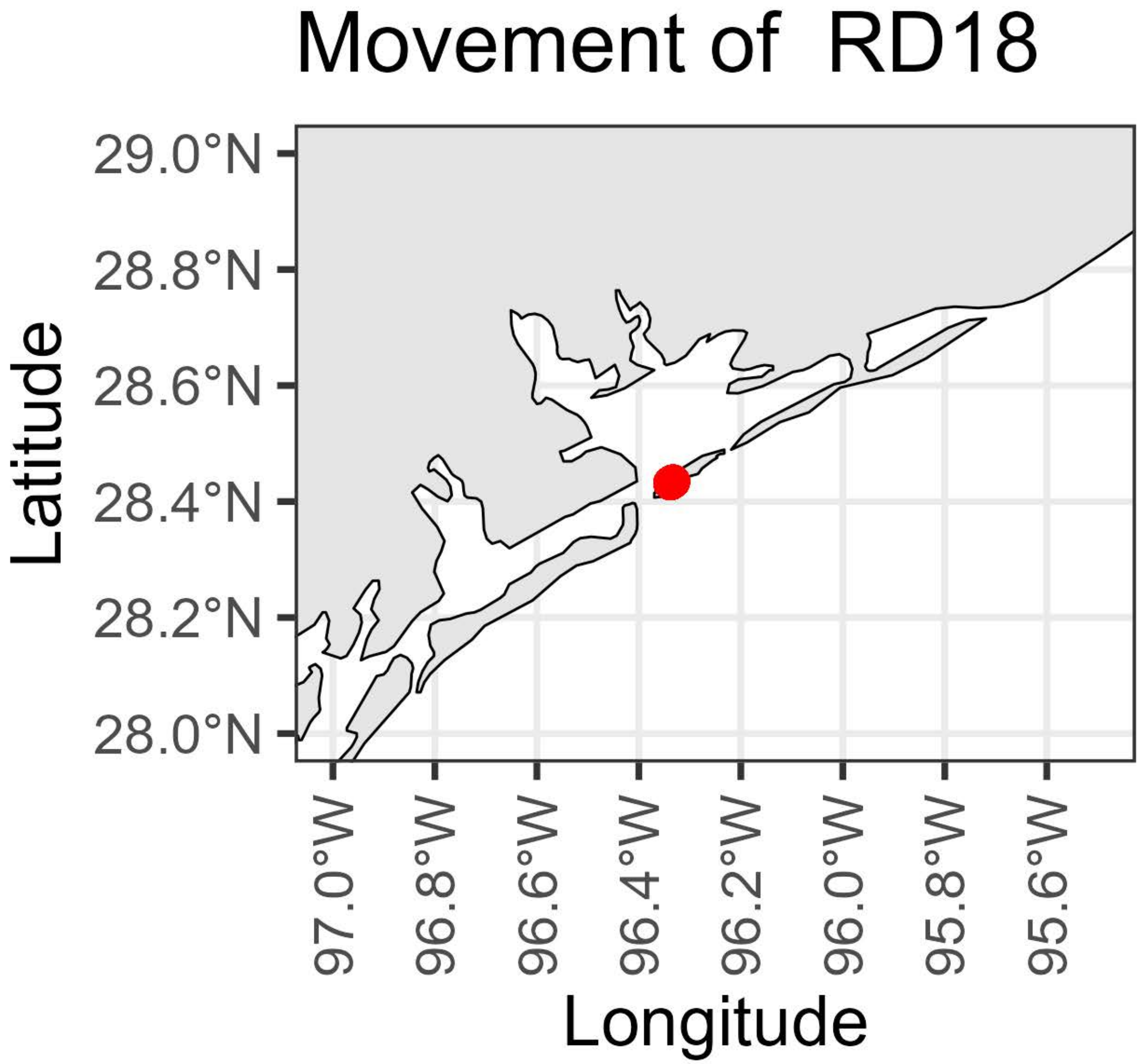
Movement of RD18
29.0°N
28.8°N
28.6°N
28.4°N
28.2°N
28.0°N
Latitude
97.0°W
96.8°W
96.6°W
96.4°W
96.2°W
96.0°W
95.8°W
95.6°W
Longitude

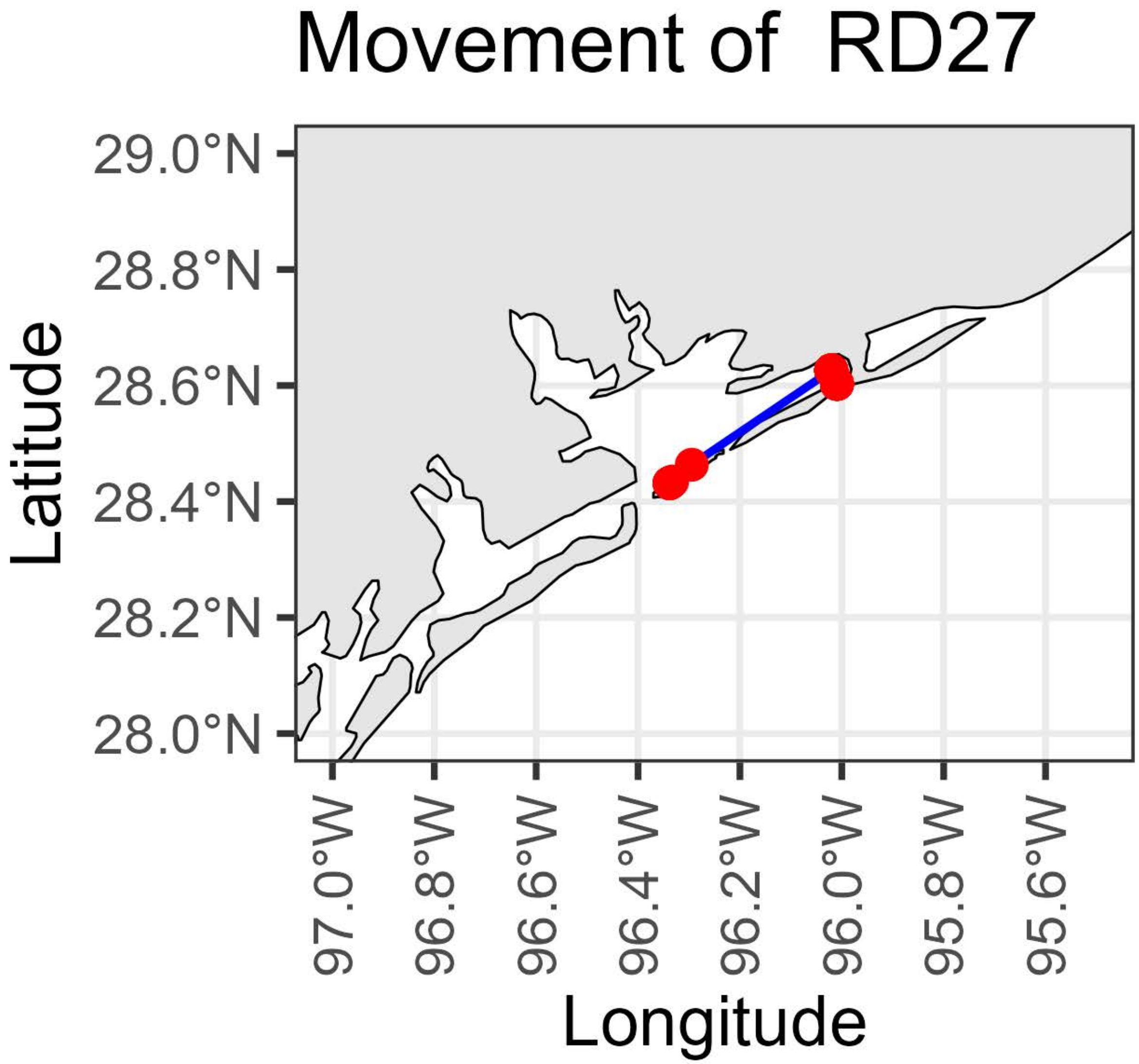
Movement of RD27
29.0°N
28.8°N
28.6°N
28.4°N
28.2°N
28.0°N
Latitude
97.0°W
96.8°W
96.6°W
96.4°W
96.2°W
96.0°W
95.8°W
95.6°W
Longitude

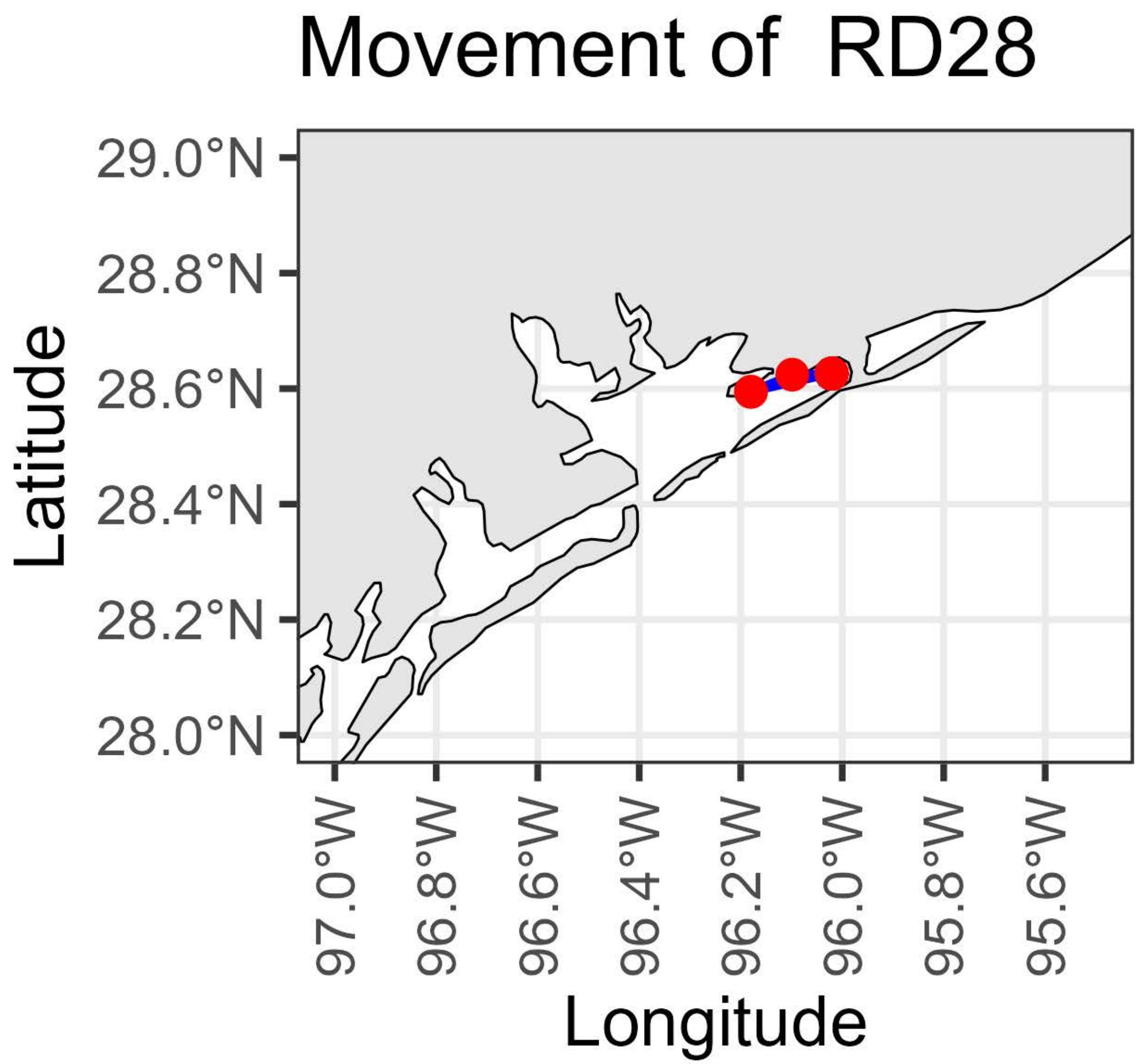
Movement of RD28
29.0°N
28.8°N
28.6°N
28.4°N
28.2°N
28.0°N
Latitude
97.0°W
96.8°W
96.6°W
96.4°W
96.2°W
96.0°W
95.8°W
95.6°W
Longitude

Spotted Seatrout

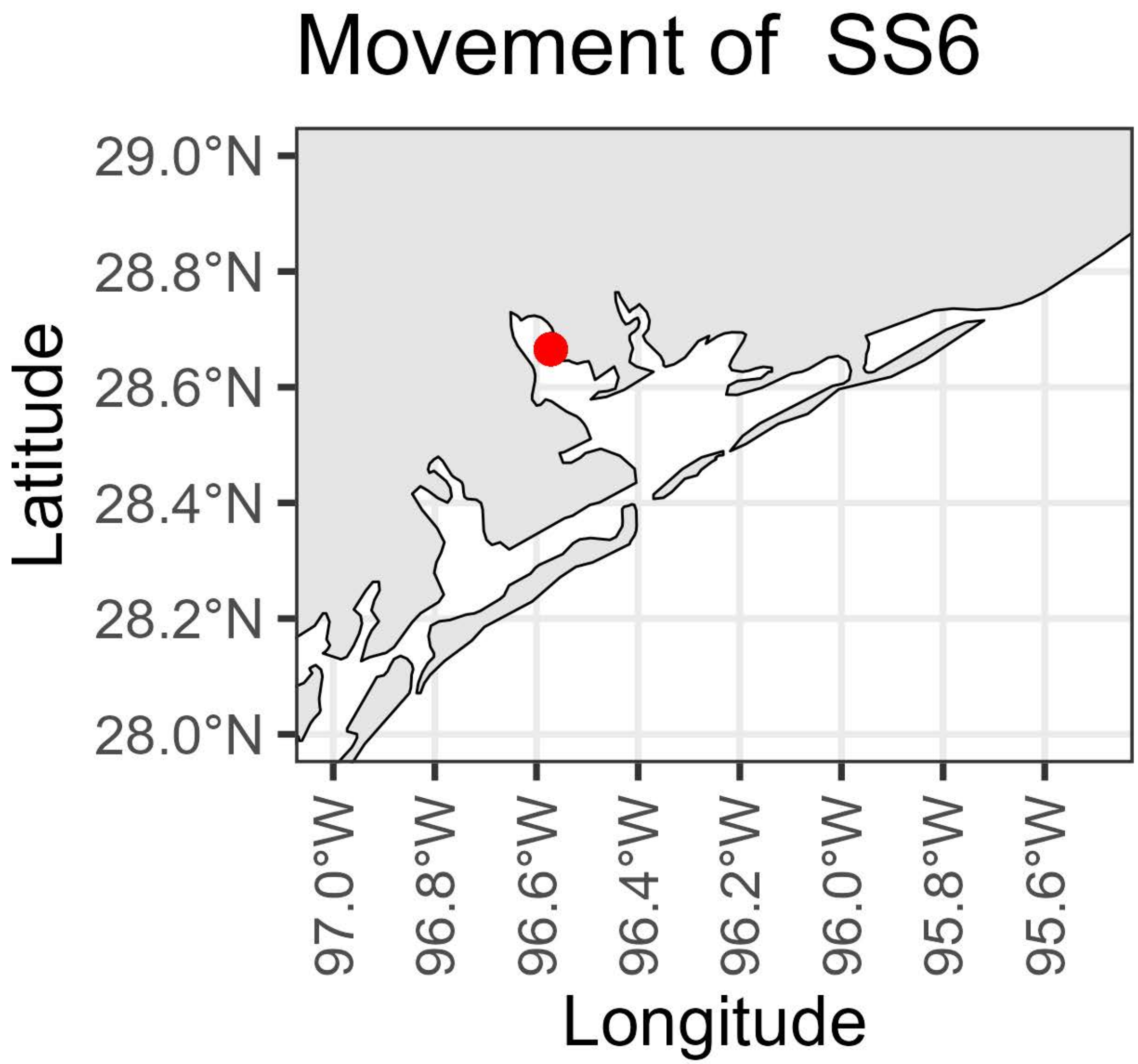

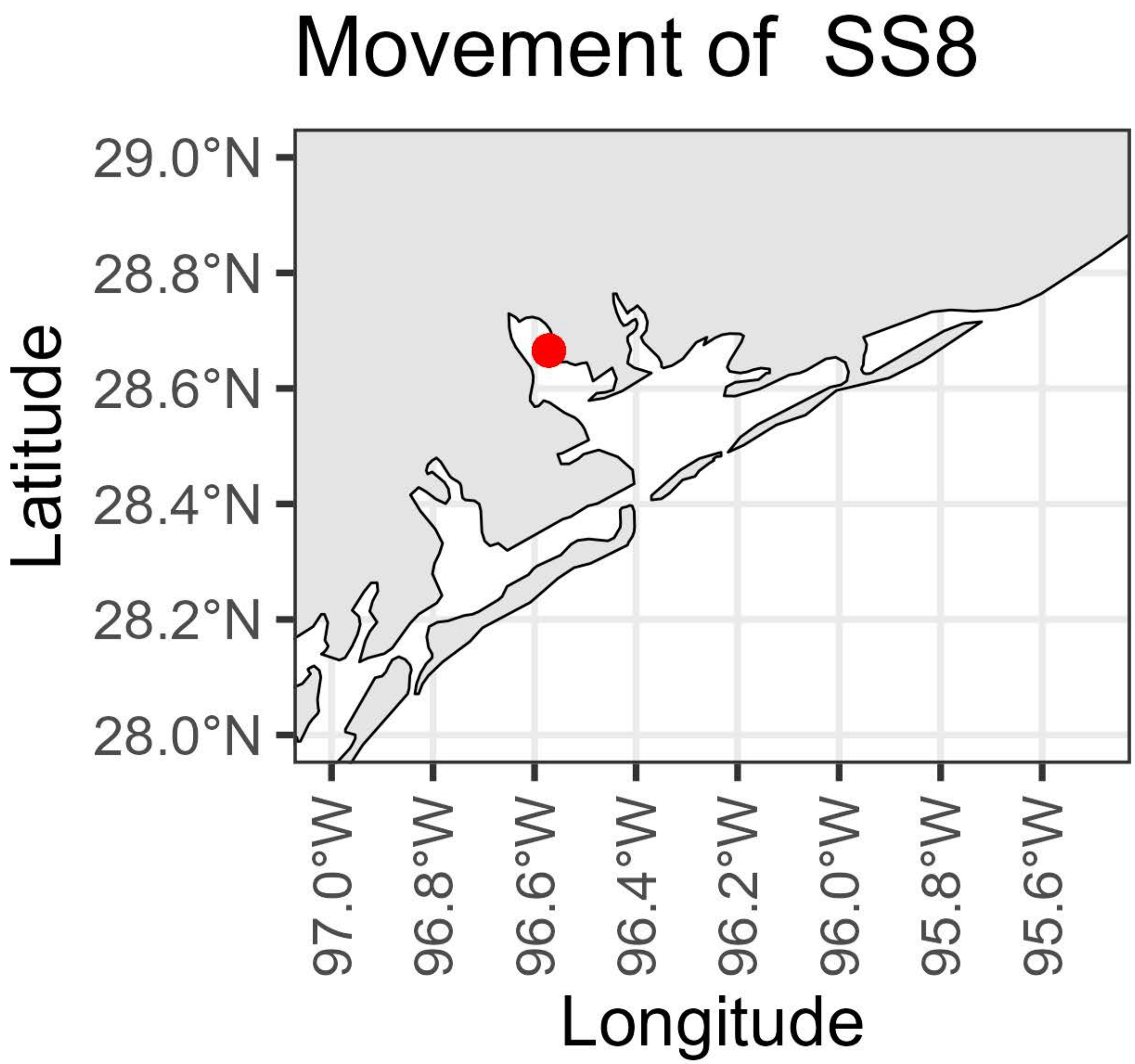
Movement of SS8
29.0°N
28.8°N
28.6°N
28.4°N
28.2°N
28.0°N
Latitude
97.0°W
96.8°W
96.6°W
96.4°W
96.2°W
96.0°W
95.8°W
95.6°W
Longitude

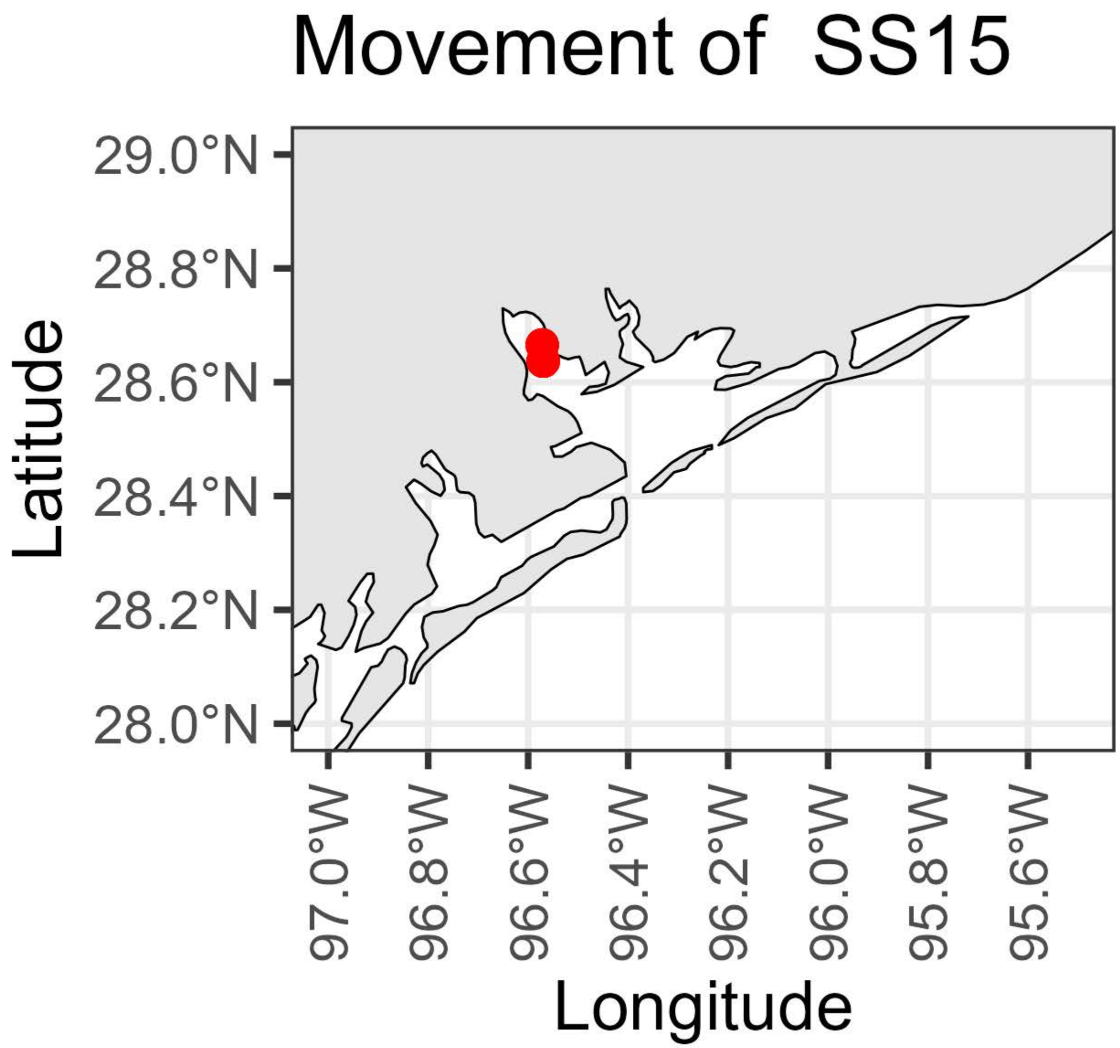
Movement of SS15
29.0°N
28.8°N
28.6°N
28.4°N
28.2°N
28.0°N
Latitude
97.0°W
96.8°W
96.6°W
96.4°W
96.2°W
96.0°W
95.8°W
95.6°W
Longitude

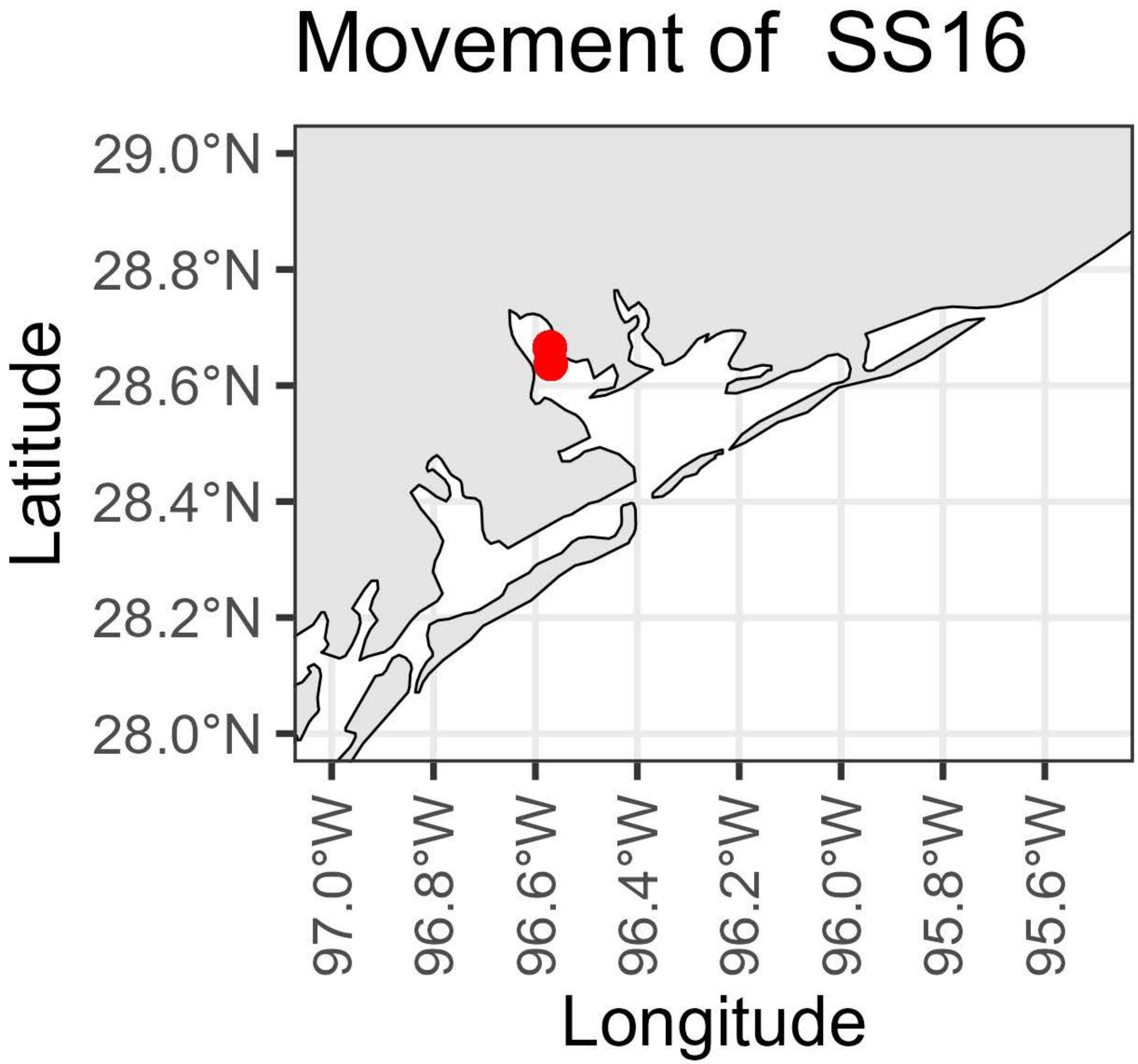
Movement of SS16
29.0°N
28.8°N
28.6°N
28.4°N
28.2°N
28.0°N
Latitude
97.0°W
96.8°W
96.6°W
96.4°W
96.2°W
96.0°W
95.8°W
95.6°W
Longitude

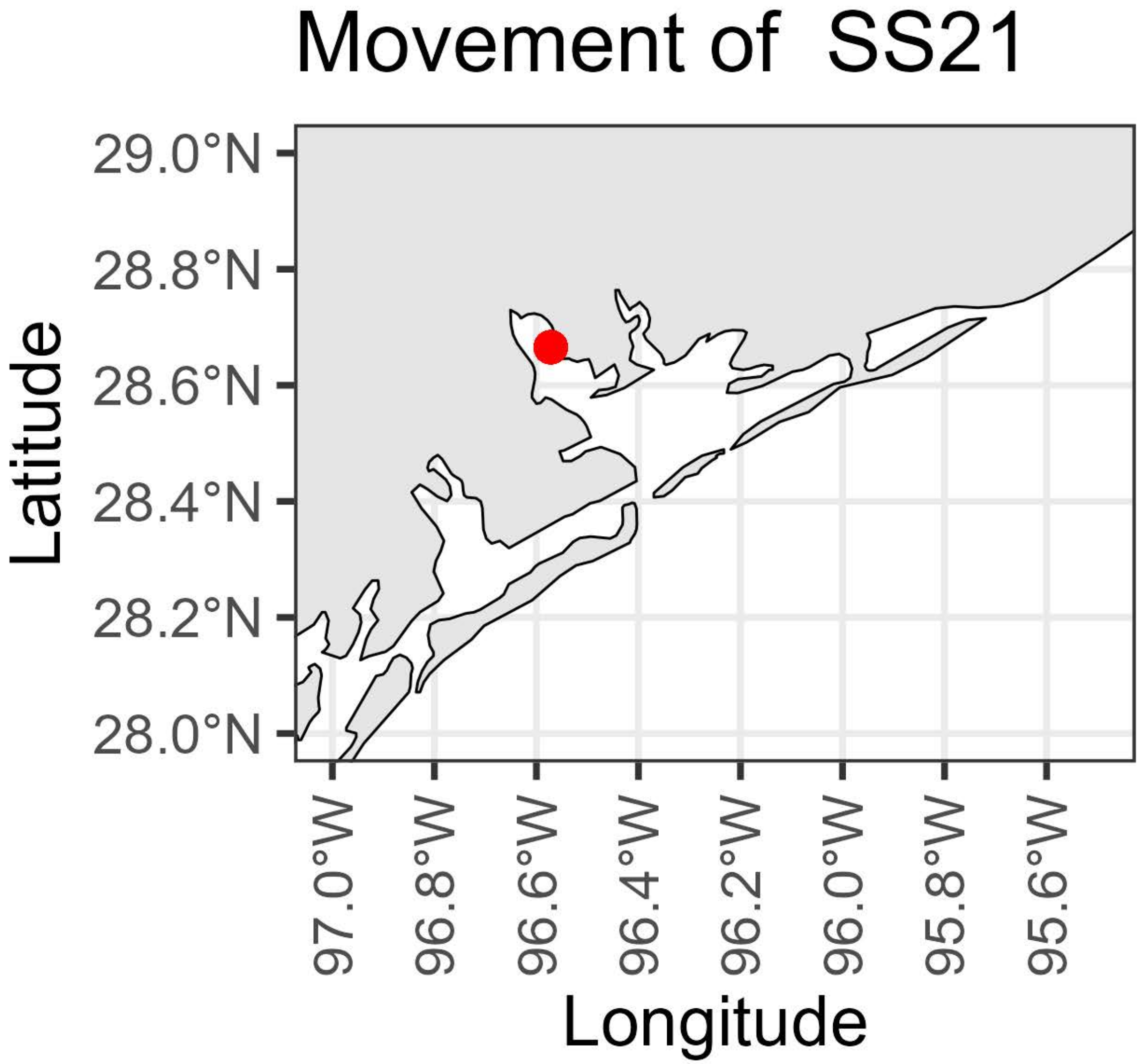
Movement of SS21
29.0°N
28.8°N
28.6°N
28.4°N
28.2°N
28.0°N
Latitude
97.0°W
96.8°W
96.6°W
96.4°W
96.2°W
96.0°W
95.8°W
95.6°W
Longitude

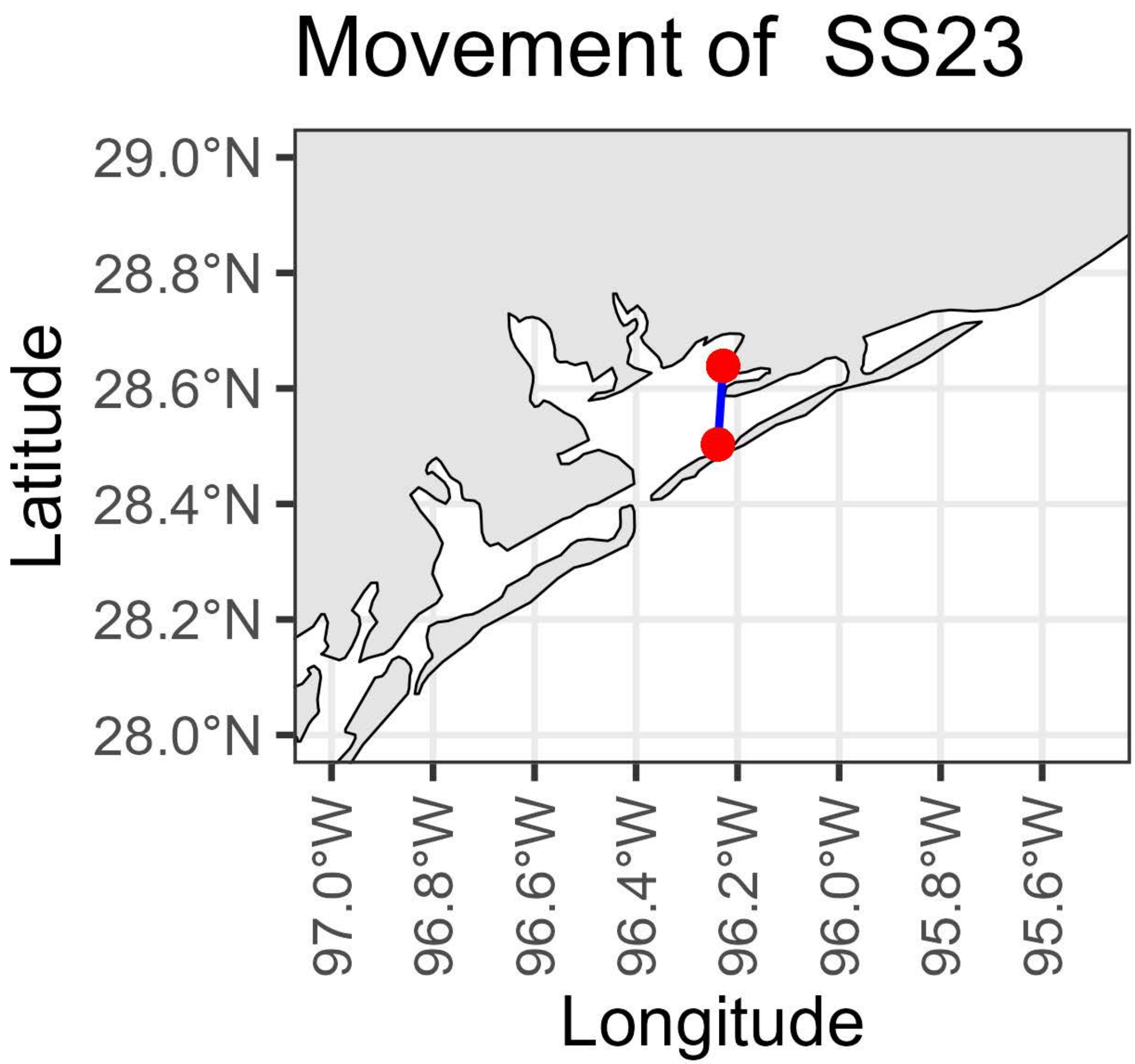
Movement of SS23
Latitude
29.0°N
28.8°N
28.6°N
28.4°N
28.2°N
28.0°N
97.0°W
96.8°W
96.6°W
96.4°W
96.2°W
96.0°W
95.8°W
95.6°W
Longitude

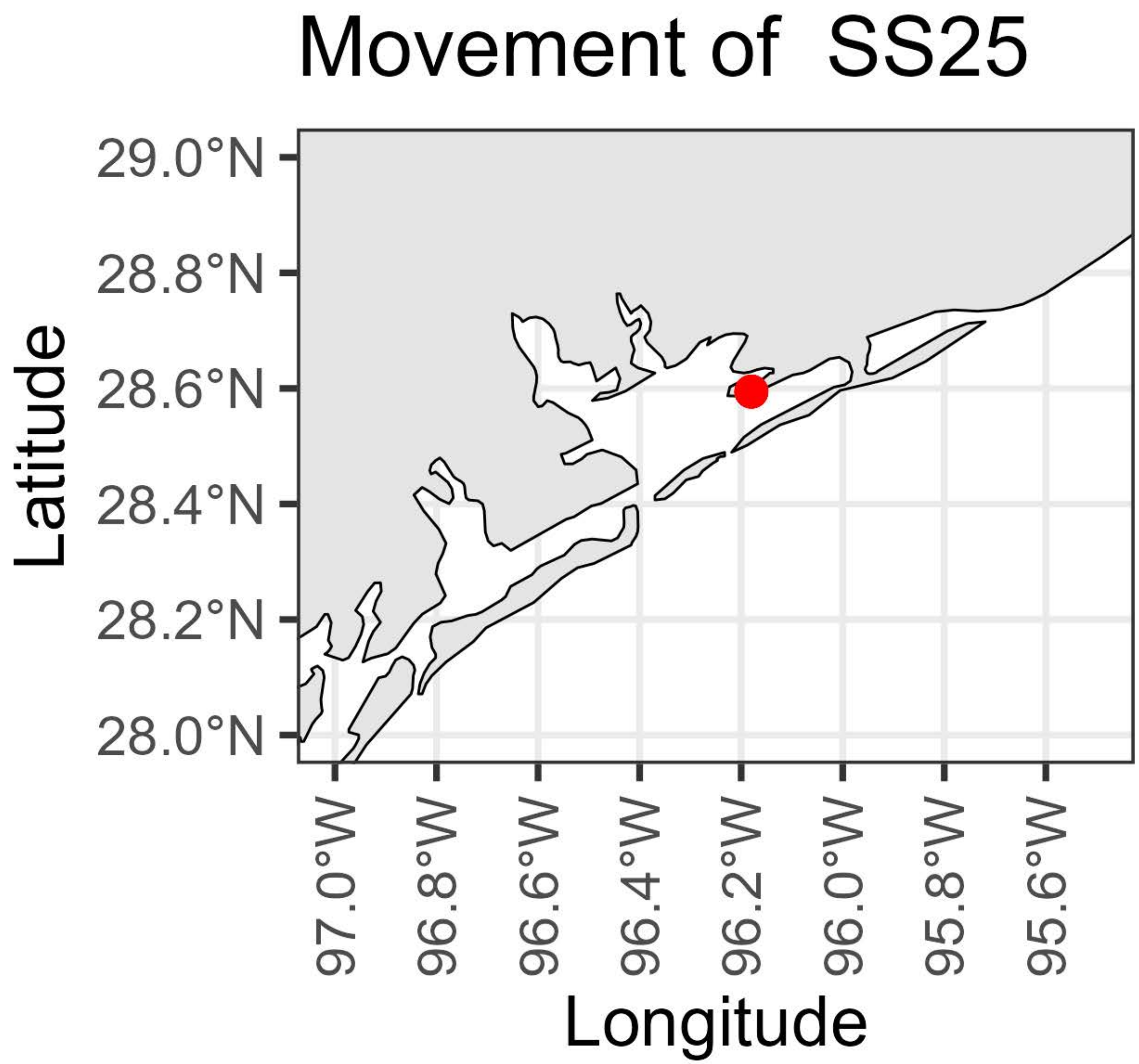
Movement of SS25
29.0°N
28.8°N
28.6°N
28.4°N
28.2°N
28.0°N
Latitude
97.0°W
96.8°W
96.6°W
96.4°W
96.2°W
96.0°W
95.8°W
95.6°W
Longitude

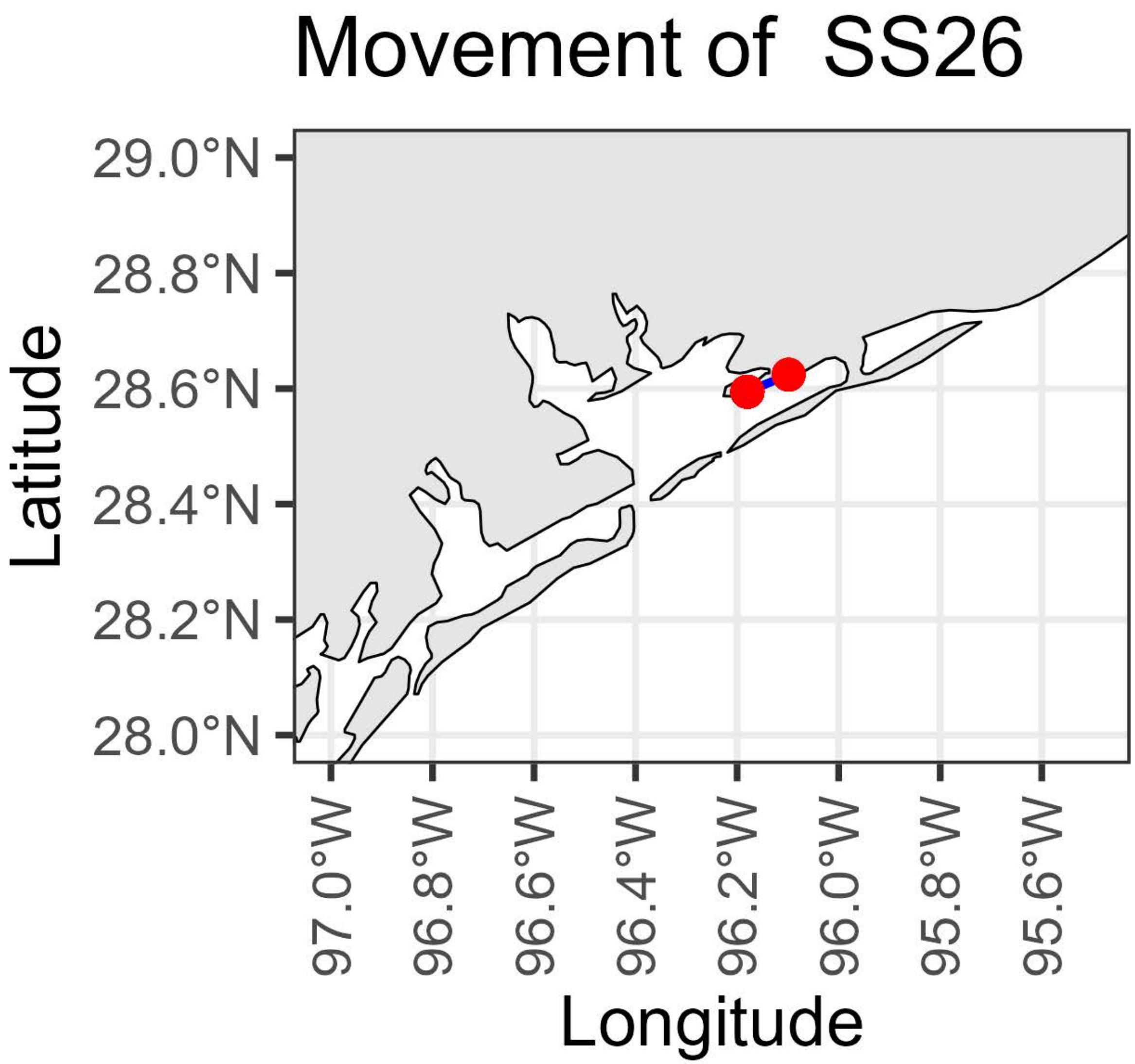
Movement of SS26
29.0°N
28.8°N
28.6°N
28.4°N
28.2°N
28.0°N
Latitude
97.0°W
96.8°W
96.6°W
96.4°W
96.2°W
96.0°W
95.8°W
95.6°W
Longitude

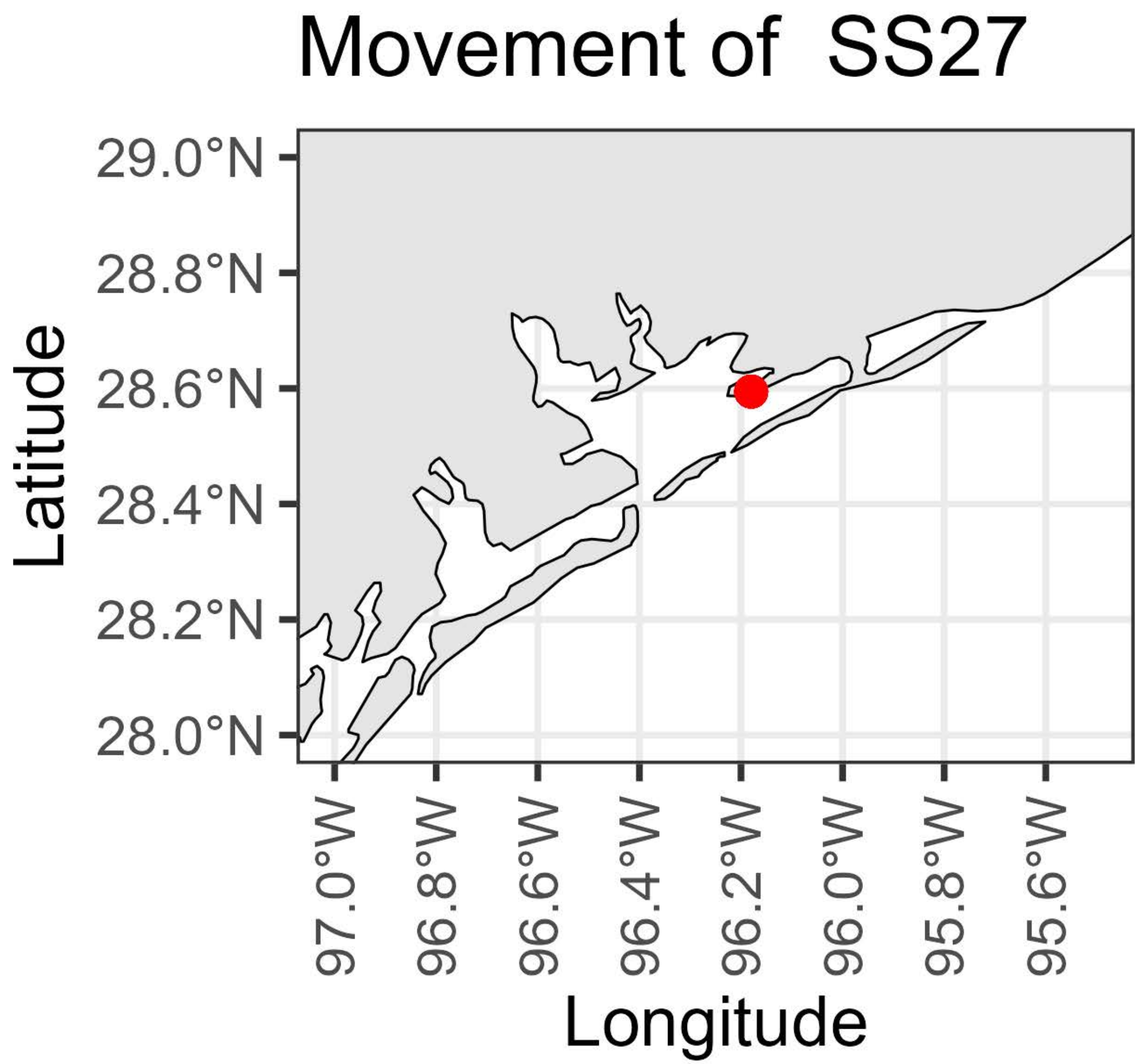
Movement of SS27
29.0°N
28.8°N
28.6°N
28.4°N
28.2°N
28.0°N
Latitude
97.0°W
96.8°W
96.6°W
96.4°W
96.2°W
96.0°W
95.8°W
95.6°W
Longitude

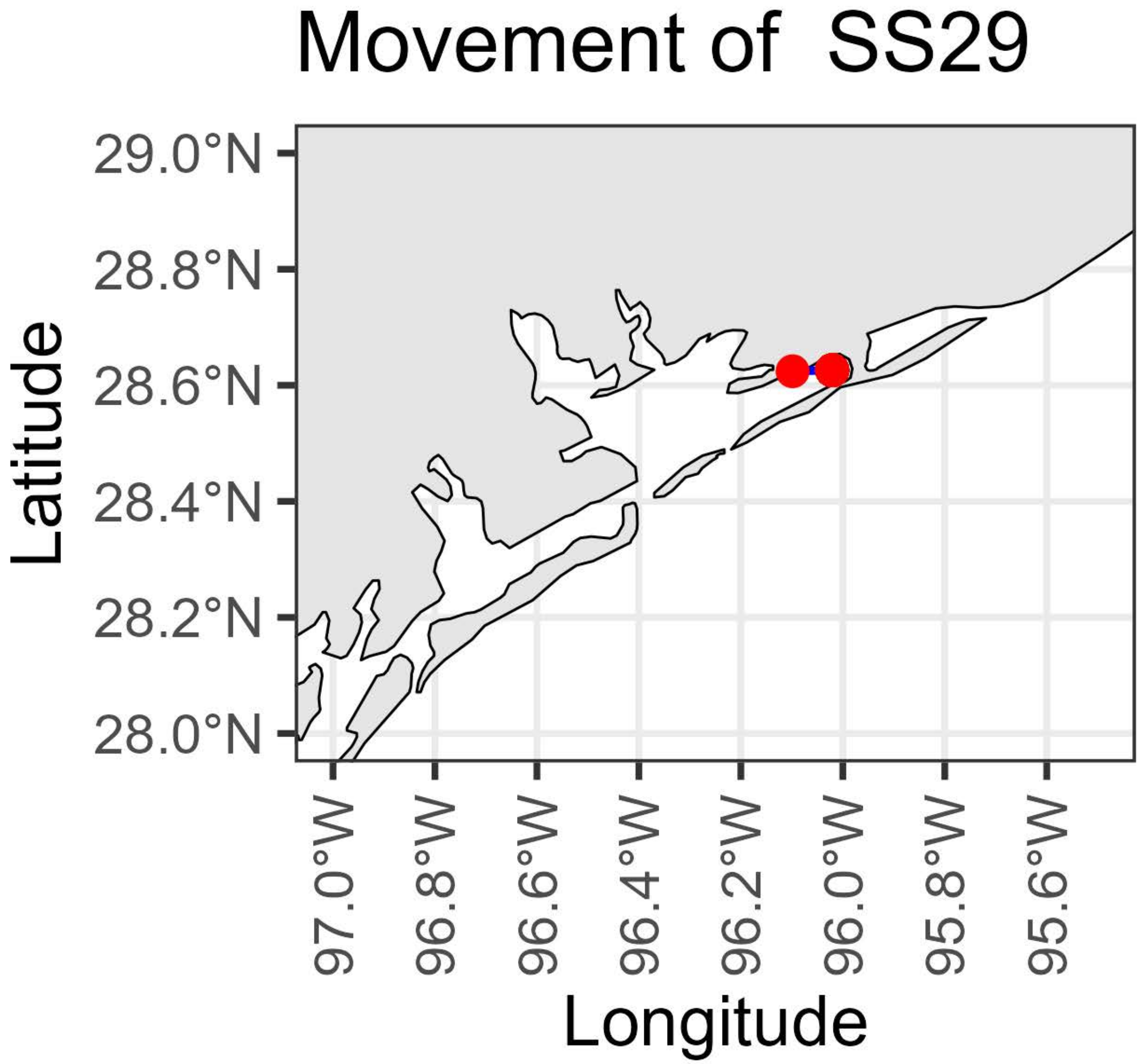
Movement of SS29
29.0°N
28.8°N
28.6°N
28.4°N
28.2°N
28.0°N
Latitude
97.0°W
96.8°W
96.6°W
96.4°W
96.2°W
96.0°W
95.8°W
95.6°W
Longitude

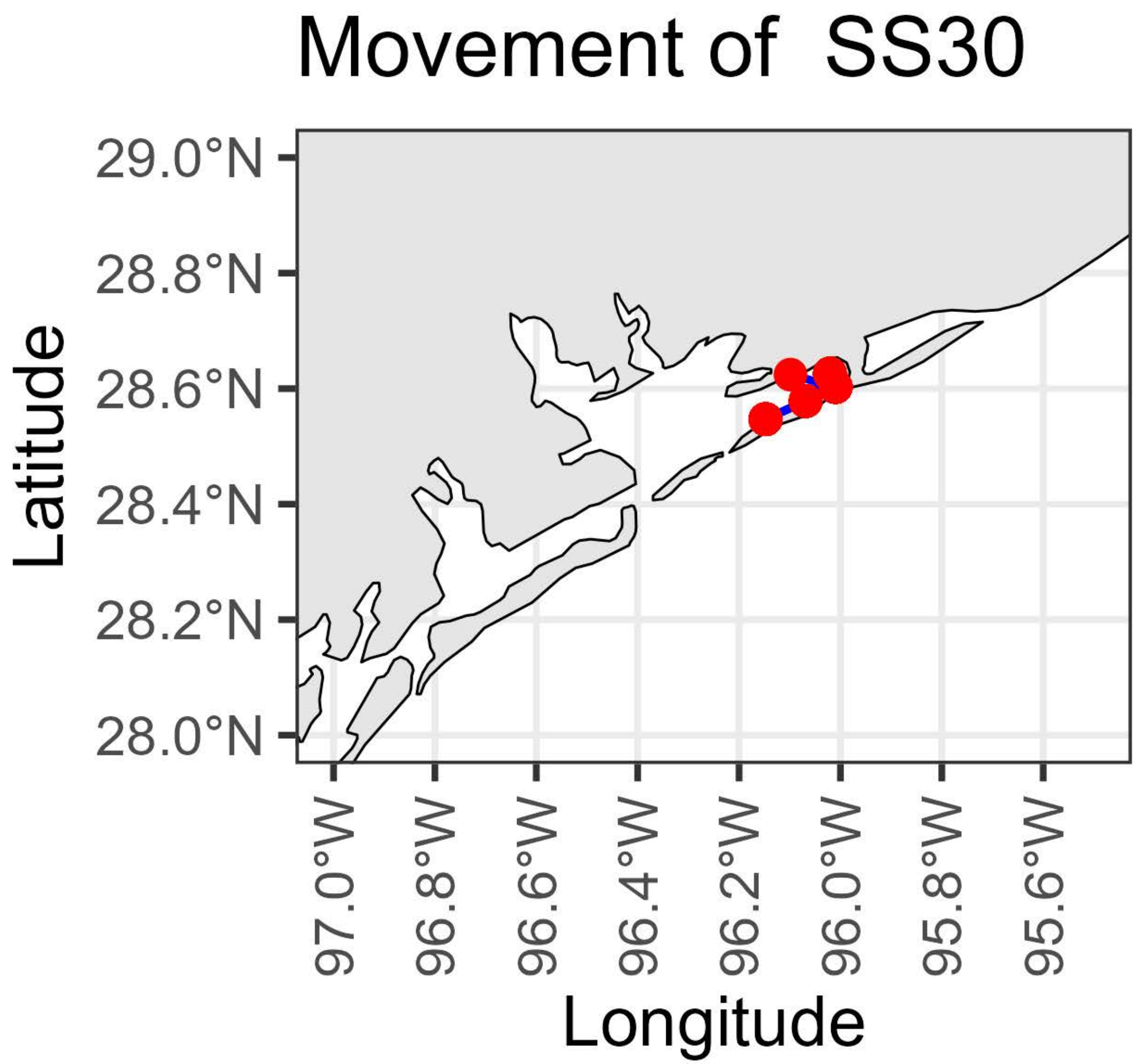
Movement of SS30
29.0°N
28.8°N
28.6°N
28.4°N
28.2°N
28.0°N
Latitude
97.0°W
96.8°W
96.6°W
96.4°W
96.2°W
96.0°W
95.8°W
95.6°W
Longitude

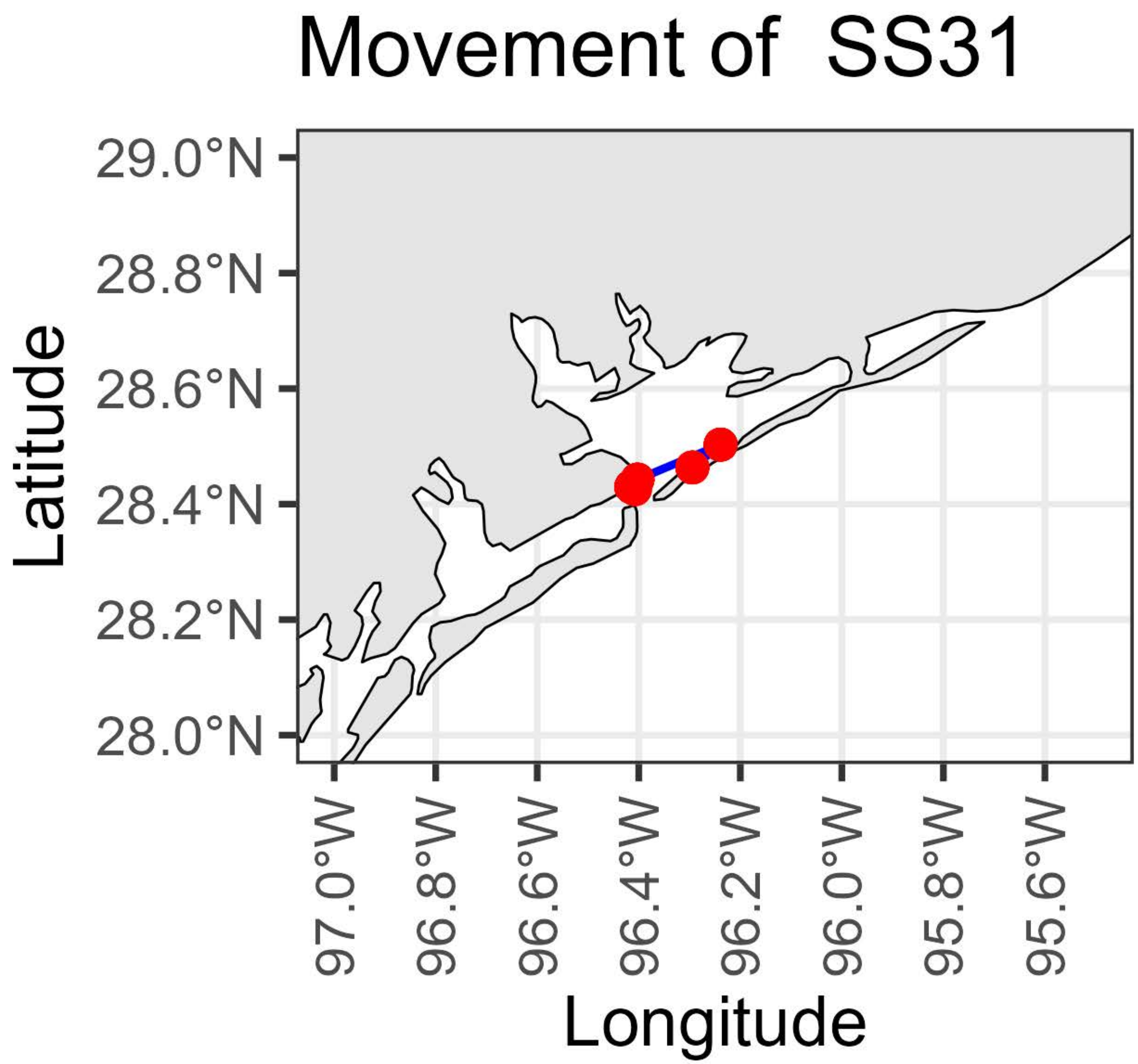
Movement of SS31
29.0°N
28.8°N
28.6°N
28.4°N
28.2°N
28.0°N
Latitude
97.0°W
96.8°W
96.6°W
96.4°W
96.2°W
96.0°W
95.8°W
95.6°W
Longitude

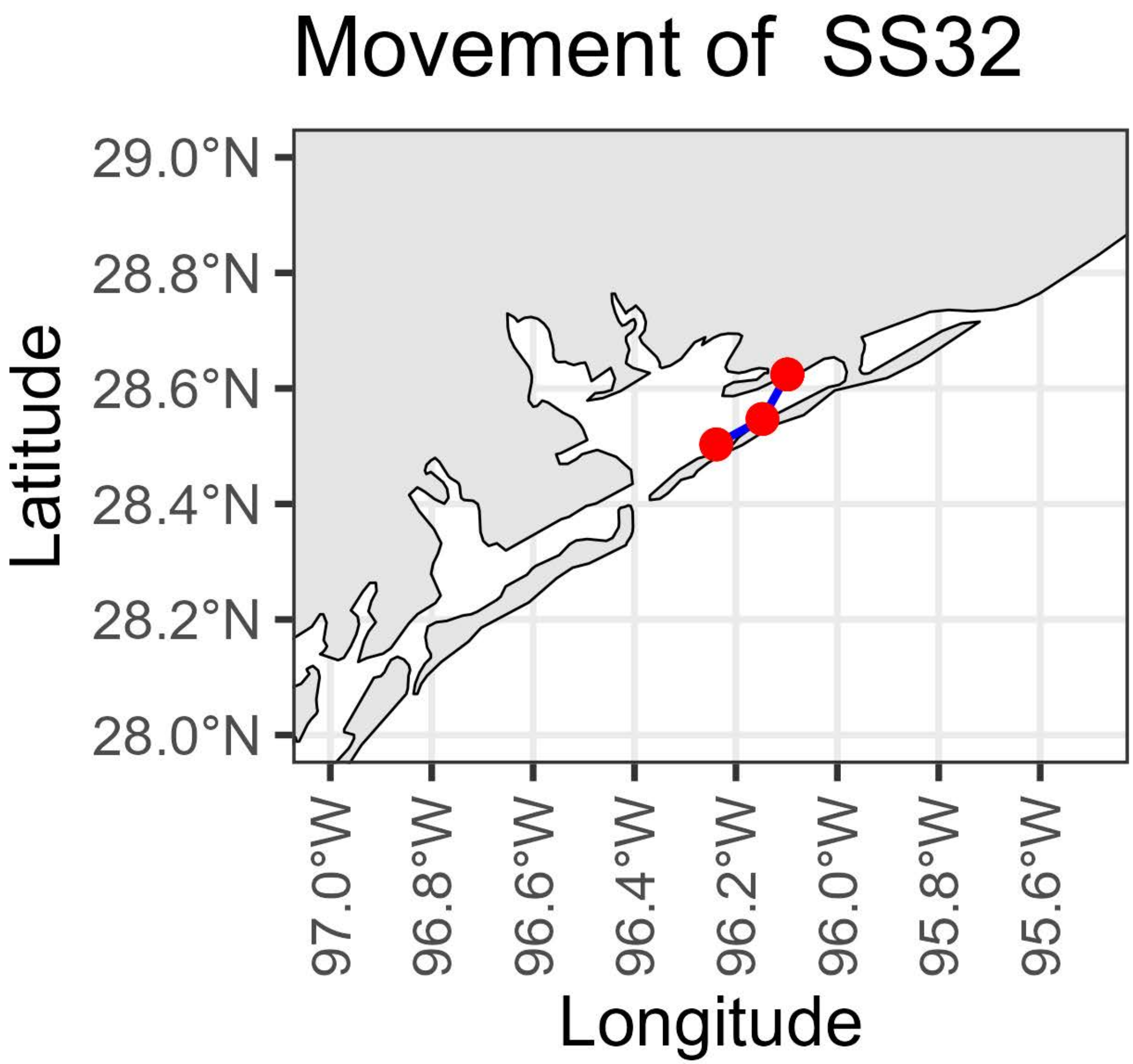
Movement of SS32
Latitude
29.0°N
28.8°N
28.6°N
28.4°N
28.2°N
28.0°N
97.0°W
96.8°W
96.6°W
96.4°W
96.2°W
96.0°W
95.8°W
95.6°W
Longitude

Appendix II: Selenium:mercury molar ratios in biota in the Alcoa Superfund site

Introduction

Selenium (Se), an essential trace element, is required to produce selenoenzymes and selenoproteins which help regulate metabolism, protect against oxidative stress, and support the immune system. Selenium has an antagonistic relationship with Hg and plays an important role in Hg detoxification by forming toxicologically inert mercuric selenide (HgSe) complexes (Ralston and Raymond, 2010). It has been proposed, and evidence supports, that if Se is present in molar excess of Hg (i.e., the Se:Hg molar ratio is >1:1) then Se may have a protective effect against Hg toxicity (Kaneko and Ralston, 2007; Raymond and Ralston, 2009). However, some studies have argued that a more conservative 5:1 Se:Hg molar ratio should be used because a 1:1 ratio assumes that all Se is bound to Hg which is not possible, therefore a 5:1 ratio assumes that 20% of Se is bound to Hg and the other 80% is potentially available for biological use (Burger and Gochfeld, 2012, 2013; Burger et al., 2012).

As a result, Se may protect biota in the Alcoa Superfund site from the toxicological effects of exposure to elevated concentrations of Hg; however, no previous study has examined this relationship. Therefore, a study was needed to investigate Hg and Se concentrations in biota throughout the food web (marsh grass, mollusks, crustaceans, teleost fishes, and elasmobranch fishes) in the Alcoa Superfund site to determine if Se may have a protective effect against Hg toxicity.

This study measured the Hg and Se concentrations and calculated the Se:Hg molar ratios in 27 species (marsh grass, two mollusk species, five crustacean species, 15 teleost species, and four elasmobranch species) collected from the Alcoa Superfund site. The relationship between mean Se:Hg molar ratio and mean Hg concentration for each species was examined and for each species, the percentage of individuals that had a Se:Hg molar ratio < 1:1, between 1:1 and 5:1, and > 5:1 was calculated.

Methods

The species (**Table S1**) were collected, processed, and the Hg analysis completed as described in the Methods section above. The Se concentration in each sample was determined by digesting ~0.25 g of dried sample in 5 ml of nitric acid (HNO_3) in a high temperature, high pressure microwave (Ethos-UP; Milestone, Shelton, CT) and diluting with 25 ml of Milli-Q water (MilliporeSigma, Burlington, MA) for a final volume of ~30 ml. The samples were then shipped to the Trace Element Analysis Core Lab at Dartmouth College (Hanover, NH) for ICP-MS analysis (Agilent 8900; Agilent Technologies, Santa Clara, CA). Quality control included blanks, certified reference materials (DORM-4, DORM-5), spiked samples, and duplicate samples. One set of quality control was included with every 20 samples analyzed.

Table S1. Species investigated in this study with the corresponding sample size (n) and body length (mean ± standard deviation; minimum – maximum in parentheses). [a] n = 5 for stem and 6 for blade. * shell height; ** shell length, *** total length; **** carapace width; ***** wingspan. ND = not determined.

	Species	Scientific name	n	Body length (cm)
Marsh grass	Smooth cordgrass	*Spartina alterniflora*	5/6[a]	ND
Mollusks	Eastern oyster	*Crassostrea virginica*	12	7.6 ± 1.5 (5.5 - 10.2) *
	Hooked mussel	*Ischadium recurvum*	9	3.5 ± 0.4 (2.9 - 4.0) **
Crustaceans	Grass shrimp	*Palaemonetes pugio*	6	3.0 ± ND (2.5 - 3.5) ***
	White shrimp	*Litopenaeus setiferus*	10	12.8 ± 1.3 (11.2 - 15.0) ***
	Fiddler crab	*Uca longisignalis*	8	1.4 ± 0.2 (1.2 - 1.8) ****
	Mud crab	*Panopeus obesus*	5	1.3 ± 0.4 (0.8 - 1.7) ****
	Blue crab	*Callinectes sapidus*	10	12.5 ± 2.7 (7.5 - 15.6) ****
Teleost fishes	Atlantic croaker	*Micropogonias undulatus*	10	16.0 ± 5.9 (9.5 - 24.2) ***
	Spot	*Leiostomus xanthurus*	3	17.0 ± 2.0 (15.7 - 19.3) ***
	Sand seatrout	*Cynoscion arenarius*	10	15.5 ± 3.5 (12.0 - 23.0) ***
	Gizzard shad	*Dorosoma cepedianum*	5	26.0 ± 1.3 (24.8 - 27.5) ***
	Gulf menhaden	*Brevoortia patronus*	10	15.7 ± 1.1 (14.0 - 17.2) ***
	Pinfish	*Lagodon rhomboides*	5	15.8 ± 2.4 (12.2 - 18.1) ***
	Ladyfish	*Elops saurus*	3	35.9 ± 13.7 (24.4 - 51.0) ***
	Striped mullet	*Mugil cephalus*	10	15.5 ± 6.5 (9.2 - 24.0) ***
	Hardhead catfish	*Ariopsis felis*	10	26.1 ± 4.9 (19.8 - 35.5) ***
	Gafftopsail catfish	*Bagre marinus*	7	33.4 ± 11.3 (19.5 - 50.0) ***
	Sheepshead	*Archosargus probatocephalus*	8	33.3 ± 4.0 (29.0 - 40.3) ***
	Southern flounder	*Paralichthys lethostigma*	10	39.9 ± 4.0 (35.5 - 47.3) ***
	Spotted seatrout	*Cynoscion nebulosus*	27	40.9 ± 9.2 (26.7 - 57.5) ***
	Black drum	*Pogonias cromis*	30	52.1 ± 28.9 (21.1 - 108.4) ***
	Red drum	*Sciaenops ocellatus*	30	45.6 ± 14.2 (27.6 - 103.0) ***
Elasmobranch	Cownose ray	*Rhinoptera bonasus*	5	52.7 ± 8.7 (46.0 - 63.4) *****
	Bonnethead shark	*Sphyrna tiburo*	3	60.6 ± 7.2 (52.4 - 65.7) ***
	Scalloped hammerhead shark	*Sphyrna lewini*	9	64.9 ± 8.4 (50.5 - 80.5) ***
	Bull shark	*Carcharhinus leucas*	9	110.1 ± 12.5 (88.9 - 123.9) ***

The Se:Hg molar ratio was calculated by dividing the concentration of Hg and Se (µg/g) by their respective atomic weight (Se = 78.96, Hg = 200.59) and the ratio determined by dividing the resulting µmol/g Se concentration by the µmol/g Hg concentration.

Key Results and Discussion

Due to the biomagnification of Hg, mean dry weight Hg concentrations (µg/g) were greatest in higher trophic level species [black drum (2.84), scalloped hammerhead shark (2.74), and blue crab (2.66)], and lowest in species at the lower trophic levels [grass shrimp (0.112), mud crab (0.108), and marsh grass blade and stem (0.0039 and 0.0013, respectively)]. The greatest Hg concentration was reported in a black drum (9.65) and the lowest concentration in a marsh grass stem (0.0011). There was no difference in Hg concentrations among mollusks (Mann-Whitney U test ; $U = 40.0$, $p = 0.320$) (**Figure S1**) however, there was a difference between marsh grass stem and blade (Mann-Whitney U test; $U = 0.000$, $p = 0.004$), and among crustaceans (Kruskal-Wallis; $H = 24.9$, $df = 4$, $p < 0.001$), teleost fishes (Kruskal-Wallis $H = 105.5$, $df = 12$, $p < 0.001$), and elasmobranch fishes (Kruskal-Wallis $H = 11.3$, $df = 2$, $p = 0.004$). The pairwise comparisons are shown in **Figure S1**.

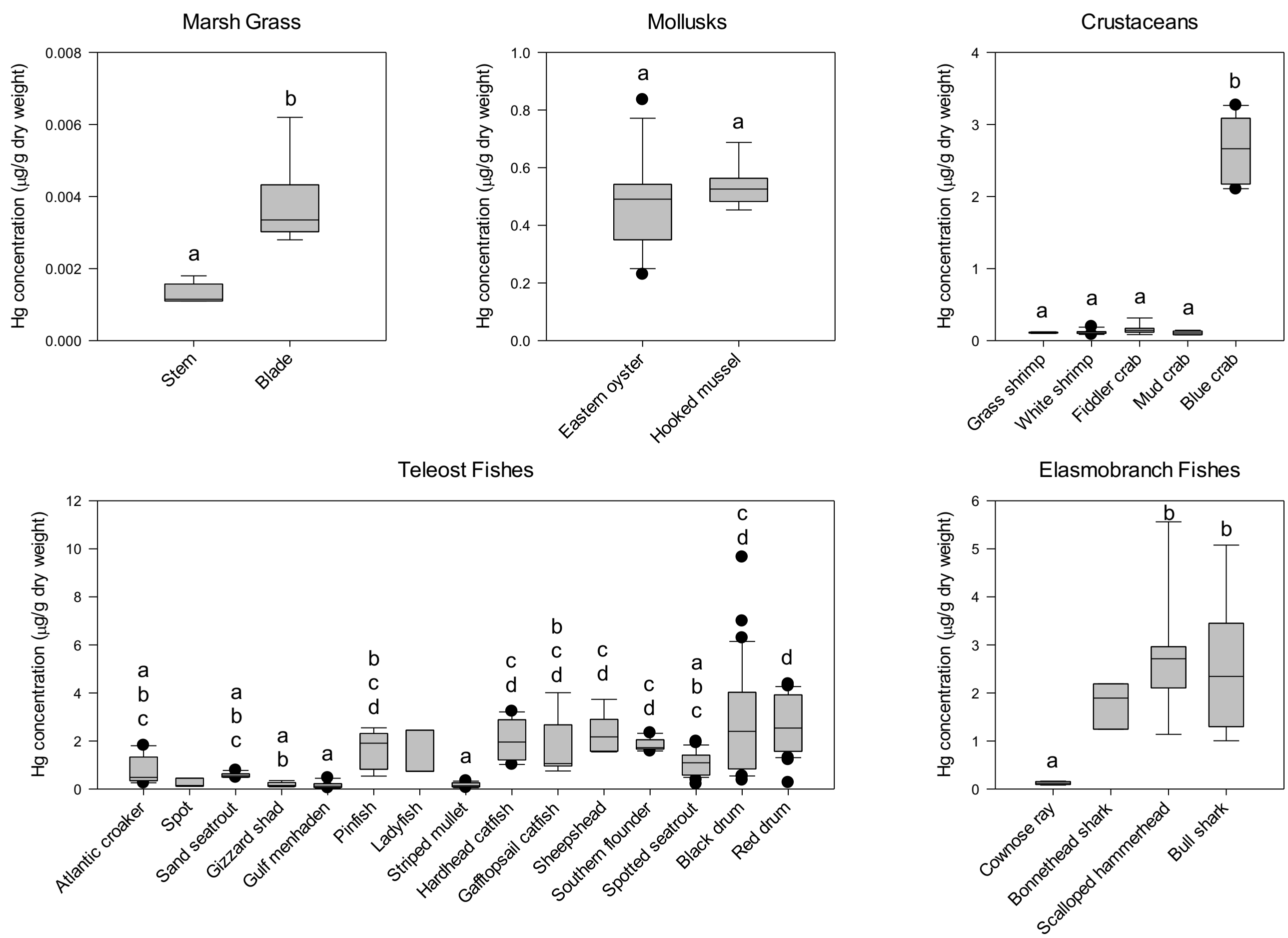

Figure S1. Comparison of dry weight Hg concentrations in marsh grass, mollusks, crustaceans, teleost fishes, and elasmobranch fishes investigated in this study. In each panel, lowercase letters represent species grouped by comparable Hg concentrations.

In comparison to Hg, mean dry weight Se concentrations (µg/g) did not follow a trend with presumed relative trophic position. Mean concentrations were greatest in hooked mussel (6.75), Atlantic croaker (6.54), and black drum (5.53), and lowest in gafftopsail catfish (1.00), mud crab (1.00), and marsh grass blade and stem (0.0239 and 0.0129, respectively). The greatest concentration was measured in a black drum (17.1) and the lowest concentration in a marsh grass stem (0.0073). There was no difference in Se concentrations between marsh grass stem and blade (Mann-Whitney U test; $U = 4.0$, $p = 0.052$) and elasmobranch fishes (Kruskal-Wallis; $H = 5.76$, $df = 2$, $p = 0.056$) (**Figure S2**). There was a difference in Se concentrations among mollusks (Mann-Whitney U test; $U = 0.000$, $p < 0.0001$), crustaceans (Kruskal-Wallis; $H = 33.5$, $df = 4$, $p < 0.001$), and teleost fishes (Kruskal-Wallis; $H = 136.3$, $df = 12$, $p < 0.001$). The pairwise comparisons are shown in **Figure S2**.

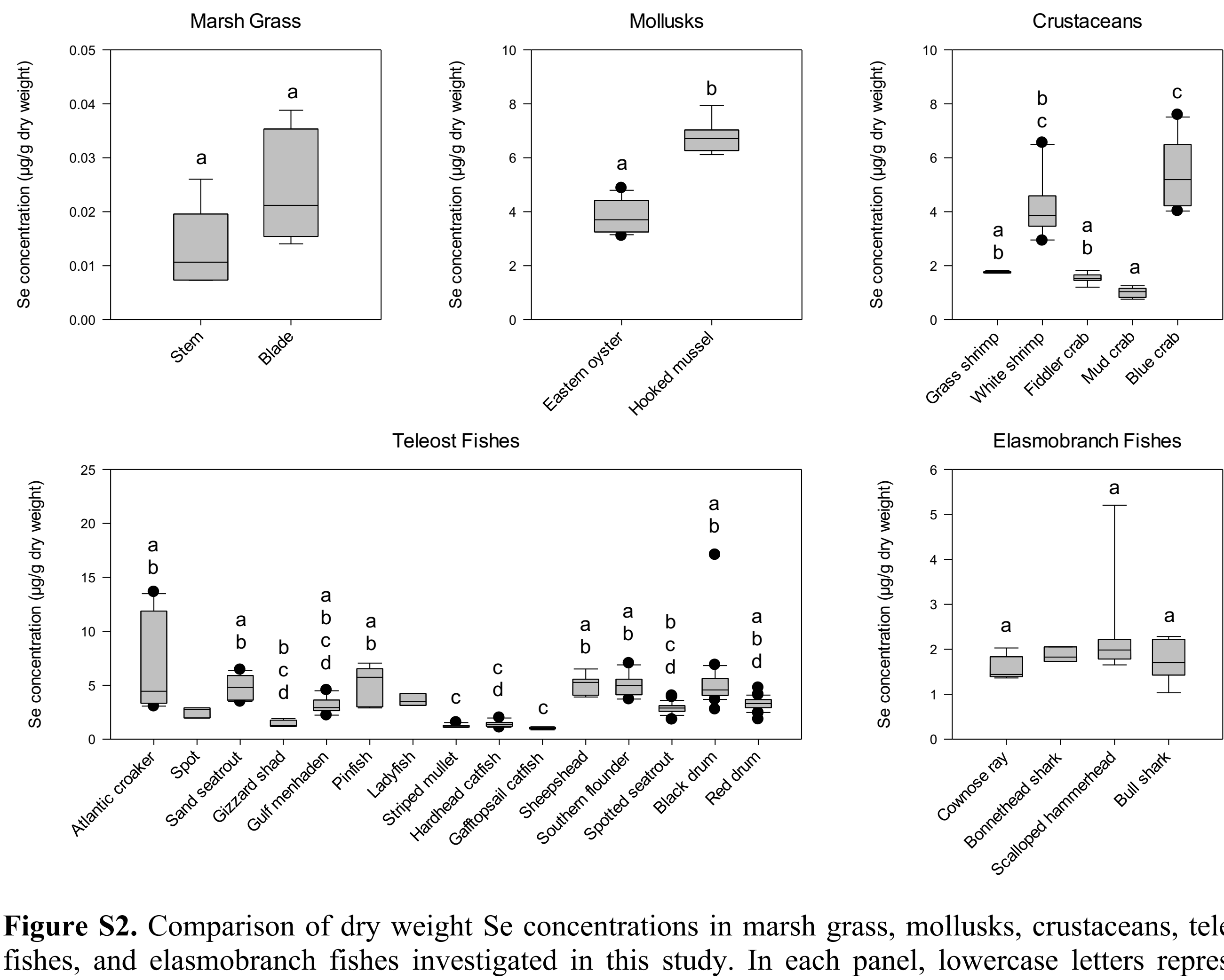

Figure S2. Comparison of dry weight Se concentrations in marsh grass, mollusks, crustaceans, teleost fishes, and elasmobranch fishes investigated in this study. In each panel, lowercase letters represent species grouped by comparable Se concentrations.

Overall, lower trophic level species had greater Se:Hg molar ratios than higher trophic level species. Mean Se:Hg molar ratios were greatest in white shrimp (89.8:1), Gulf menhaden (82.3:1), and grass shrimp (39.9:1), and lowest in hardhead catfish (2.15:1), bull shark (2.08:1), and gafftopsail catfish (2.04:1). The greatest Se:Hg molar ratio was reported in a Gulf menhaden (177:1) and the lowest in a gafftopsail catfish (0.601:1). There was no difference in Se:Hg molar ratios between marsh grass stem and blade (Mann-

Whitney U test; U = 10.0, p = 0.429) and mollusks (Mann-Whitney U test; U = 28.0, p = 0.065) (**Figure S3**). There was a difference in Se:Hg molar ratios among crustaceans (Kruskal-Wallis; H = 34.2, df = 4, $p < 0.001$), teleost fishes (Kruskal-Wallis; H = 114.8, df = 12, $p < 0.001$), and elasmobranch fishes (Kruskal-Wallis; H = 11.5, df = 2, p = 0.003). The pairwise comparisons are shown in **Figure S3**.

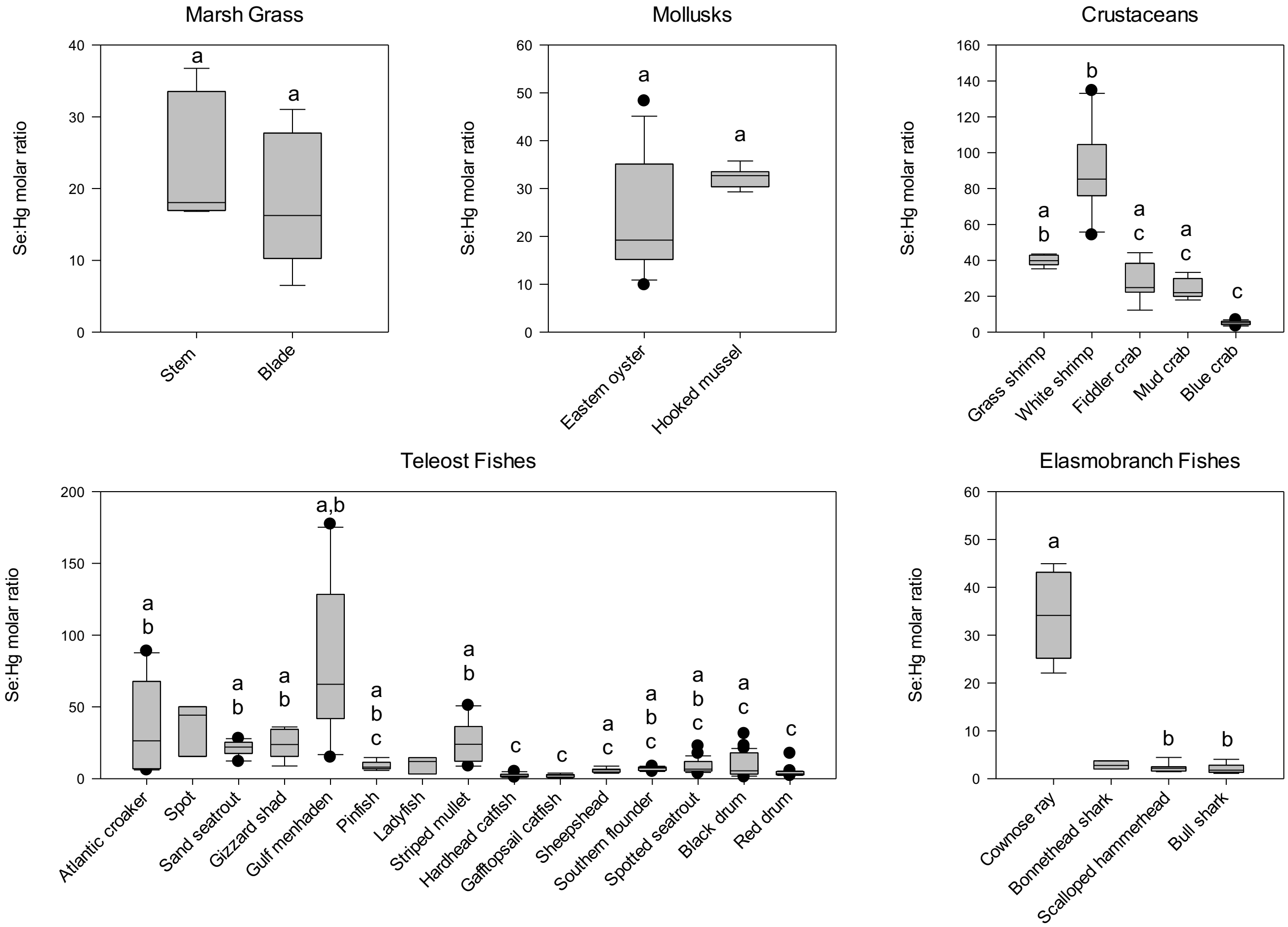

Figure S3. Comparison of Se:Hg molar ratios in marsh grass, mollusks, crustaceans, teleost fishes, and elasmobranch fishes investigated in this study. In each panel, lowercase letters represent species grouped by comparable Se:Hg molar ratios.

There was a strong negative correlation (Spearman's rank correlation; $r_s = -0.761$, $p < 0.001$) between the mean Se:Hg molar ratio and mean dry weight Hg concentration for the 27 species examined in this study (**Figure S4**). Mercury bioaccumulates in organisms and biomagnifies in estuarine food webs whereas Se often does not; as a result, the Se:Hg molar ratio decreases as Hg concentration increases.

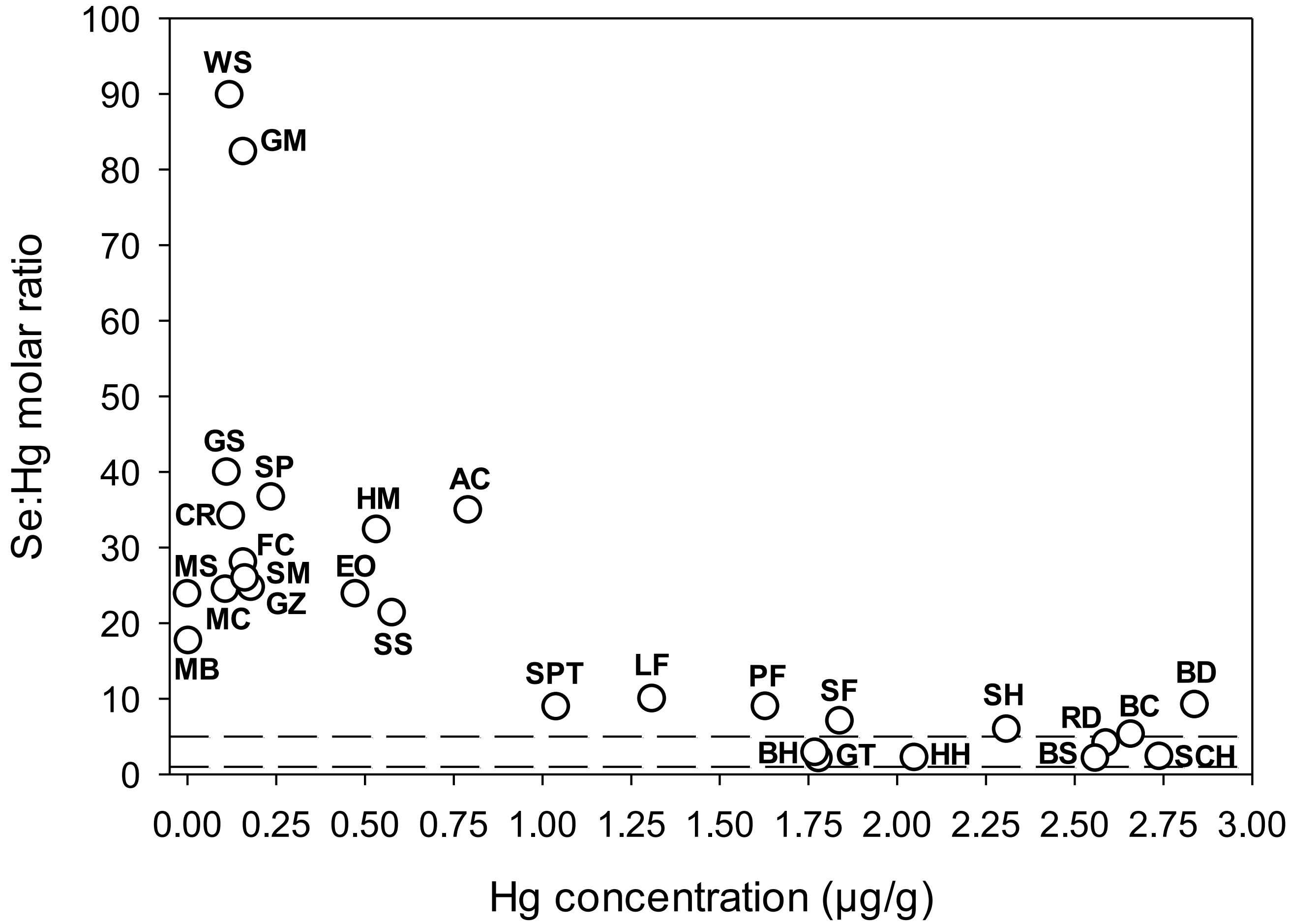

Figure S4. Relationship between the mean Se:Hg molar ratio and mean dry weight Hg concentration in the species examined in this study. The horizontal dashed lines are the 1:1 and 5:1 Se:Hg molar ratios. MS = marsh grass stem, MB = marsh grass blade, EO = eastern oyster, HM = hooked mussel, GS = grass shrimp, WS = white shrimp, FC = fiddler crab, MC = mud crab, BC = blue crab, AC = Atlantic croaker, SP = spot, SS = sand seatrout, GZ = gizzard shad, GM = Gulf menhaden, PF = pinfish, LF = ladyfish, SM = striped mullet, HH = hardhead catfish, GT = gafftopsail catfish, SH = sheepshead, SF = southern flounder, SPT = spotted seatrout, BD = black drum, RD = red drum, CR = cownose ray, BH = bonnethead shark, SCH = scalloped hammerhead shark, BS = bull shark.

All species had a mean Se:Hg molar ratio > 1:1, suggesting that Se may have a protective effect against Hg toxicity in biota in the Alcoa Superfund site. However, if the more conservative 5:1 Se:Hg molar ratio is applied, then six species (hardhead catfish, gafftopsail catfish, red drum, bonnethead shark, scalloped hammerhead shark, bull shark) had a mean Se:Hg between 1:1 and 5:1, suggesting the Se may not be protective against Hg toxicity in these species. However, on an individual-basis, 10% of hardhead catfish and 28.6% of gafftopsail catfish had a Se:Hg molar ratio < 1:1, indicating that Se may not have a protective effect against Hg toxicity for all individuals within a species. If the 5:1 Se:Hg molar ratio is used, then 12 species (blue crab, ladyfish, hardhead catfish, gafftopsail catfish, sheepshead, southern flounder, spotted seatrout, black drum, red drum, bonnethead shark, scalloped hammerhead shark, bull shark) had individuals with a Se:Hg molar ratio between 1:1 and 5:1.

Overall, there was large inter- and intraspecies variability in Hg and Se concentrations and Se:Hg molar ratios in biota collected from the Alcoa Superfund site. Risk assessment should not only evaluate the mean Se:Hg molar ratio but also examine the percentage of individuals that have a Se:Hg molar ratio < 1:1 and > 5:1. Except for hardhead catfish and gafftopsail catfish, based off the 1:1 Se:Hg molar ratio, Se concentrations may be great enough to protect species within the Alcoa Superfund site from Hg toxicity. However, the Se:Hg molar ratio that is truly protective and whether that ratio varies among tissues and taxa needs to be determined before Se:Hg molar ratios can extensively be used in risk assessment.

Presentations at conferences

Rehkopf, J., K. Banks, M. Streich, W. Nowlin, and J. Dutton (2024) Mercury concentrations in biota from the Alcoa/Point Comfort Superfund site (Lavaca Bay, Texas). Society of Environmental Toxicology and Chemistry North America 45th Annual Meeting. Fort Worth, TX.

Rehkopf, J., K. Banks, M. Streich, and J. Dutton (2024) Mercury concentrations in biota from the Alcoa Superfund site in Lavaca Bay (Point Comfort, Texas). South-Central Regional Chapter of the Society of Environmental Toxicology and Chemistry Annual Meeting. Kerrville, TX.